Doctoral Dissertation

Ultraprecision Micromachining of Hard Material with Cutting Point Swivel Machining by Using a Non-rotational Tool with Special Chamfer

TANG Xinrui

January 2013

Graduate School of Engineering,
Osaka University

Doctoral Dissertation

Ultraprecision Micromachining of Hard Material with Cutting Point Swivel Machining by Using a Non-rotational Tool with Special Chamfer

TANG Xinrui

January 2013

Graduate School of Engineering,
Osaka University

本論文の概要

近年，各種情報機器の高性能化・小型化に伴い，それらを支える基幹部品である光学素子に対して，高精度化・高機能化が要求されている．このような光学素子は，金型で成形して量産されるため，特にその金型には高精度化・複雑化の要求が高まっている．硬度の高い金型材料の加工において，工具を被削材に押しあてて，不要な部分を除去するため，工具の形状がそのまま転写される．高精度な形状を得るために，工具摩耗を抑制することが一番の課題になる．この課題に対して，工具材料，工具形状，表面処理，加工条件などといった様々な面から盛んに研究が行われている．しかし，高硬度材料の加工において，高精度な加工を長時間に継続するために，工具寿命が足りていないということが大きな問題となっている．

そこで本研究では，工具寿命を長くするために，『加工方法』という点に着目し，これまでにないポイントから工具摩耗を抑制することを目的とし，工具摩耗を抑制できる加工法の提案を行った．さらに，提案した加工法のメカニズムを解明し，その応用として曲線溝と自由曲面の加工に適用していた．

第 1 章では，高硬度材料の加工技術，特に工具摩耗に関する研究の概要をまとめ，本研究に着手するに至った背景を述べる．

第 2 章では，硬脆材料を加工する際に，発生する脆性破壊の原因と負のすくい角を持つ工具を使用する効果について述べる．均一な負のすくい角と円弧形状の断面を持つ特殊チャンファ付き工具を使用し，工具摩耗の抑制を期待できる『刃先移動加工法』を提案した．セッティングの誤差を補正することにより，高精度な加工を実現できた．さらに，SiC での検証実験において，従来の加工法より工具寿命を倍以上に伸ばすとともに，工具摩耗を抑制することにより，良好な表面性状が得られていた．

第 3 章では，刃先移動加工法のメカニズムを解明している．加工した表面の観察から，刃先移動加工法は実質的な切削方向を変化させられるとともに，速度比と切削力の関係についての実験から，速度比を増加させると，切削力を低減できることが分かった．また，速度比を増加させると，工具摩耗を低減でき，さらに増加させると，工具摩耗が逆に激しくなることから，最適な速度比が存在していることを明らかにした．

また，複雑な形状を加工するために，第 4 章で刃先移動加工法を曲線状な溝加工と曲面加工に適用した結果を述べる．任意の曲率を持つ溝加工において，良好な加工結果を得られることが分かった．従来の自由曲面加工法には，ボールエンドミリングが多用されてきたが，高硬度材料の加工においては，工具摩耗が激しくなることから，刃先移動加工法を適用すると工具摩耗を抑制しながら高精度な自由曲面の創成が可能になることを示した．

以上のように，本論文では新しい切削法，刃先移動加工法を提案し，それを自由曲面・自由曲線の加工に適用したところ，工具摩耗を抑制しながら複雑な形状を加工できることを実証した．このような新しい加工技術によって，金型加工の高精度化かつ複雑化に大きく貢献できる．

Abstract

Recently, in accordance with the technical development and miniaturization of information equipments, the demand of optical elements with high precision and miniaturization has been increasing. The optical elements including lenses are manufactured by the mold, so it is requested to fabricate the mold with high precision, miniaturization and complex shape. In the machining of the mold, the tool is pushed into the material, and the unnecessary part is removed by moving the tool, so the shape of tool is transferred into the surface. To obtain the surface with high shape accuracy and roughness, there is a proposition that of how to suppress the tool wear in the machining. There are a large number of investigations to solve this proposition, from the view-point like tool materials, the shape of tool, surface treatment, machining conditions and so on. However, in the machining of hard material, to keep the high precision machining as long as possible, the serious issue is the shortage of tool life.

This study focuses on the 『Machining method』 to suppress the tool wear and to increase the tool life in the machining of hard material. This study aims to create a new machining method which has the ability to suppress the tool wear, and to realize high precision machining at the same time. Then, by investigating the mechanism of the proposed machining method and applying it to the machining of complex shape, it is confirmed that a new machining method which has the ability to suppress tool wear and to realize ultraprecision machining is constructed.

In Chapter 1, the machining technology of the hard material, especially the investigations of the tool wear are summarized, and the background of this research work is introduced.

In Chapter 2, the mechanism of the brittle fracture in the machining of hard material and the effect of the tool with negative rake angle is introduced. Then, a method which is called 『cutting point swivel machining』 , by using the tool with special chamfer, which has the same negative rake angle along the rake face and the circle cross section of tool shape, is proposed. By compensating the setting error, it is confirmed that ultraprecision machining can be realized by using this cutting point swivel machining. The effect of the tool wear suppression is verified by the cutting experiment of SiC. It is found that good surface can be obtained by suppressing the tool wear at the same time.

In Chapter 3, it aims at investigating the mechanism of the cutting point swivel machining. It is found that the cutting point swivel machining has the ability to change the actual cutting direction in the machining. At this time, the moving distance of the cutting edge becomes longer than the conventional machining to remove the same volume of workpiece. Thus, the actual cutting width can be reduced and the cutting force can be reduced at the same time. In addition, by using the broad part of the cutting edge, the tool wear can be reduced substantially. Then, the relationship between cutting force and the speed ratio is investigated. It is found that the cutting force can be reduced by increasing the

speed ratio. After that, it is found that the tool wear can be suppressed by increasing the speed ratio. However, when the speed ratio is increased furthermore, the tool wear becomes severe. As a result, it is shown that there is an appropriate speed ratio which has the ability to suppress the tool wear to the least.

In Chapter 4, to machine the complex shape, the cutting point swivel machining is applied to the creation of curved microgrooves. It is confirmed that microgroove with arbitrary curvature can be machined with good accuracy by using cutting point swivel machining. Then, to compare with ball end milling, which is mostly used in the machining of curved surface, it is found that although the efficiency of cutting point swivel machining is worse, the tool wear is less than that of ball end milling, and high precision machining can be obtained for a longer time. At last, the cutting point swivel machining is applied to the machining of curved surface. It is confirmed that both good shape accuracy and surface roughness can be obtained by using cutting point swivel machining.

In Chapter 5, this study is summarized.

As above, a new machining method which is called cutting point swivel machining is proposed in this study. The cutting point swivel machining is applied to curved microgrooving and the machining of curved surface. As a result, it is confirmed that the machining of complex shape with tool wear suppression can be realized. The use of this new machining technology can contribute significantly to the machining technology with high precision and complex shape, which is requested in the machining of mold.

CONTENT

Chapter 1
INTRODUCTION

1.1Back ground of this study

The cutting operation is a machining method which removes the unnecessary parts of material to get target shape by pushing the cutting tool into workpiece and moving the cutting tool. The feature of cutting operation can be shown as follows:

1) High machining efficiency
2) Comparatively low cost in variety and small amount of manufacturing
3) High machining accuracy
4) Ability of various target shape
5) Ability of various materials
6) Low energy to remove unit volume of material

As shown as above, there are a lot of advantages of the cutting operation, so it is one of the most basic and important machining method [1], and it is used in large numbers of manufacturing of all kinds of products.

By the advancement of optical region, it is requested to machine the hard material with high dimension accuracy, high shape accuracy, good roughness, miniaturization and high efficiency. To realize these exacting requirements, the cutting operation assumes a great role, and the requirement to cutting operation becomes harder and harder.

The machine tools, machining methods, cutting tools and cutting fluid are investigated to satisfy these hard requirements. As an important element of cutting operation, the cutting tool is pushed into the workpiece, so it has a direct influence on the accuracy of machined shape and surface. Especially in the cutting of hard material, there is the occurrence of severe tool wear on the cutting edge because of the hardness of workpiece, and tool wear makes a huge impact to the machining quality. It is necessary to suppress tool wear in the machining. There are several methods to suppress tool wear just as improvement of tool material, surface treatment and coating of cutting tool, and development of machining method and so on. In this study, to machine the complex shape with high precision, miniaturization and high efficiency, a new machining method is proposed. The effect of this machining method is verified and it is applied to the machining of complex shape. Then, the requirement of cutting hard material with complex shape is explained to introduce the background of this research.

1.2 Manufacture of optical elements

In recent years, the optical elements come into wider use in our life. For example, they are used in camera, mobile phone, CD/DVD driver, and so on. The optical elements are used from long time ago [2]. The mirror used around 16th century B. C. was unearthed in Egypt, and the lens used around 7th century B. C. was found in Iraq. Then, the glasses is diffused from 14th century, and the scope and microscope are made from 16th century. As this, the mirror and lens are used from long time ago, and they are used widely in our life.

Shape of optical elements

The spherical lens is used for long time. However, as shown in Fig. 1-1(a), it is found that the spherical lens does not have the ability to focus the incident light to one point, because of the difference of location where the light transmit and the wavelength of light [3]. This phenomenon is called aberration. Although the aberration can be compensated by using several lenses, the equipment becomes larger and heavier, and the transmittance of light becomes worse at the same time. As the method to compensate aberration, the aspheric lens is proposed. As shown in Fig. 1-1(b), to focus the incident light, the curvature radius is different according to location on lens. By using the aspheric lenses, compensation of aberration can be realized by few lenses, and optical equipment can be produced with miniaturization and lightweight [4].

However, because the wavelength of each colored light is different, by using this kind of refracting lens, different colored lights focus to different points, and it causes the chromatic aberration. To solve this problem, the diffractive optical element (DOE) is proposed. The proposal of DOE can trace back to 1870s [5], the Fresnel zone plate (FZP). At 1898, Wood confirmed that the efficiency can be improved by using DOE with surface relief [6]. Then, it is proposed to compensate the color aberration by combining refractive lens and diffractive lens in the 1960`s [7]. After that, it is reported that DOE are used to vary design of lenses [8], [9]. For example, by using pickup lens with microgrooves which are arranged in a concentric pattern on aspheric surface, CD and DVD with different thickness can be

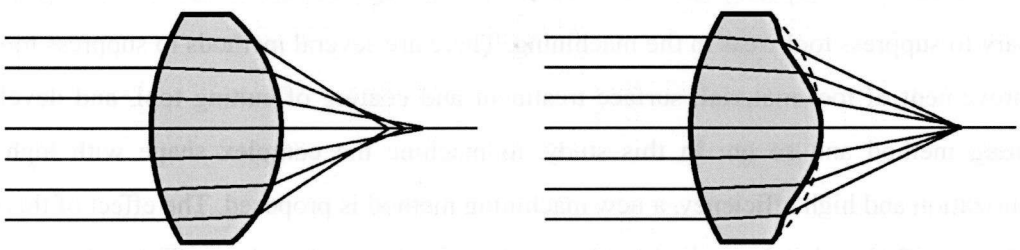

(a) Spherical lens (b) Aspheric lens

Fig.1-1 Effect of aspheric lens

regenerated by one lens, by changing the focal point distance of diffracted light [10]. There are a large number of investigations about the structure of surface and optical property [11], [12]. In addition, the micro lens is requested to be used by the miniaturization of optical equipments.

Material of optical elements

Glass is used as the material of optical elements from long time ago. Plastic is researched to be used as the material of optical elements as a substitute for glass from 19 century [13]. At about 1920, the clear and colorless urea resin is developed. However, by the demerit of non-durable and crack, it is not considered as the optical material. Then, methyl methacrylate (MMA) is developed at about 1930, with good durable and mechanical intensity. However, MMA belongs to thermoplastic resin, so there are problems that it is easy to be hurt and the heat resistance is not enough to all products. After that, a lot of investigations which use plastic as the material of optical elements is made during World War 2. As a result, thermo hardening resin CR-39 (diethylene glycol bisallyl carbonate) is developed with good heat resistance and hardness.

To compare with the glass, the plastic lens has the merit of ①low density, ②impact-resistance, ③ low molded temperature, ④low cost, and so on. At the same time, the plastic has the demerit as follows: [14], [15]

Transparence: There are many kinds of plastic with the property of clear and colorless. So there is scarcely any problem on the transparence. However, by the advancement of optical equipments, it is requested to consider the transparence of invisible ray such as infrared ray and ultraviolet ray.

Homogeneity: By managing the production process, the pore and impurity can be discharged from feedstock. However, because the forming process of plastic lens is injection mold, it is easy to occur the heterogeneity by the different lots, or products with the same lot. Then, there is a problem that the generation of strain by the character of water absorbability and surface oxidation.

Variation of temperature: The coefficient of thermal expansion of plastic is 10 times to that of glass, so the variation of refraction which is caused by the change of temperature is 40-60 times to that of glass. Then, the molding shrinkage occurs in the molding processing to cause the deterioration of the shape accuracy.

Hardness: The hardness of plastic is not enough and the coefficient of elasticity is so small that plastic is easy to be hurt and to be deformed after molding to cause the deterioration of surface accuracy.

Table 1-1 Property of optical plastic and glass

	Glass	PMMA	PS	CR-39	PC
Refraction index N_d	1.50~1.52	1.48~1.50	1.56~1.58	1.50	1.58
Dispersion γ_d	—	57.0	30.9	57.8	31.0
Elastic modulus (10^4 kg/cm^2)	50~90	2.5~3.5	2.8~4.2	2.1	2.2~2.5
Tensile strength (10^2 kg/cm^2)	4.0~10.0	5.6~7.0	3.5~6.3	3.5~4.2	5.9~6.6
Difference of N_d by temperature ($\times10^{-5}$/K)	-12	-14	-15	-16	-1
Thermal conductivity (10^{-4} cal/sKcm)	23	4~6	2.4~3.3	—	4.6
Coefficient of thermal expansion (10^{-5} /K)	0.9~1	9	6~8	8~15	7
Soften point (°C)	450~500	65~100	70~100	140	138~142
Coefficient of water absorption (%) (24 h)	—	0.3~0.4	0.03~0.05	0.2	0.8
Oriented strain	None	Small	Medium	—	Medium
Density (g/cm^3)	2.5	1.18~1.19	1.04~1.07	1.32	1.2

Secular change: Plastic, especially thermoplastic resin, is easy to be deformed by the rise of temperature. Then, there is always the strain in the material by the machining. The release of strain causes the deformation of plastic. In addition, there is a problem that devitrification occurs by the oxidation of light and heat, when optical elements are irradiated by the sun light.

As above, there are still several problems to use plastic instead of glass. The properties of glass, PMMA, PS, CR-39 and PC are shown in Table 1-1. As shown in this table, it is known that glass has the excellent temperature properties, humidity properties and optical properties. So glass is used as the material of optical elements when the request of optical elements is high.

Manufacture of glass lens

Traditionally, glass lenses are manufactured by cold working (grinding and polishing process) after material forming by melt glass [16]-[19]. It costs a lot of time and the complex shape like aspheric surface is difficult to be fabricated. To solve this problem, the molding technology is investigated from 1970, and it is in practical used from 1982, by Eastman Kodak Company to manufacture glass lens of disk camera [20], [21]. After 1985, molding technology is used widely in the manufacture of glass lens.

In recent years, there are a lot of investigations for cutting and grinding glass lens directly. For example, Kawada et al. reported that optical glass can be grinded in ductile mode when the depth of grind is less than 0.1 μm [22]. As the cutting of glass, Matsumura et al. found that good machining result can be obtained by using the end mill with small radius [23]-[26], and Warisawa et al. observed the transition between plastic deformation, ductile and brittle cutting for glass [27]. Then, Obigawa et al. simulated the transition between ductile and brittle cutting of glass [28] and cut glass with micro ball end mill [29]. Iizuka et al. used the fly cutting to the machining of glass, to discuss the relationship

between surface and the material of tool [30]. As a result, good shape accuracy and surface can be obtained by cutting and grinding glass lenses. However, the process costs a lot of time so it is not available for mass production. The press forming by molds is used in the manufacture of glass lens. The press molding is shown in Fig. 1-2 [31]. Glass is set between upper mold and lower mold, and it is heated to be softened. The gas is used to avoid the oxidization of glass. By this way, glass lenses can be manufactured with the same shape as the mold.

The mold of plastic is usually made by Ni-P which is coated on aluminum alloy, cooper and steel. Then, the coated Ni-P is machined to the shape of lens by an ultraprecision machining center [32], [33]. However, when the mold with Ni-P coating is heated to 700 K [34], the crystal architecture transforms from amorphous to crystalline. There is the volume constriction of metallic skin to cause the occurrence of crack [35]. The molded temperature of glass is about 900 K, which is much higher than the temperature that the crack occurs on Ni-P. So the hard material including cemented carbide and ceramics are used as the material of molds. As the common denominator of these materials, they have the properties of high hardness, high heat resistance and low coefficient of thermal expansion, which are needed as the mold material.

Fabrication of the mold

Traditionally, hard materials for molds need to be fabricated by several processes. For example, after the rough machining by a machining center, the molds need hardening process, electrical discharge machining and polishing process. However, when micro molds are fabricated, it is difficult to produce the electrode of electrical discharge machining, and there is the threat of the broken part of mold by

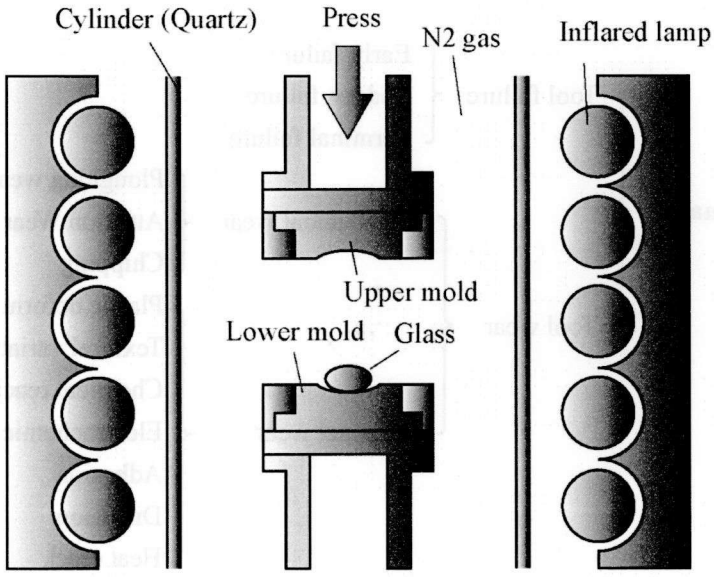

Fig. 1-2 Glass molding process

using electrical discharge machining. Then, it is difficult to keep the shape accuracy and create complex shape by polishing process. Recent years, by the development of ultraprecision machining center, the resolution of translation axis is fine down from 10 nm to 1 nm. Good surface can be obtained by the machining. At the same time, good shape accuracy can be obtained because of the correct transfer of tool path. So ultraprecision cutting is used as the finish machining of mold to obtain good shape accuracy and surface roughness.

There are a large number of investigations about the cutting of hard material, these investigations are almost about ①Character of tool wear, ②Cutting forces, ③Material of cutting tool, ④Shape of cutting tool, ⑤Cutting conditions, ⑥Machining method.

Character of tool wear

The classification of tool damage in the machining is shown in Fig. 1-3 [36], [37]. The tool wear can be divided into mechanical wear and thermal wear. The tool wear in the machining of hard material almost belongs to the mechanical wear because of the hardness of the workpiece. In the machining of cemented carbide, which is a representative hard material, it is reported that chippings occur on the cutting edge, and tool life depends on the tool wear on flank face [38]. The tool wear is involved to the grain size of WC grains. When the grain size of WC is large, the probability of abrasion between tool and grain becomes large, and tool wear becomes severe [39]. Then, the energy dispersion spectroscopy (EDS) is used to observe the flank face of tool. The tungsten constituent can be observed on the flank face [40]. It can be considered that there are 2 reasons of the tool wear, one is the mechanical wear which is caused by the friction between tool and workpiece, and the other one is adhesion wear by the

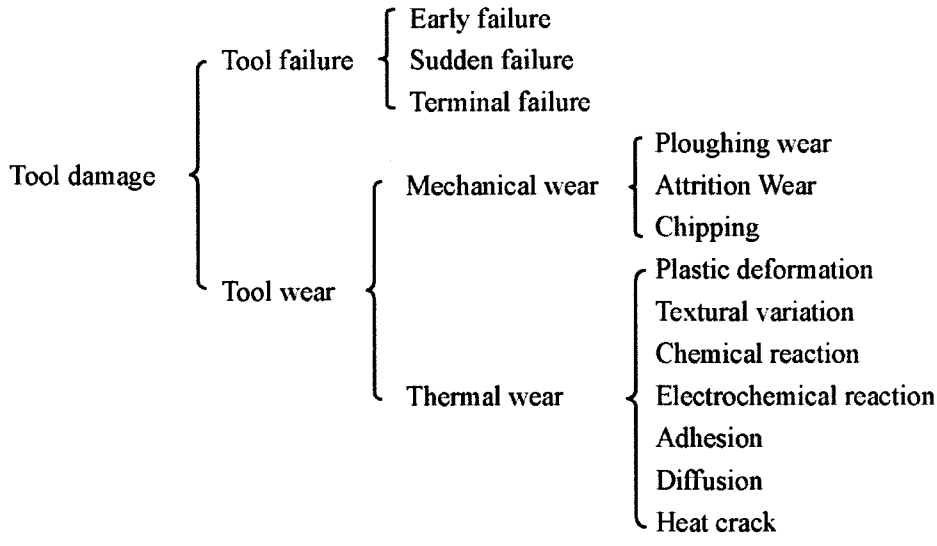

Fig. 1-3 Reason of tool damage

desorption of incrustation. Then, there are investigations about the machining of silicon carbide (SiC) [41], [42]. It is known that chippings occur on the flank face with high feed rate because of the impact between cutting tool and SiC grains, and scratch mark can be observed with low tool feed rate because of the abrasive scratch of SiC grains.

Then, as the chemical wear of cutting tool, it is reported that there is the chemical aspects of tool wear in the machining of electro less nickel by single point diamond [43].

Cutting force

Cutting forces are measured in the lathe turning of tungsten carbide. It is known that the thrust force is about twice to three times as much as cutting force in the machining [40]. So it is requested to use the machine tools with high stiffness at the direction of thrust force. Then, the cutting forces become large when the content of WC becomes high, because the hardness of workpiece is increased.

Material of cutting tool

At 1976, by the diffusion of polycrystalline sintered compact, it is reported that there is the possibility of cutting cemented carbide by Tanaka et al [44], [45]. In the cutting process, the hardness of tool is expected to be more than 4 times of that of workpiece. The hardness of these hard materials are more than 1500 HV, so the material of tool is limited. Single crystal diamond (SCD), sintered diamond (PCD) and cubic boron nitride (cBN) are majorly used as the material of tool. The single crystal diamond has the maximum hardness in the material of tool, and because of its directional property, the cutting edge can be made sharp. However, because of this directional property, in the machining of hard material, the chippings occur on the cutting edge and the tool life becomes very short. Then, although the cutting edge of PCD is worse than that of SCD, the tool life can be extended substantially by its directionless property [46]. In the machining of cemented carbide, it is reported that tool wear can be suppressed by using PCD tool with coarse grained diamond and low content of cobalt [47]. It is considered as that the diamond grain is difficult to be dropped by using coarse grained diamond. There are a large number of researches to investigate the mechanism of tool wear by using PCD tool [48]-[51].

In recent years, the binderless nano polycrystalline diamond tool is developed [52], [53]. This tool is made at 16 GPa and 2300 ℃, sintered by high purity graphite directly, and the radius of grain is less than 50 nm [54]. The hardness of the tool is higher than that of SCD, and the problem of SCD that the difference of hardness depends on the plane direction can be solved because of the use of polycrystalline diamond. It is reported that the tool life of binderless nano polycrystalline diamond can be extended to more than 3 times as that of coarse grained PCD tool [41].

Then, it is reported that if the content of cobalt in the tungsten carbide is more than 20%, the tool wear of cBN tool is less than that of PCD tool [55]. So cBN tools are used at point of production with the merit of low cost. The binderless cBN tool is developed and its availability for cutting cemented

carbide is verified. At the same time, there are several investigations by using the tool with chemical vapor deposited (CVD) diamond [56], [57].

Shape of cutting tool

Suzuki et al. developed a new micro milling tool made of PCD, and it is reported by using this new tool, the mold of Fresnel lens with shape accuracy under 0.1 μm, and roughness R_y under 20 nm can be obtained [58]-[61]. Fukui et al. focused on the tool of diamond grains [62]-[64]. By using the tool with small radius, the complex shape can be machined on the cemented carbide. Kato et al. used the tool with the shape of cone, which is made of sintered diamond, to the milling of cemented carbide. The radius of tool is 0.035 - 0.04 mm, and the rotation speed of spindle is 20,000 to 70,000 rpm. As a result, surface with flatness of 0.5 μm, roughness of 0.3 μm can be obtained [65].

Cutting conditions

The cutting condition is a very important part in the machining. The effects of cutting fluid are lubrication and cooling. Fujiwara et al. has investigated the effect of cutting fluid in the machining of cemented carbide, and it is found that tool wear on flank face and defluxion of diamond grain can be suppressed by the lubrication effect when the depth of cut is large [66]. Yui et al. investigated the relationship among different kinds of cutting fluid, atmosphere and tool wear. As a result, the effect of cutting oil is bigger than that of water solubility fluid, and Zinc Dialkydithiophosphate (ZnDTP) has the most ability to suppress the abrasive wear and chipping. Then, wear of the tool which is used in the atmosphere of air is less than that used in the atmosphere of N_2 and Ar_2 [67]-[70].

In the machining of alumina and cordierite, by PCD tools, tool life with cutting fluid can be extended to 10 times as that without cutting fluid. It is necessary to use cutting oil in the machining of hard material [71].

Machining method

In the traditional investigations of machining hard material, lathe turning are almost used as the machining method. By the advancement of the machine tools and development of new machining method, there are lots of reports about the high precision machining of hard material. Shamoto et al. applied the elliptical vibration cutting to the machining of cemented carbide, and found that ductile mode machining can be realized with the frequency from 0.1 Hz to 20 kHz [72]-[74]. Nath et al. use the technology of ultrasonic elliptical vibration cutting (UEVC) to investigate the relationship among roughness, tool wear, cutting force and nose radius of tool [75], [76]. As a result, it is found that when the nose radius is 0.6 mm, good result can be obtained. Then, when the speed ratio is reduced, in UEVC, the cutting force and tool wear on flank face can be reduced, and the roughness can be improved. There are several researches about ball end milling of cemented carbide by using SCD, PCD and nano polycrystalline diamond tools [52], [53], [77], [78].

As introduced above, the fabrication of mold is very important in the manufacturing optical elements. However, there is still a big problem that how to suppress tool wear. The tool life is expected as long as possible to keep the ultraprecision machining for long time.

1.3 Ultraprecision micro machining of complex shape

On the other hand, to fabricate the optical elements with complex shape, it is requested to machine the complex shape on the mold material with high precision and miniaturization. There are several machining methods that used in the machining of complex shape. Then, as the machining of complex shape, the grinding and cutting are introduced as follows. Here, the cutting is divided into vibration cutting, ball end milling and sharp operation.

Grinding

Grinding process is shown in Fig. 1-4 (a). The grinding wheel, which is made of the abrasive grains, bonding material, is rotating to remove the workpiece. To compare with the cutting tool, the grinding wheel is combined with a large number of abrasive grains, so there are a lot of cutting points in the grinding process and the machining efficiency is better than cutting. In addition, the size of chips becomes small so good roughness and shape accuracy can be obtained.

The grinding can be divided into cross grinding and parallel grinding. The cross grinding is that the rotation direction of grinding wheel is perpendicular with the feed direction [79]. Only one point is used in the grinding so there is no influence on shape accuracy by the shape error of grinding wheel. However, the wear of grinding wheel becomes severe, and the setting needs to be executed with high accuracy. To compare with this, the parallel grinding is that the rotation direction of grinding wheel parallels to the feed direction [80]. The width of grinding wheel which is used in the machining

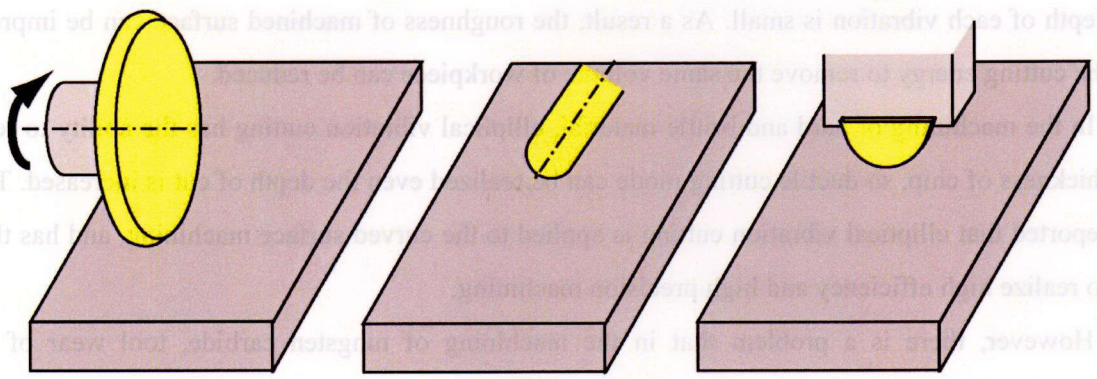

(a) Grinding (b) Ball end milling (c) Sharp operation

Fig. 1-4 Mechining method of comples shape

becomes large so that the wear of grinding wheel can be reduced. In addition, the machined surface shows good roughness. However, the shape error of grinding wheel exerts influence of shape accuracy, and it usually needs a compensation grinding. Then, the arc envelope grinding method [81], [82] is proposed in the grinding of curved surface. The grinding wheel with cross-section of circle is used in the grinding, and it is fed by three dimensions to grind the aspheric surface. It is reported that shape accuracy and roughness can be controlled under 0.1 μm by using this method.

However, grinding wheel need to be truing and dressing before grinding to make the wheel sharp. There is a problem that the best shape accuracy of grinding wheel is over 2 μm, and it needs compensation grinding after the first grinding. In addition, when the radius of grinding wheel becomes small, the grains in the grinding wheel become less, and there is a problem of the deterioration of grinded surface, which is caused by the reduction of cutting teeth.

Vibration cutting

Vibration cutting is the cutting that the tool is subjected to a forced vibration with the frequency of 50 to 30k Hz, which is proposed in 1960s [83]. The vibration cutting has the advantages as follows [84].

① Reduction of the cutting forces

② Reduction of the friction coefficient on the rake face of tool

③ Improvement of roughness

④ Reduction of affected layer

⑤ Increase of tool life

Especially, the elliptical vibration cutting is proposed at 1996 by Shamoto et al [85]-[87]. It is named because the vibration trace of tool is like ellipse. To compare the cutting speed, the vibration speed is so large that the direction of friction force on the rake face is the same as the ejection direction of chip. The chip can be ejected easily by this friction force. At this time, the shear area becomes small and the cutting force can be reduced. In addition, the thickness of chip can be reduced because the cutting depth of each vibration is small. As a result, the roughness of machined surface can be improved and the cutting energy to remove the same volume of workpiece can be reduced.

In the machining of hard and brittle material, elliptical vibration cutting has the ability to reduce the thickness of chip, so ductile cutting mode can be realized even the depth of cut is increased. Then, it is reported that elliptical vibration cutting is applied to the curved surface machining, and has the ability to realize high efficiency and high precision machining.

However, there is a problem that in the machining of tungsten carbide, tool wear of elliptical vibration is more than that of conventional machining because the contact distance between the flank face and workpiece becomes too long [73]. In addition, to realize elliptical machining, it is necessary to use the special equipment [90] which estimates cost increase.

Ball end milling

Ball end milling is shown in Fig. 1-4 (b). The tool is rotating while being fed, so it is easy to machine arbitrary shape of surface by controlling the tool posture and tool path. The ball end milling is mostly used in the cutting of curved surface. Especially in recent years, ball end mill with radius under 50 μm and shape accuracy under 500 nm has been developed [91] and micro machining can be realized by using a ball end mill with small radius. In the ball end milling, the tool is usually rotated to more than 10,000 rpm by using a high speed spindle so that the feed rate of tool can be set higher to increase the machining efficiency. The theoretical roughness of ball end milling can be shown in Eq. (1-1). Here, f is pick feed and R is the radius of tool. The roughness can be controlled by the feed rate and pick feed.

$$R_y \approx f^2/(8R) \tag{1-1}$$

However, there are several problems of the ball end milling. For example, the stiffness of tool is decreased when the radius of tool becomes small, and there is the occurrence of vibration when the tool is rotating with high speed. In the ultraprecision micro machining, the vibration will cause the deterioration of the roughness and the shape accuracy.

Sharp operation

Sharp operation is shown in Fig. 1-4 (c). The non-rotational tool is used in sharp operation. By controlling tool posture and tool path, complex shape can be machined by sharp operation. Feed rate cannot be set high because of the use of non-rotational tool. Therefore, it is pointed out that there is a problem of the efficiency of machining. However, because the non-rotational tool is used in the machining, there is no problem on the vibration of tool, tool shape can be transferred into the surface correctly, and good shape accuracy and roughness, which cannot be obtained by ball end milling [92], [93], can be obtained in the sharp operation. By the high needs of the molds of optical elements, it requests the finish machining with high precision, and the volume of workpiece which needs to be removed is not so much. Therefore, sharp operation with low efficiency and high precision attracts attentions as the method of finish machining.

1.4 Purpose of this study

It is known that the mold is so important in the manufacturing of glass lens that optical elements with high precision cannot be fabricated without the ultraprecision mold. In the machining of mold, the tool is pushed into the material to remove the unnecessary part of workpiece, and the tool shape is transferred into the created surface. As a result, the tool life acts an important part on the accuracy of optical elements.

In the machining of hard materials, there is a large problem that how to keep the tool life as long as

possible. The character of tool wear in the machining of hard material has been investigated. As the method to suppress tool wear, large numbers of investigations are focused on 『Material of tool』, 『Cutting conditions』 and 『Shape and surface treatment of tool』. As a result, new materials including nano polycrystalline diamond and various kinds of tool have been developed. By using these tools, the tool life can be lengthened substantially. However, to realize the ultraprecision machining as long as possible, the serious issue is the shortage of tool life.

This study focuses on the 『Machining method』 to suppress tool wear and to increase tool life in the machining of hard material. As introduced in Section 1.2, there are several investigations about the machining method in the machining of hard material. However, some of them just discuss the possibility of machining hard materials without the increase of tool life. By using the elliptical vibration cutting, it is reported that ductile mode machining can be realized easily. However, the tool wear becomes more severe, and there is a problem that the cost of the elliptical vibration cutting machine. Under this back ground, this study aims to create a new machining method which has the ability to suppress tool wear, and to realize ultraprecision micro machining at the same time. By using 5-axes machining center, a machining method called "cutting point swivel machining", which use an R-shape non-rotational tool, is proposed, and its effect is verified by the cutting experiment. Then, by investigating the mechanism of cutting point swivel machining and applying it to the machining of complex shape, it is confirmed that a new machining method which has the ability to suppress tool wear and to realize ultraprecision machining is created.

1.5 Organization of the dissertation

This dissertation includes 5 chapters, as shown in Fig. 1-5. In Chapter 1, the needs which are the machining of complex shape on the hard material and the problems in the machining hard material are introduced. Then, the objective of this study, which is the creation of a machining method which has the ability to suppress tool wear and to realize ultraprecision machining, is described.

In Chapter 2, the mechanism of the brittle fracture in the machining of hard material and the effect of the tool with negative rake angle is summarized. Then, a method which is called 『cutting point swivel machining』, by using the tool with special chamfer, which has the same negative rake angle along the rake face and the circle cross section, is proposed. By compensating the setting error, it is confirmed that ultraprecision machining can be realized by using cutting point swivel machining. And its effect of the tool wear suppression is verified by the cutting experiment of SiC. It is found that good surface can be obtained by suppressing the tool wear.

Next, in Chapter 3, it aims at investigating the mechanism of the cutting point swivel machining. It is found that the cutting point swivel machining has the ability to change the actual cutting direction in the machining. At this time, the moving distance of the cutting edge becomes longer than the conventional machining to remove the same volume of workpiece. So the actual cutting width can be reduced and the cutting forces can be reduced at the same time. In addition, by using the broad part of cutting edge, the tool wear can be reduced substantially. Then, the relationship between cutting force and the speed ratio is estimated and verified by the experiment. It is found that the cutting force can be reduced by increasing the speed ratio. After that, it is found that the tool wear can be suppressed by increasing the speed ratio. However, when the speed ratio is increased furthermore, the tool wear becomes more severe. As a result, it is shown that there is an appropriate speed ratio which can suppress the tool wear to the least.

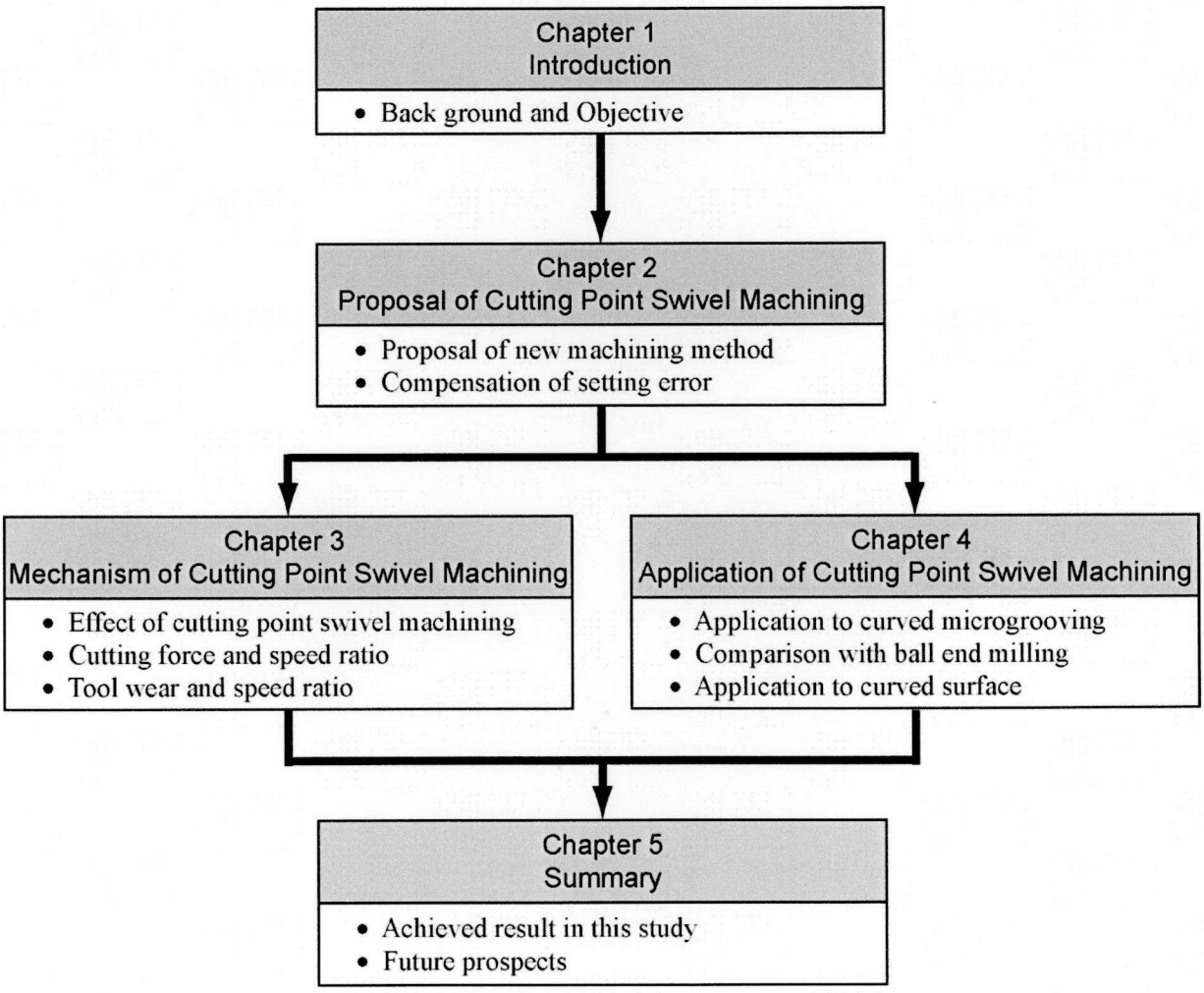

Fig. 1-5 Flow chart of this study

To machine the complex shape, the cutting point swivel machining is applied to the curved microgrooving in Chapter 4. And it is confirmed that microgroove with arbitrary curvature can be machined with good accuracy by using cutting point swivel machining. Then, to compare with ball end milling, which is mostly used in the machining of curved surface, it is found that although the efficiency of cutting point swivel machining is worse, the tool wear can be suppressed substantially, and high precision machining can be obtained for a longer time. At last, the cutting point swivel machining is applied to the machining of curved surface. It is confirmed that both good shape accuracy and roughness can be obtained by using cutting point swivel machining.

Finally, Chapter 5 summarizes this research and descripts the future prospects.

Chapter 2

PROPOSAL OF CUTTING POINT SWIVEL MACHINING

2.1 Introduction

There are mainly two problems in the machining of hard material, one is the occurrence of severe tool wear, which is introduced in Chapter 1, and the other one is the occurrence of brittle fracture which causes the deterioration of surface roughness and shape accuracy. As shown in Fig. 2-1, when hard material is machined, the generation of chip is crack type [1], so brittle fracture occurs and good surface is difficult to be obtained. It is known that brittle fracture can be suppressed by reducing the depth of cut [94]-[98]. The maximum depth of cut without brittle fracture is called the critical depth of cut. The critical depth of cut depends on the rake angle, and the rake angle with the maximum critical depth of cut is called the best rake angle. To machine with high efficiency, it is expected to use the tool with the best rake angle in the machining.

There are several investigations about the critical depth of cut and rake angle. For example, the relationship between the critical depth of cut and rake angle in the machining of silicon and germanium is investigated by using the single crystal diamond tool [99]-[102], and there is the cutting experiment of silicon and germanium by inclination plunger cutting. At the same time, there are several investigations about the machining of glass. For example, there is the cutting experiment of BK7 and low-expansion glass [103], research about the effect of rake angle to the critical depth of cut in the machining of F2 glass [104], and the critical depth of cut for glass by arc cutting machine tool [105]. In these investigations, it is found that the tool with negative rake angle has the ability to increase the critical depth of cut and to suppress brittle fracture in the machining of hard brittle fracture.

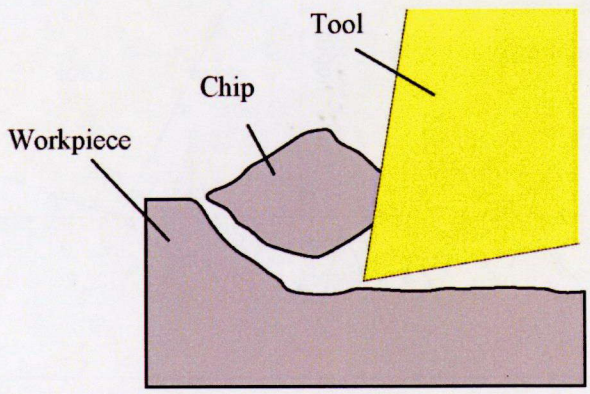

Fig. 2-1 Crack type chip

In this chapter, the mechanism of brittle fracture in the machining of hard material and the effect of using the tool with negative rake angle is introduced in Section 2.2. Then, in Section 2.3, a cutting method which is expected to have the ability of tool wear suppression is proposed, called "Cutting Point Swivel Machining". However, there is a large setting error by using the cutting point swivel machining, so a method to compensate this setting error is developed in Section 2.4. In Section 2.5, the effect of cutting point swivel machining is verified by the cutting experiment of SiC.

2.2 Effect of tool with negative rake angle and cutting tool

2.2.1 Effect of tool with negative rake angle in the machining of hard material

Figure 2-2 shows the model of brittle mode cutting. When the depth of cut is large, the crack is proceeded to break by the tensile stress which locations on the anteroinferior portion of cutting edge [106, 107]. By this reason, the proceeding route of crack depends on the stress state, and when it is nearby the surface, the inclination θ becomes gentle, and the inclination θ becomes steep when it is far from the free surface. So when the depth of cut h is small, the crack is easy to inflect to the surface, and the material can be removed by the crush and shear failure on the rake face of tool. The inclination of crack θ and crater depth d can becomes small by reducing the depth of cut h, and the generation of chips can be transitioned from the crack type to the shearing type. On the other hand, when the inclination degree θ is too large, the growing of crack stops, and there is the occurrence of residual crack [108].

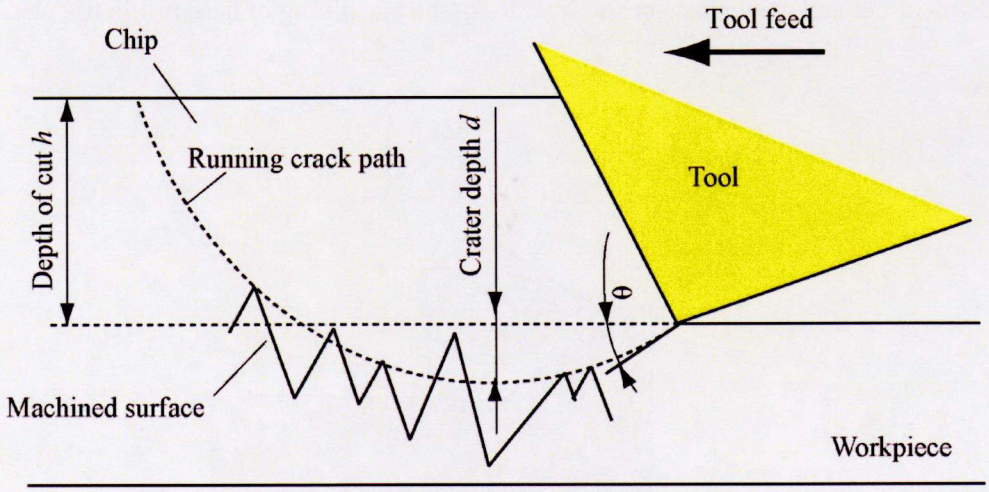

Fig. 2-2 Machining by fracture mode

The transmission of crack is also acted upon by the dormant failure of material by the preprocessing. When the depth of cut becomes large, the number of dormant failure in the stress field becomes large, and the fracture behavior becomes instability at the same time. Then, when there are a large number of dormant failures, the unstable transmission of crack which from these failures becomes more, the chip is easy to be crushed and the length of chip becomes short. By reducing the depth of cut, the dormant failure in the stress field can be lessened, and the irregular transmission of crack can be reduced.

Then, the ductile mode cutting can be obtained by the change of stress state in the cutting area when the depth of cut is reduced, as shown in Fig. 2-3. And that is, when the depth of cut is large, the tensile stress locations on the anteroinferior part of cutting edge holds a commanding position, and it is easy to cause the crack anteroinferior the cutting edge. By reducing the depth of cut, the shear stress anterosuperior the cutting edge becomes a commanding position, and there is the occurrence of shear slip. In the simulation analysis of the generation of chips in the cutting of glass [28], it is found that there is a transition of crack which occurs under cutting edge from tensile mode to shear mode, by reducing the depth of cut. When the rake angle becomes negative, the hydrostatic pressure effect becomes large by the pressure from the rake face of tool. At this time, the component of tensile stress is lowered so that the crack can be reduced and the critical depth of cut can be increased.

On the other hand, when the rake angle becomes larger in negative direction, a part of workpiece can become chip by moving to the upside along the rake face. However, most of the workpiece is moved to the lower side of tool, and by the elastic and plastic deformation, it moves to the backward of the cutting edge. If the ratio of workpiece which is moved to the lower side of cutting edge is regardless of the depth of cut, and only depends on the rake angle, the absolute amount of workpiece becomes large

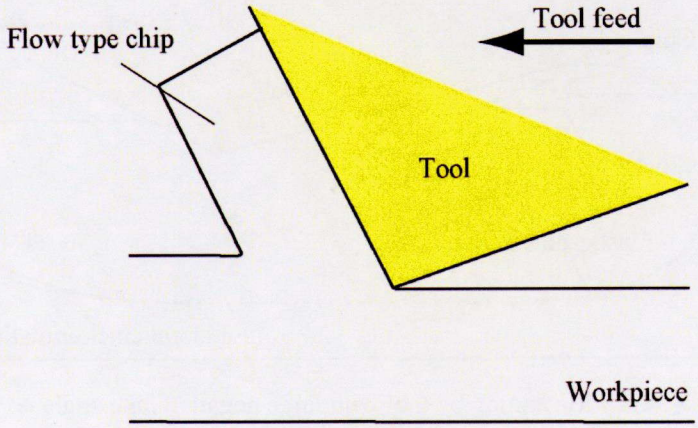

Fig.2-3 Machining by ductile mode

when the depth of cut is increased. At this time, as shown in Fig. 2-4, the workpiece which is located under the cutting edge is subject to a great hydrostatic pressure. The deformation which is only subject to hydrostatic pressure is elastic deformation [109], so the plastic deformation occurs on the surface of workpiece, and elastic deformation occurs in the deep layer of workpiece. Then, the elastic deformation is released in bursts at the backward of cutting edge, there is the occurrence of remnant stress between superficial site and deep layer. The remnant stress in the superficial site is compression stress and that in the deep layer is tensile stress. As a result, there is the occurrence of vertical tensile stress on the elastic-plastic boundary [110]. The lateral crack initiation occurs if this tensile stress is larger than the limit. The lateral crack initiation is confirmed from the pressing of brittle material [110], scratching of glass [111] and grinding of single crystal Silicon [112]. Then, in the cutting of cemented carbide by R-shape tool, it is found that microgroove cannot be obtained when the rake angle of tool is set to be over than 60 degree in negative direction [113]. So when the rake angle becomes large in negative direction, the amount of workpiece which moves to the lower side of tool is increased to cause the reduction of the critical depth of cut [101].

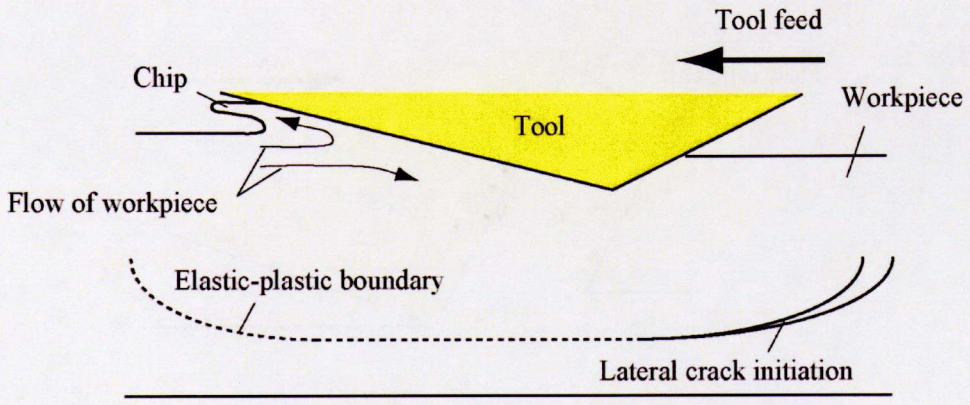

Fig. 2-4 Machining by tool with large negative rake angle

2.2.2 Cutting tool used in this study

It is reported that the tool with chamfer has the ability to suppress tool wear in the machining of steel. The tool with chamfer is the tool that has negative rake angle and obtuse tip angle, as shown in Fig. 2-5. The tool tip angle is obtuse so that the stiffness is larger than the tool without chamfer, and the chippings can be suppressed substantially. In addition, the rake angle of tool with chamfer is negative so it is able to increase the critical depth of cut in the machining of hard material.

However, as shown in Fig. 2-5 (a), the conventional tool with chamfer is made by cutting a part of tool tip, so there is a problem that the angle between the surface perpendicular to the cutting edge and chamfer at point A is different from that at point B. Therefore, the rake angle along the cutting edge is different. As a result, the form of chip is changed along the cutting edge, and there is the influence of the machined surface. In addition, the shape of tool tip is like ellipse to cause the shape error in the machining, especially in the machining with arc interpolation.

To solve these problems, the tool with special chamfer which is shown in Fig. 2-5 (b) is developed [114]. The rake face of this tool which is the angle between chamfer and vertical plane is constant along the cutting edge. By this, there is no change of rake angle and the radius of tool tip along the cutting edge. In addition, the shape of tool is circle so that there is no deterioration of the shape accuracy even in the machining by arc interpolation.

The non-rotational cutting tool (A. L. M. T. Corp.) with special chamfer used in this study is made of

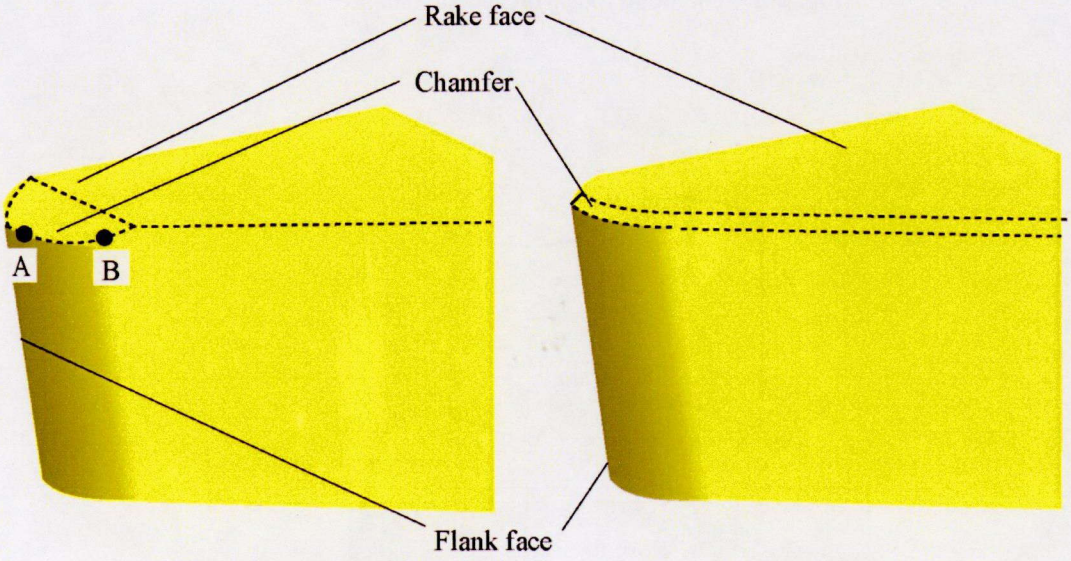

(a) Conventional type (b) Special type

Fig. 2-5 The tool with chamfer

a single crystal diamond with the radius of 0.1 mm. The tool is shown in Fig. 2-6, (a) shows the whole view and (b) shows the enlarged view of tool tip. There is special chamfer along the tool tip, and the width of chamfer is about 2 to 4 μm.

In the machining of hard material, the depth of cut is usually set to be tens to hundreds nanometers to suppress brittle fracture. The machining by using the tool with special chamfer is shown in Fig. 2-7, only chamfer is used in the machining and the rake angle is the same as the angle of chamfer. It is found that the best rake angle is -25 to -40 deg in the machining of silicon and germanium, and the best rake angle of machining cemented carbide is about -30 to -40 deg, so the angle of chamfer is set to be -30 deg.

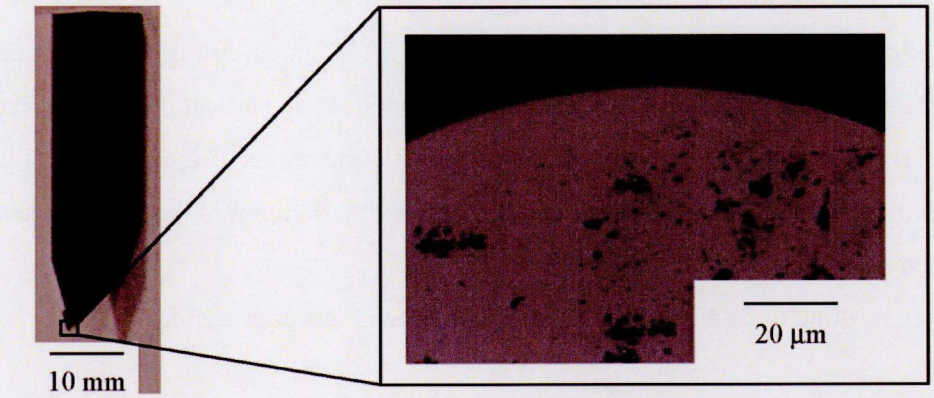

Fig. 2-6 Diamond tool with special chamfer

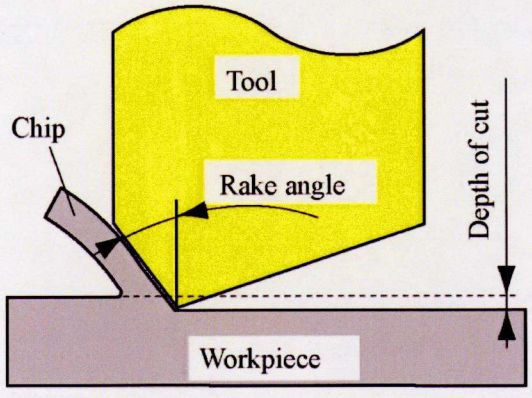

Fig. 2-7 Machining by tool with chamfer

2.3 Summary of cutting point swivel machining

2.3.1 Ultraprecision machining center

Summary of the machining center

The ultraprecision machining center used in the experiment is ROBOnano made by FUNUC [115]. The whole view is shown in Fig. 2-8. The specifications are shown in Table 2-1. This machining center is composed of 3 translation axes, X, Y and Z, and 2 rotation axes, B and C. X and Z axes are set on the base, Y and B axes are set on X axis, and C axis is set on Z axis. In the ultraprecision machining, the fluctuation from exterior influences the result of machining such as roughness and shape accuracy. So, part which can block this fluctuation is set in the machining center. Air-oil damper is set between base and floor, and the base is made by cast iron with concrete.

Translation axis

The translation axes X and Z have the same structure. As shown in Fig. 2-9, these axes are moved by a ball screw with the structure of aero-static and slide. The air screw to transmit the driving force is sustained by aero-static on both radial and thrust direction, and the air screw is made as the integral construction with servo motor. As shown in Fig. 2-9 (b), the nut surface of guide is grinded as a concave face to form the aero-static.

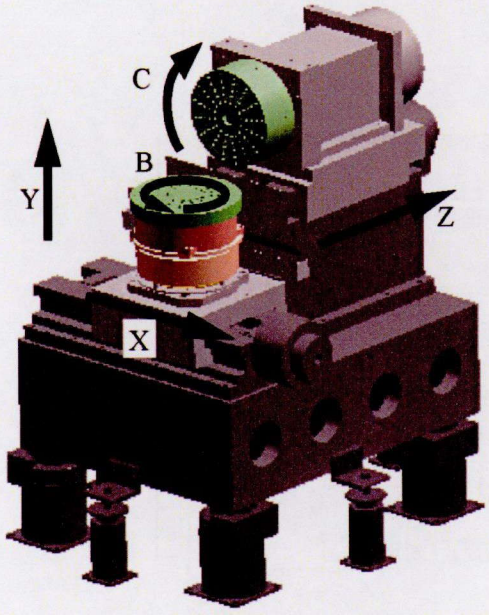

Fig. 2-8 Ultraprecision machining center

Table 2-1 Specification of ROBOnano

Stroke	X axis	200 mm
	Y axis	20 mm
	Z axis	100 mm
	B, C axes	360 deg
Command resolution	X, Y, Z axes	1 nm
	B, C axes	10^{-5} deg
Maximum command speed	X, Z axes	100 mm/min
	Y axis	20 mm/min
	B, C axes	360 deg/min
	Synthesis	720 min^{-1}

Then, the structure of Y axis is constructed by translation axis and rotation axis, as shown in Fig. 2-10. The rotation is transformed to vertical move by aero-static screw.

Rotation axis

The rotation axes B and C are constructed with the same structure. As shown in Fig. 2-11, the aero-static bearing is used in both radial and thrust direction. The transmission of driving force is decelerated by the worm gear which is treated by lubrication film.

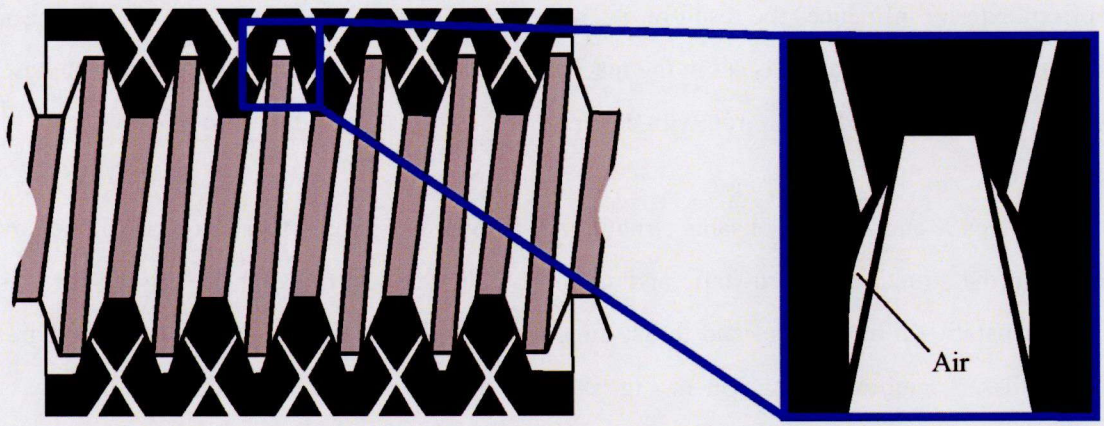

(a) Whole view (b) Enlarged view

Fig. 2-9 Air screw

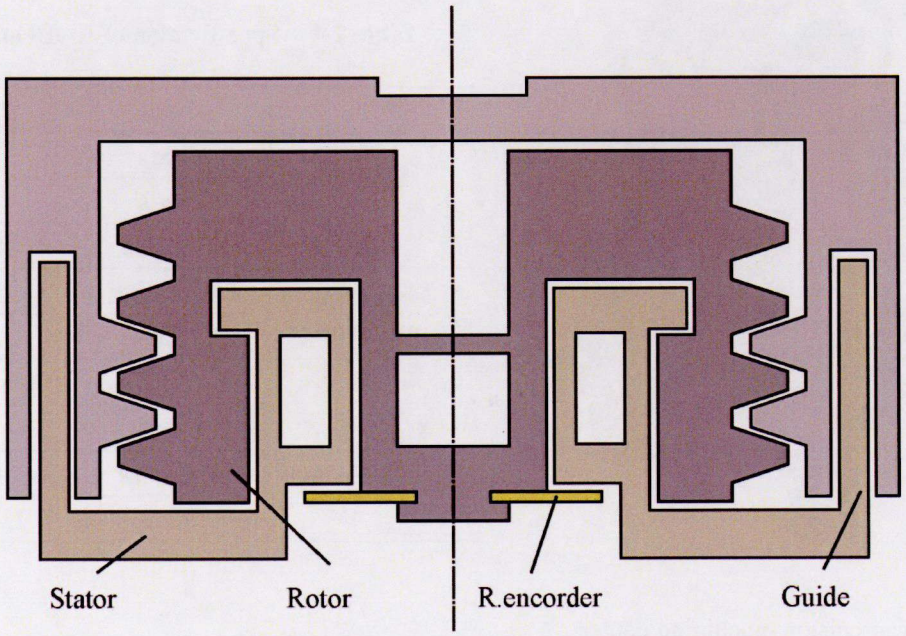

Fig. 2-10 Structure of Y axis movement

Spindle

The target shape in the ultraprecision micro machining is very small, so the tool with small radius is used in the machining. However, there is a problem that the cutting edge of small-diameter tool is nearby the rotational axis. Rotation radius of the tool is so small that the cutting speed becomes low. To get the enough cutting speed the spindle needs to be rotated with high revolution. An air turbine spindle is used in the experiment, as shown in Fig. 2-12. Aero-static is used as the bearing so there is no friction when the spindle is rotating. Compressed air is used to rotate the spindle, and the rotation speed is proportional to the pressure of compressed air.

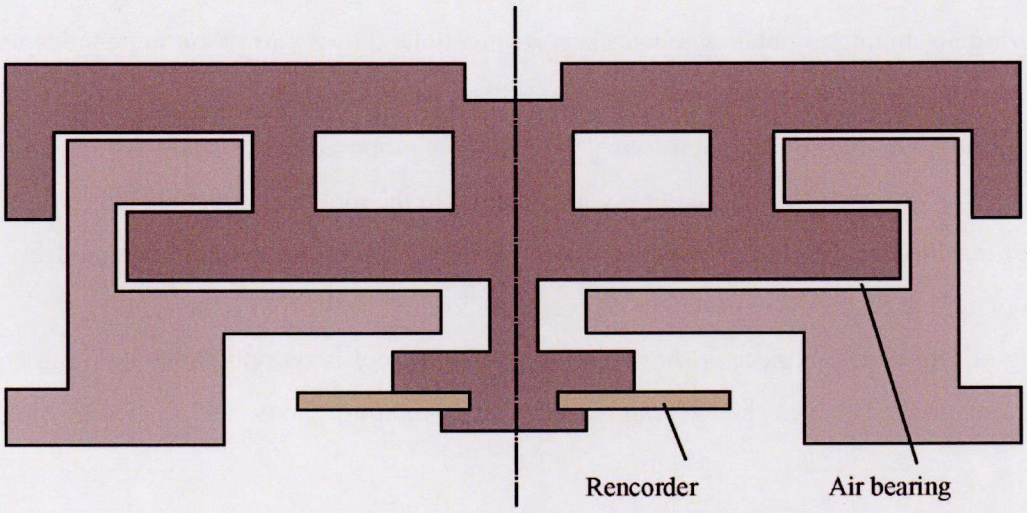

Fig. 2-11 Structure of B axis movement

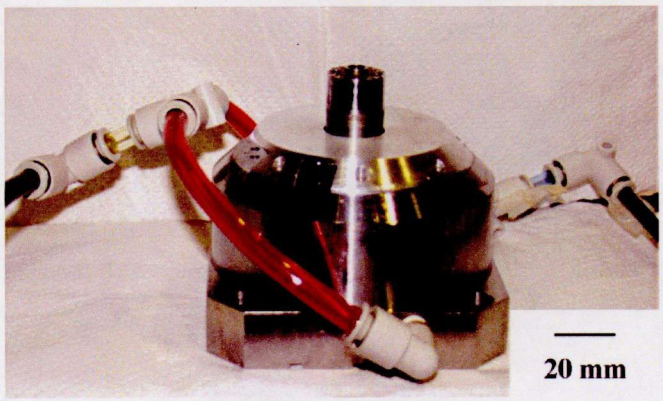

Fig. 2-12 Air turbin spindle

Environment

In the ultraprecision machining, the environment is important because there is the influence of the roughness and shape accuracy by the temperature changes and fluctuation. The base which is made by cast iron with internal concrete and fluctuation blocking device with air and oil attenuation are used. As a result, the fluctuation from exterior and machining center can be reduced to nano meter level. Then, the temperature of air which is supplied into the machining center is controlled as 23 ± 0.01℃ and the room temperature is managed with 23 ± 1℃.

2.3.2 Proposal of cutting point swivel machining

As shown in Fig. 2-13, in the conventional machining by R-shape tool, the posture of tool is not changed during machining to obtain good surface. At this time, only a part of cutting edge is used in the machining, and there is a problem that tool wear is centered at this part.

To solve this problem, the cutting point swivel machining is proposed in this study. As shown in Fig. 2-14, the tool is always swiveled in the plane perpendicular to the tool feed direction. By using cutting point swivel machining, the cutting point is always changing along the cutting edge, and by using abroad part of cutting edge, it is expected to suppress and to average the tool wear.

The setting of tool and workpiece is shown in Fig. 2-15, the tool is set on C table by a jig, and the workpiece is set on the B table. The tool can be swiveled by rotating C axis, and it is fed by moving Z axis.

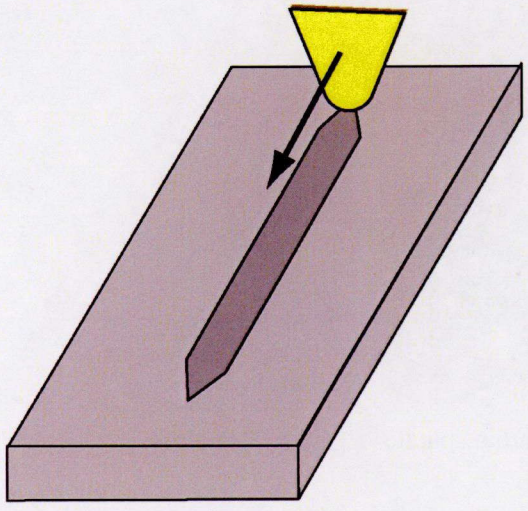

Fig. 2-13 Conventional machining

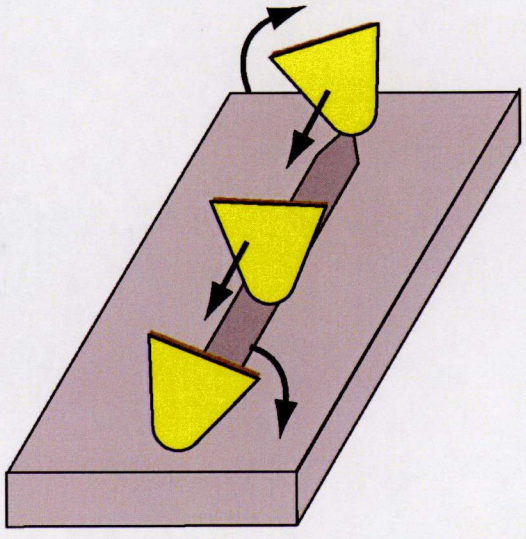

Fig. 2-14 Cutting point swivel machining

The system of cutting point swivel machining consists of the following.

1. The rotatable range without tool interference is calculated by the parameter including the tip angle of tool, radius of tool and cutting depth.
2. The distance of cutting is calculated, and it is divided into small segments by the rotatable range and cutting shape.
3. The system determines the appropriate tool posture of each segment.

In the machining by the tool with conventional chamfer, because the shape of tool is like ellipse, there is the occurrence of shape error when the tool is swiveled. However, because the shape of the tool with special chamfer is like circle, there is no error when the tool is swiveled.

2.4 Setting error and compensation

2.4.1 Setting error

The NC data which controls the tool posture and tool path is made in the condition that the tool center point is not changed by the rotation of C table, so it is necessary to set the tool center point the same as the center of C table correctly [116].

When the tool center point is not at the same position with center of C table, the setting is done by the principle that the trajectory of tool center point is the circle around center of C table by rotating C table. A microscope is used in the setting of tool center point and the center of C table. The microscope

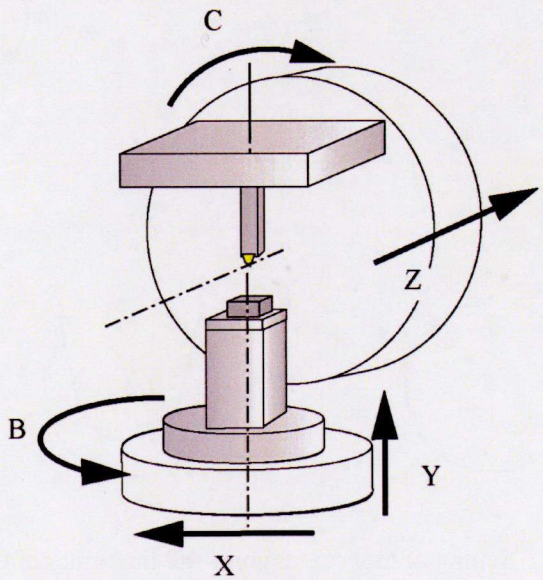

Fig. 2-15 Setting of the tool and workpiece

is set to observe the tool from front. As shown in Fig. 2-16 (a), the tool is observed in the monitor, and as shown in (b) to (d), the trajectory circle is written by rotating C table step by step. At last, as shown in (e), the tool center point is moved to be the same as the center of trajectory circle. The position of tool is adjusted by the micrometer head which is set on the jig to hold the tool. By repeating this work, the tool center point can converge to the center of C table.

However, hand working is used to adjust the position of tool center point with the use of micrometer head and microscope by this method, so it is difficult to realize the microscopic displacement, and it costs a lot of time to adjust. In addition, it is difficult to understand the tool center point on the monitor. As a result, it is impossible to set tool center point the same as the center of C table correctly.

As shown in Fig. 2-17, the position of the tool center point P is (X_0,Y_0), when C table is rotated to α deg, there is the displacement (δ_x, δ_y) of tool center point P, and the displacement can be shown in Eq. (2-1).

$$\begin{cases} \delta_x = X_0 \cos\alpha - Y_0 \sin\alpha - X_0 \\ \delta_y = X_0 \sin\alpha + Y_0 \cos\alpha - Y_0 \end{cases} \tag{2-1}$$

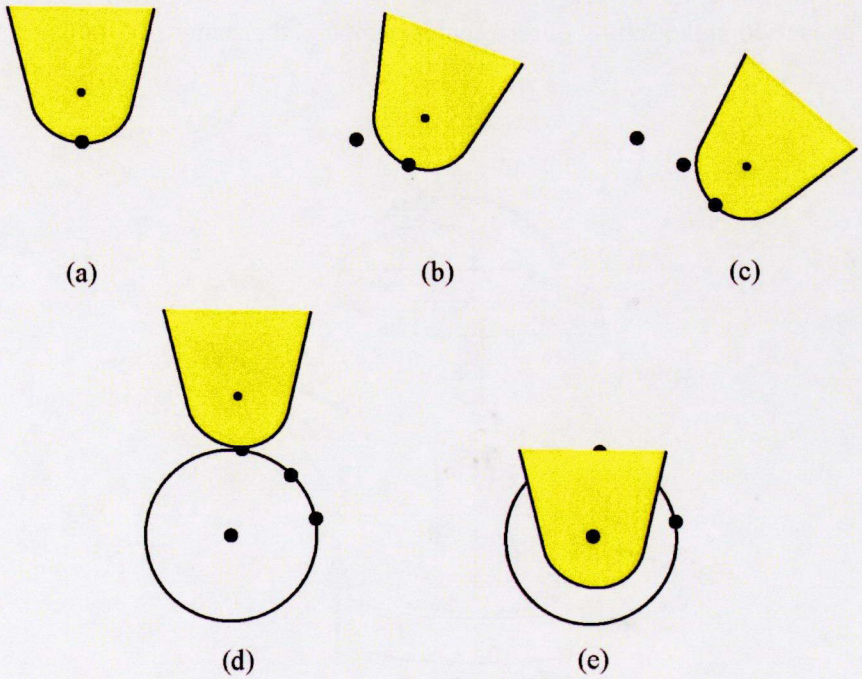

Fig. 2-16 Setting of tool center point and the center of C table

2.4.2 Compensation of setting error

A try cutting is conducted to calculate the position of tool center point (X_0, Y_0) by the depth of machined microgroove. As shown in Fig. 2-18, the difference D_1 in the depth of two microgrooves with the same depth of cut can been shown in Eq. (2-2). One is machined without the rotation of C table, and the other one is machined by rotating C table to α_1 degree. By the same method, there is another microgrooving by rotating C table to α_2 degree so that two equations with two unknowns (X_0, Y_0) can be set up by taking difference in the depths of machined microgrooves, as shown in Eq. (2-3). Then, the position of the tool center point can be known by solving these equations.

$$D_1 = Y_0 - X_0 \sin\alpha_1 - Y_0 \cos\alpha_1 \tag{2-2}$$

$$\begin{cases} X_0 = \dfrac{D_1(1-\cos\alpha_2)-D_2(1-\cos\alpha_1)}{(1-\cos\alpha_1)\sin\alpha_2-(1-\cos\alpha_2)\sin\alpha_1} \\ Y_0 = \dfrac{D_1\sin\alpha_2-D_2\sin\alpha_1}{(1-\cos\alpha_1)\sin\alpha_2-(1-\cos\alpha_2)\sin\alpha_1} \end{cases} \tag{2-3}$$

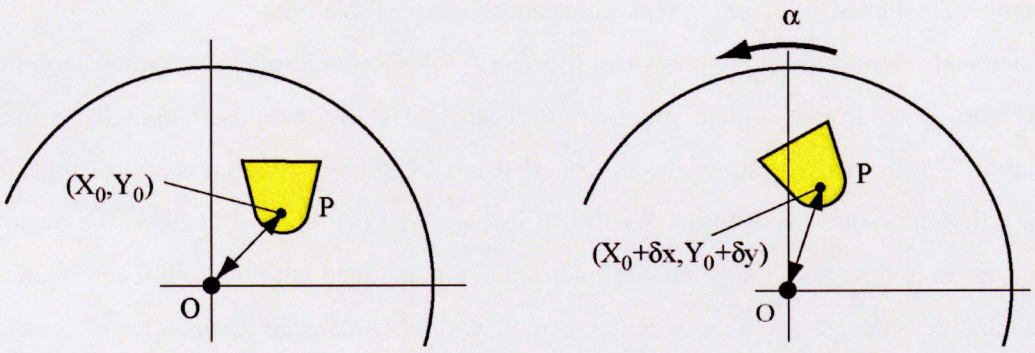

(a) Setting error (b) Error by rotation of C table

Fig. 2-17 Error in the setting of C table

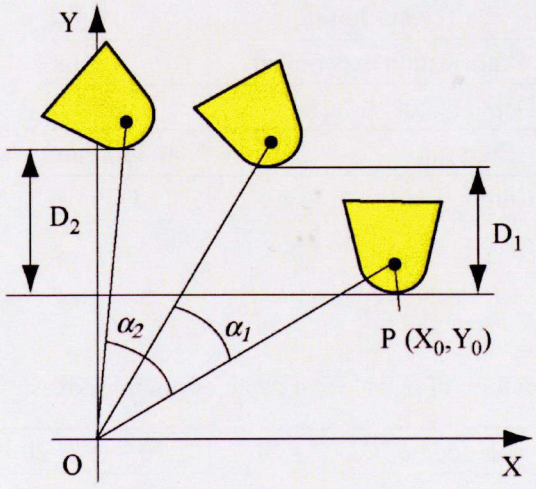

Fig. 2-18 Microgrooving for compensation setting error

In response to the position of the tool center point (X_0, Y_0), NC data, written under the condition that the position of the tool center points is coaxial of the center of C table, should be compensated by using the following relationship (2-4).

$$\begin{cases} X \rightarrow X - (X_0 \cos C + Y_0 \sin C) \\ Y \rightarrow Y - (X_0 \sin C + Y_0 \cos C + Y_0) \end{cases} \quad (2\text{-}4)$$

2.4.3 Verification experiment

There is a verification experiment of the compensation of setting error. The workpiece is made by aluminum alloy A5056, and the cutting conditions are shown in Table 2-2. The depth of cut is set to be 1 μm and feed rate is 40 mm/min. Three microgrooves are machined with C table rotating to 0, 10 and 20 degree. The depth of machined microgrooves with each C table rotation is shown in Table 2-3. By the rotation of C table and depth of machined microgroove, the coordinate of tool center point can be calculated as (-5.348, 53.430) μm. By this calculated position of tool center point, a verification experiment is conducted. The cutting conditions are shown in Table 2-2.

The machined microgrooves are shown in Fig. 2-19. (a) show microgroove without compensation, and (b) show microgroove with compensation. Then, (1) show the observation by a microscope (Keyence VF-7500), and (2) show the measured result by surface roughness measuring instrument (Kosaka Laboratory Ltd. SE 3500K). As shown in Fig. 2-19 (a), because there is the occurrence of displacement in X direction, the machined microgroove is inclined with the tool feed direction. Then, the depth of side is deeper than that of center, and the width of side is larger than that of center. The

Table 2-2 Cutting conditions

Workpiece		A5056
Total depth	Try machining	10 μm
	Varification experiment	5 μm
Depth of cut		1 μm
Feed rate		40 mm/min
Cutting fluid		Oil mist

Table 2-3 Rotation of C table and depth of microgrooves

Rotation of C table (degree)	0	10	20
Depth of microgroove (μm)	13.337	13.220	14.730

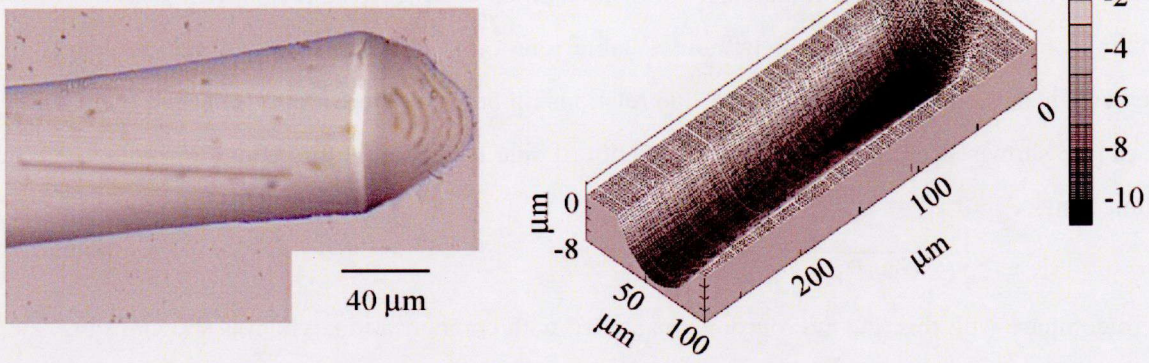

(1) (2)

(a) Without compensation

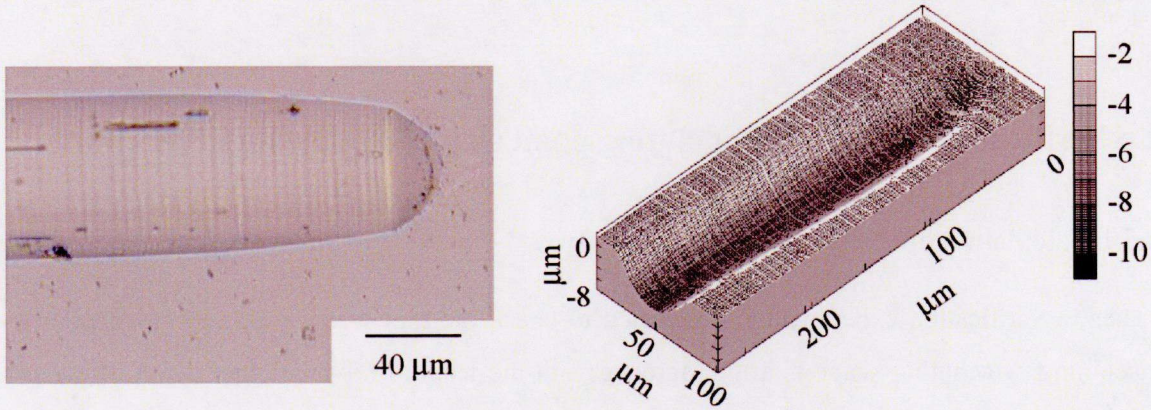

(1) (2)

(b) With compensation

Fig. 2-19 Machined microgrooves

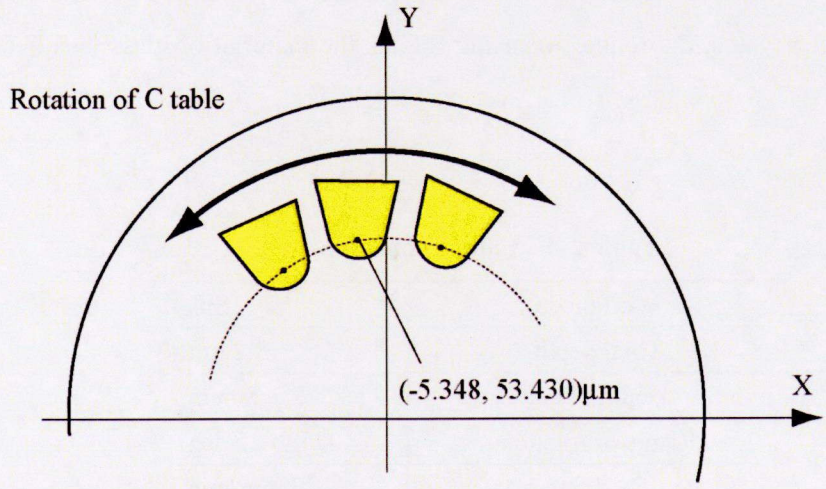

Fig. 2-20 Error induced by the rotation of C table

displacement of tool when the position of tool center point is (-5.348, 53.430) μm is shown in Fig. 2-20. At this time, the Y coordinate becomes small when C table is rotated, and the depth of machined microgroove is deeper than that without C table rotation so that the depth of side is deeper that of center. Then, the radius of tool tip is R, the relationship between the width of microgroove b and depth d can be shown in Eq. (2-5). Because the depth of side is deeper, so the width becomes larger at the same time.

$$b = 2\sqrt{(2R - d)d} \tag{2-5}$$

To compare with this, the microgroove machined with compensation, which is shown in Fig. 2-19 (b), is paralleled with tool feed direction and the depth is the same along the microgroove. It is confirmed that the proposed method has the ability to compensate the setting error and to realize high precision machining.

2.5 Verification experiment of cutting point swivel machining

2.5.1 Calculation of tool rotatable range

Then, a verification experiment is conducted to check the tool wear by using cutting point swivel machining. Machining shape is a microgroove with the length of 14 mm, and depth of 3.2 μm. the cutting conditions are listed in Table 2-4, the depth of cut is set to be 80 nm, and the tool is moved for 40 times to machine a microgroove.

The workpiece used in the experiment is SiC (Nippon Steel Materials Co. Ltd. C101R). Its physicality is shown in Table 2-5. As shown in this table, this material has the property of heat resistance, hardness and low coefficient of thermal expansion, which are necessary as the property of molds. So in recent years, the request of using SiC as the material of glass lens becomes higher and higher.

Table 2-4 Cutting conditions

Workpiece	SiC
Total depth	3.2 μm
Depth of cut	80 nm
Range of rotation	-25 to 25 deg
Feed rate	3 mm/min
Cutting fluid	Oil mist

At first, the tool rotatable range without tool interference is calculated. As shown in Fig. 2-21, the tip angle of tool is β, the radius of tool tip is R, the depth of microgroove is d, and tool rotatable range C can be shown in Eq. (2-6).

$$|C| < \beta/2 - \cos^{-1}((R-d)/d) \tag{2-6}$$

In this study, the tip angle of tool is 90 degree, the radius of tool is 0.1 mm and the depth of microgroove is 3.2 μm. The rotatable range of C table can be calculated as 30.466 deg. in this experiment, the rotation range of C table is set to be -25 to 25 deg. To consider the length of microgroove and tool rotation range, the microgroove is divided into small segments with the length of 7 nm, and the tool rotation degree is 0.00005 deg per each segment.

2.5.2 Compensation of feed rate

It is necessary to compensate the feed rate by using cutting point swivel machining. In the conventional machining, only two translation axes are used in the machining. However, by using the

Table 2-5 Physicality of SiC

Machanical properties	Density	3.16 g/cm^3
	Young's modulus	430 GPa
	Hardness HV	2100
	Poisson's ratio	0.16
Thermal properties	Coefficient of linear thermal expansion(α)	2.3×10^{-6}/K*
	Thermal conductivity	128 W/m·K
	Specific heat	0.63 J/g·K

* 23 ℃

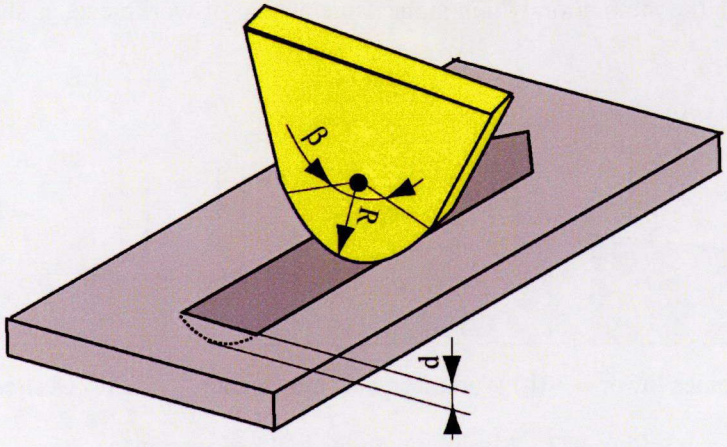

Fig. 2-21 Range without tool interference

cutting point swivel machining, it is necessary to use two translation axes and one rotation axes. In addition, simultaneous control of 4 axes is used when the setting error is compensated. To get the same efficiency with the conventional machining, it is necessary to compensate the feed rate. In the conventional machining, the tool is fed by moving Z direction, and the feed rate equals to the speed in Z direction. To realize the same machining efficiency, the feed rate in Z direction is set to be the same.

Then, when the tool is moved from nth machining point to n+1th machining point, the variation of (X, Y, Z, C) axes is (x, y, z, c), so the length between these two points l can be shown in Eq. (2-7). Then, the command feed rate F can be calculated by the feed rate in Z direction as Eq. (2-8). Here, the unit of each translation axis is mm, and that of each rotation axes is deg.

$$\mathrm{l} = \sqrt{x^2 + y^2 + z^2 + c^2} \tag{2-7}$$

$$\mathrm{F} = F_z \times l/z \tag{2-8}$$

2.5.3 Inclination of workpiece

In the machining of hard material, because of the hardness of workpiece, it is impossible to make the plane as the pre-stage machining. So in the machining, the surface of workpiece is not horizontal but inclined.

In the machining, tool path is made to feed the tool horizontal. Figure 2-22 shows the machining with inclined workpiece. (a) shows the machining that the surface of workpiece becomes lower by feeding the tool, and (b) shows the surface of workpiece becomes higher. As shown in these figures, if the surface of workpiece becomes lower, the tool will separate from the workpiece and it is impossible to realize the machining. On the other hand, if the surface of workpiece becomes higher, there is the threat of that the depth of cut becomes several tens micrometer by the inclination of workpiece to cause the broken of tool and workpiece. So it is expected to make clear the inclination of workpiece, and feed the tool with the inclination which is the same as that of workpiece, as shown in Fig. 2-22 (c)

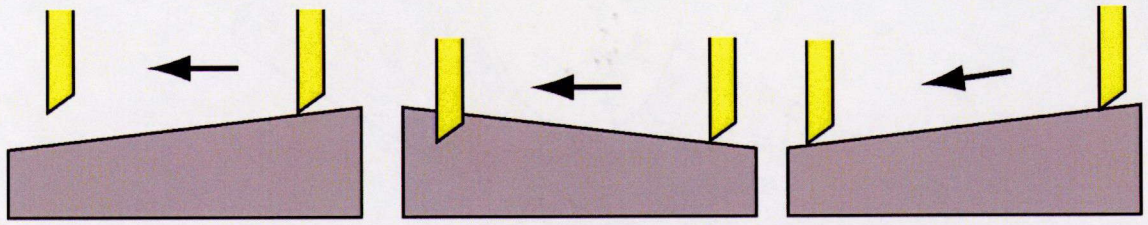

(a) Workpiece becomes lower (b) Workpiece becomes higher (c) Desired machining

Fig. 2-22 Machining on the inclined workpiece

Figure 2-23 shows the method to calculate the inclination of workpiece. As shown in this figure, several points are selected in the tool feed direction, and the origin setting of Y axis is done at these points to evaluate the coordinate in Y direction. Then, by the coordinate (z, y) of this point group, the inclination of workpiece can be calculated by using least-square method.

2.5.4 Tool wear

The tool which is used in the conventional machining and observed by a microscope is shown in Fig. 2-24. (a) shows the tool before machining and (b) shows the tool which has machined 4 microgrooves. The machining time is 15 hours and 36 minutes, and the cutting distance is 2,240 mm. As shown in Fig 2-24 (b), severe tool wear occurs on the rake face of the tool. The tool wear only occurs in the center of tool tip and there is scarcely any tool wear on the side of tool tip. It can be known that chippings occur on the tool tip, and by the progress of these chippings, there is about 8 μm broken part on the rake face of the tool. By using this broken tool, there is the threat of the deterioration of the roughness and shape accuracy.

Then the tool which is used in the cutting point swivel machining is shown in Fig. 2-25. (a) shows the tool before machining and (b) shows the tool after 8 microgrooves are machined. The machining

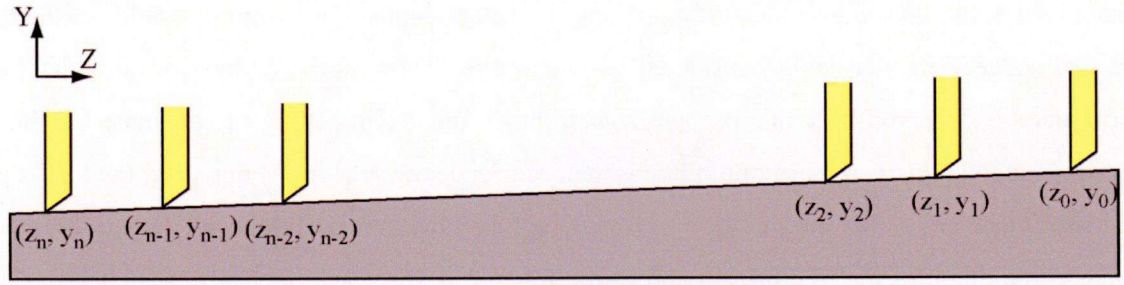

Fig. 2-23 Method to calculate the inclination of workpiece

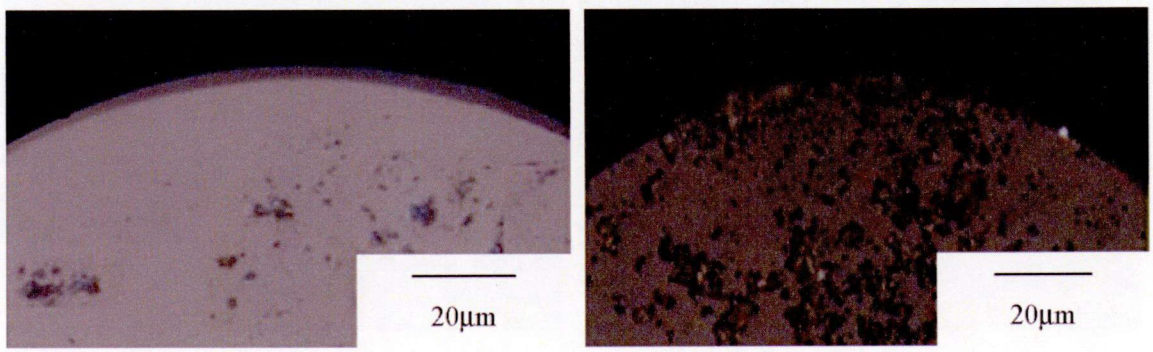

(a) Before machining (b) After machining

Fig. 2-24 Tool used in conventional machining

time is 31 hours and 12 minutes, and the cutting distance is 4,480 mm. As shown in Fig. 2-25 (b), there is uniform tool wear on the part of chamfer, and the width of chamfer becomes a little narrow, but there is no broken part on the cutting edge, and the shape of tool is still like circle. There is no problem of the shape accuracy in the machining with this tool. To compare with the conventional machining, the cutting distance is double. However, tool wear can be suppressed substantially.

2.5.5 Machined surface

Figure 2-26 shows the machined microgrooves by conventional machining. (a-1) and (b-1) show the SEM photos of the 1st and 4th microgroove, (a-2) and (b-2) show the measured result by surface roughness measuring instrument, respectively. The poreless processing of the workpiece is not executed, so large numbers of pores can be observed on the surface of workpiece and microgroove. Because the cutting mark can be observed on the surface of microgroove, it can be known that it is ductile mode machining. Except the pore in the workpiece, a lot of micropit can be observed on the surface of microgroove. The workpiece is sintered by SiC grains, there are a large number of SiC grains and Si grains in the workpiece. If the cutting force is larger than the combining force between these grains, there is the occurrence of grain drops on the machined surface, and it causes a lot of nanometer level micropit on the surface. Then, the actual depth of microgroove is lower than that of desired value. The reason is considered as the setting error of the Y axis origin. The tool and workpiece is observed by a microscope from front. In the origin setting of soft material, the tool is approximated to the workpiece until there is the occurrence of the chip. At this time, the tool is cut into the workpiece about 300 nm to 400 nm. However, when the tool is cut into the material for 400 nm, there is the threat of the tool broken and brittle fracture in the machining of hard material. So in the origin setting of Y axis, the shadow of tool is observed, and the origin of Y axis is set to be the

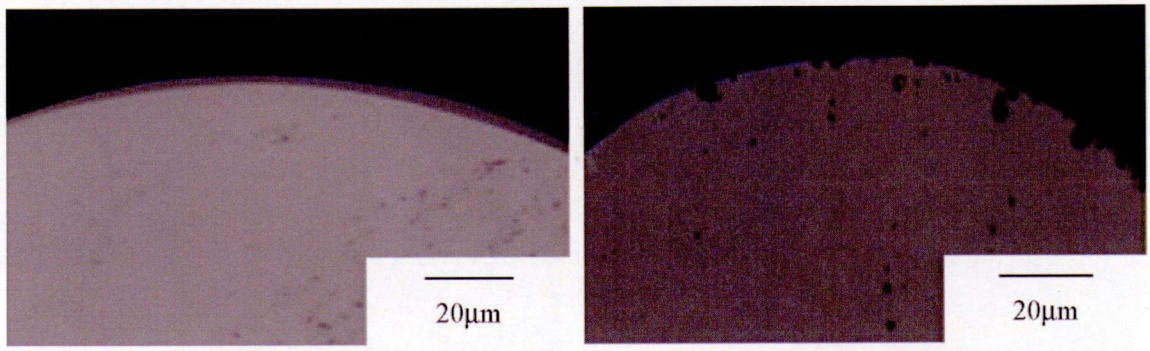

(a) Before machining (b) After machining

Fig. 2-25 Tool used in cutting point swivel machining

coordinate that the cutting edge of tool overlaps with that of the shadow. At this time, there is the aperture between the workpiece and tool so that the depth of machined microgroove becomes shallow.

Then, the transition of the roughness is shown in Fig. 2-27. The roughness R_z of the 1st microgroove is 97 nm, and that of the 4th microgroove is 207 nm. The 1st microgroove shows the good roughness. To compare with this, the roughness of 4th microgroove becomes worse. Then, as shown in Fig. 2-26, the cross-section of the 1st microgroove is like circle, and in the machining of 4th microgroove, there is the shape error on the cross-section of the microgroove. The reason is considered that chippings occur on the cutting edge, and it is transferred in to the surface to cause the deterioration of both shape accuracy and roughness.

To compare with this, Fig. 2-28 shows the machined microgroove by cutting point swivel machining. (a-1) and (b-1) show the SEM photos of the 1st and 8th microgroove, (a-2) and (b-2) show the measured result, respectively. The transition of the roughness in the tool feed direction is shown in Fig. 2-27. At first, the roughness of the 1st microgroove machined by conventional machining and cutting point swivel machining is almost the same. The tool posture is changed in the machining by using cutting point swivel machining. However, the cutting point swivel machining has the ability to realize

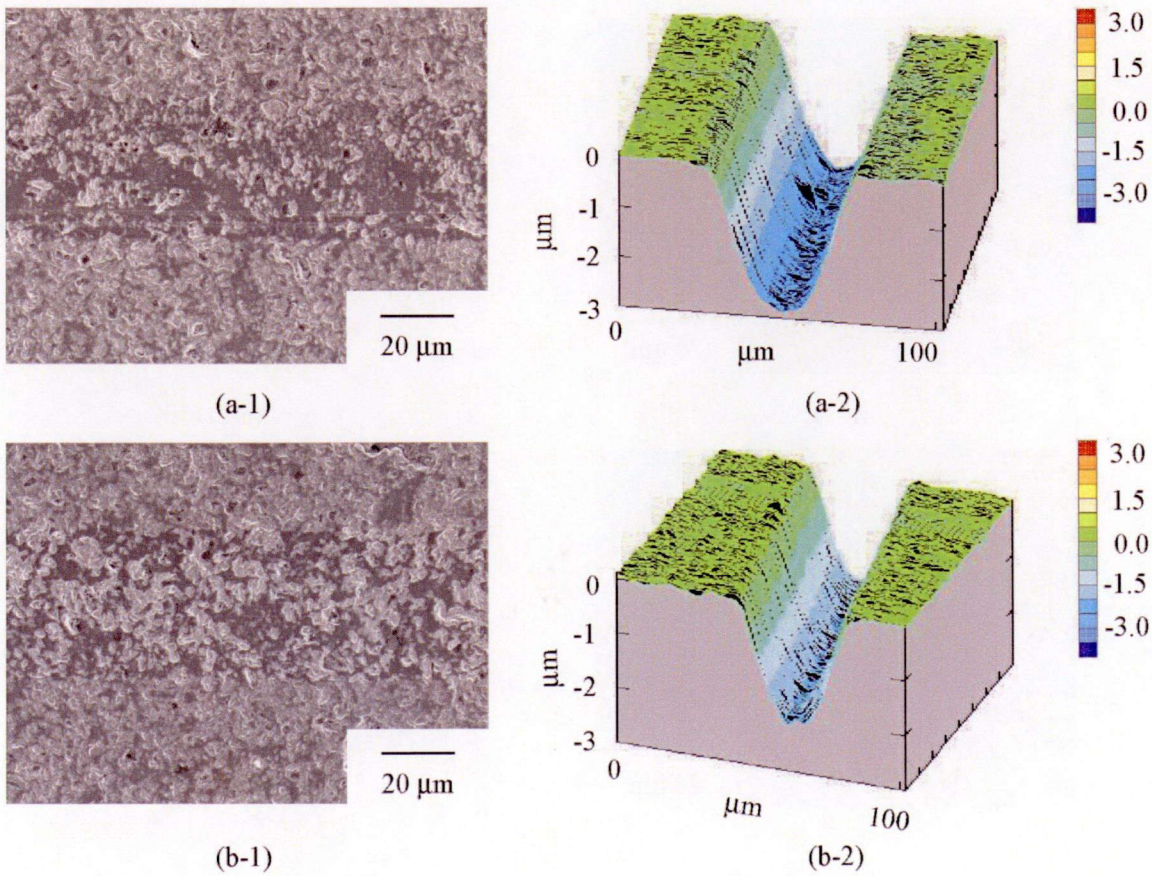

Fig. 2-26 Microgrooves machined by conventional machining method

the same roughness as conventional machining. Then, the roughness of 8th microgroove machined by cutting point swivel machining is 127 nm, and it is known that good roughness can be obtained until 8th microgroove. In addition, the cross-section of both 1st and 8th microgroove is like circle because of the suppression of tool wear.

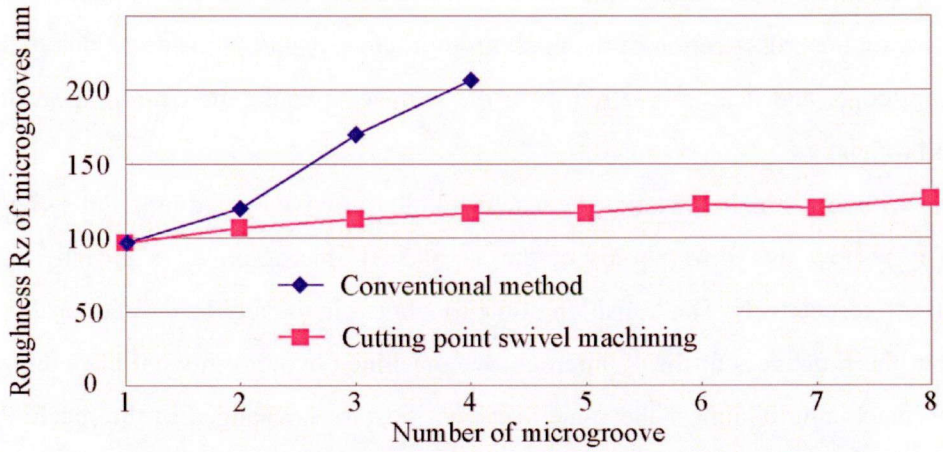

Fig. 2-27 Relationship between roughness Rz and microgrooves

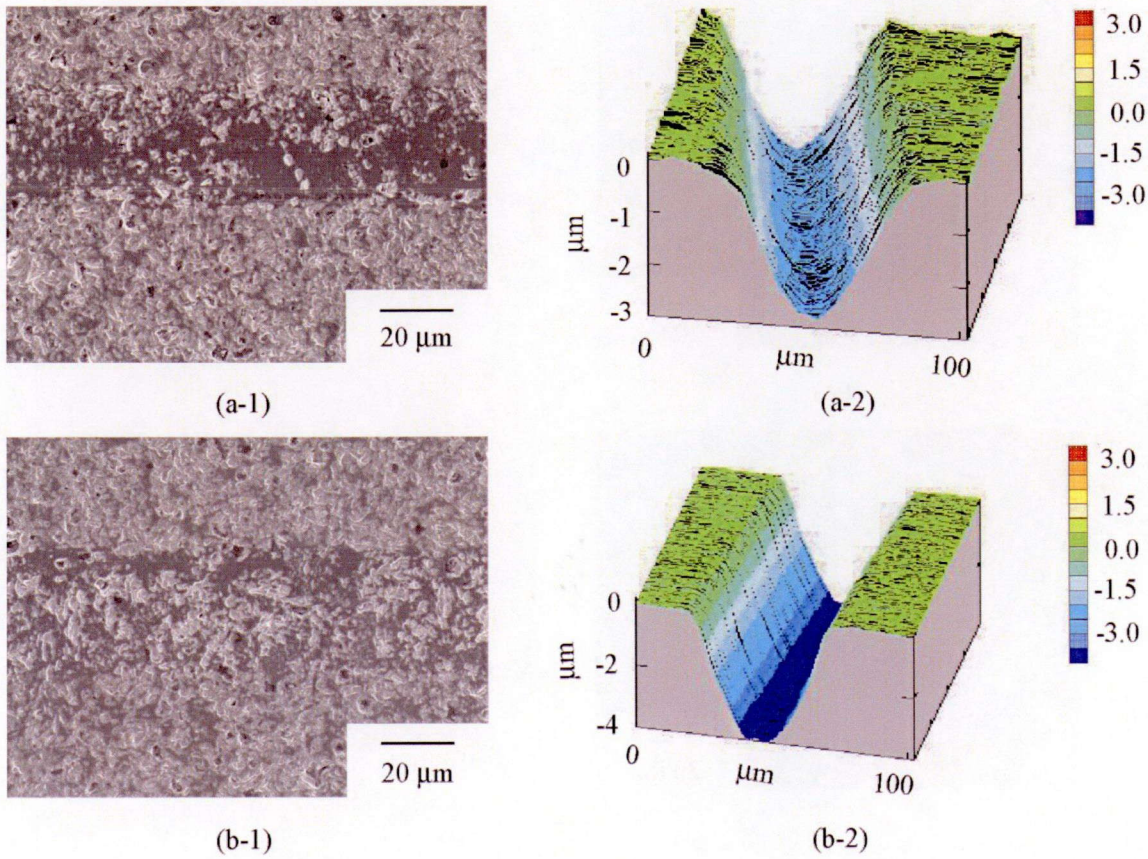

Fig. 2-28 Microgrooves machined by cutting point swivel machining

Figure 2-27 shows the transition of the machined microgroove by conventional machining and cutting point swivel machining. It is known that the deterioration of roughness by conventional machining is rapid. To compare with this, the deterioration of roughness by cutting point swivel machining is gentle, and good roughness can be obtained until 8^{th} microgroove. From the above, it is confirmed that the cutting point swivel machining has the ability to suppress tool wear and to realize high precision machining.

2.6 Summary

In this chapter, the machining of hard brittle material is introduced. In the Section 2.1 and 2.2, the mechanism of brittle fracture and the effect of the tool with negative rake angle are summarized. Then, the tool with special chamfer which has the same negative rake angle along the cutting edge and the circle cross section on the rake face is introduced. By using these past investigations, the rake angle of the cutting tool is decided to be -30 deg.

Then, From Section 2.3, a new machining method called cutting point swivel machining is proposed. As the result of verification experiment, the conclusion can be summarized as follows.

1) By using the tool with special chamfer, the cutting point swivel machining, that the tool is swiveled in the plane perpendicular to the tool feed direction, is proposed. To compare with other machining method, the cutting point swivel machining can be realized easily by using the rotation axis, and it is expected to suppress and average the tool wear.
2) In the cutting point swivel machining, there is a problem of the setting error between the tool center point and the center of C axis. Then, a try cutting is proposed to calculate the coordinate of tool center point. By using this calculated coordinate, the setting error can be compensated by modifying the NC data, which controls the tool path and tool posture. By the result of the verification experiment, it is confirmed that the proposed method has the ability to compensate the setting error and to realize ultraprecision machining.
3) By the verification experiment of SiC, it is confirmed that to compare with the conventional machining, the cutting point swivel machining can extend tool life to more than two times. In addition, good roughness and shape accuracy can be obtained by using cutting point swivel machining, because of the suppression of tool wear, and the machining with high precision can be continued for long time.

As summarized above, it is confirmed that the cutting point swivel machining, which is proposed in this chapter, has the ability to suppress tool wear in the machining of hard material, and to realize ultraprecision machining for a long time.

Chapter 3
MECHANISM OF CUTTING POINT SWIVEL MACHINING

3.1 Introduction

The mechanism of machining process is very important. For example, by understanding the mechanism of cutting process, it can make predictions including the force and energy which is necessary in the cutting, the deformation and vibration of machine tool, the accuracy of machined surface and tool wear, and so on. So the mechanism of cutting process is investigated from 1930s. From that, there are a large number of investigations to research the mechanism of two dimensions cutting, three dimensions cutting, rotary machining, and elliptical vibration cutting and so on. In the Chapter 2, a machining method, called cutting point swivel machining, which has the ability to suppress tool wear is proposed. By compensating the various setting errors, it is confirmed that ultraprecision machining can be realized by using cutting point swivel machining. As a new machining method, it is necessary to investigate the mechanism of cutting point swivel machining.

In this chapter, the effect of cutting point swivel machining is investigated in Section 3.2. And then, the relationship between the cutting force and the speed ratio, which is the ratio of the circumferential velocity to the feed rate, is investigated in Section 3.4. At last, the relationship between the speed ratio and tool wear is researched in Section 3.5.

3.2 Change of actual cutting direction

At first, the effect of cutting point swivel machining is investigated. The SEM photos of machined microgrooves are shown in Fig. 3-1. Figure (a) shows the microgroove machined by conventional machining. Figure (b) and (c) show the microgrooves machined by cutting point swivel machining. The tool rotation speed of cutting point swivel machining is 16 and 286.5 deg/min, respectively. Cutting conditions are shown in Table 3-1, the depth of cut is set to be 80 nm. The part between white dashed lines is the surface of microgroove. It can be known that all microgrooves are machined in ductile mode because the cutting mark can be observed on the surface of microgrooves.

In the microgroove machined by conventional machining, it is confirmed that cutting mark is paralleled with the feed direction. To compare with this, by using the cutting point swivel machining, when the tool rotation speed is 16 deg/min, the cutting marks are almost paralleled with the feed

direction, which is the same as the conventional machining. However, when the tool rotation speed is increased to 286.5 deg/min, the cutting mark is inclined with feed direction, and the angle between cutting mark and feed direction is about 26 deg. The reason is considered as follows. As shown in Fig. 3-2, the tool is fed, while being rotated by using the cutting point swivel machining, so the workpiece is subject to the force F_z in the tool feed direction and the force F_x in the tool rotation direction at the same time. At this time, the actual cutting direction is inclined. When the tool rotation speed is 16 deg/min, the circumferential velocity is so slow to compare with the feed rate that the cutting mark is almost paralleled with the feed direction.

Then, as shown in Eq. (3-1), the ratio r_v (Named as speed ratio) of the circumferential velocity V_x to the feed rate V_z is calculated by the tool rotation speed and the radius of tool tip. In this experiment, the radius of tool is 0.1 mm, and the feed rate V_z is 1 mm/min. When tool rotation speed is set to be 16 and 286.5 deg/min, the speed ratio r_v can be calculated as 0.028 and 0.5, respectively. By the calculated speed ratio r_v, as shown in Eq. (3-2), the angle between actual cutting direction and feed direction γ can be calculated as 1.604 and 26.565 deg, respectively. The angle between feed direction and actual cutting direction which is calculated is the same as the inclination of cutting mark. So it is confirmed that the use of the cutting point swivel machining changes the actual cutting direction by rotating the tool.

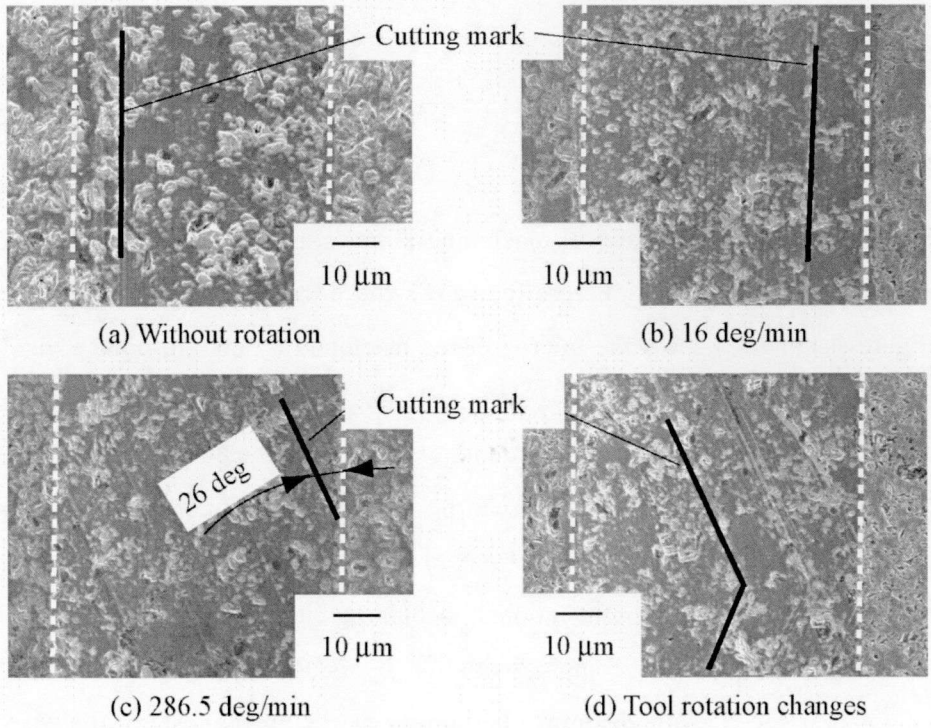

Fig. 3-1 Machined microgrooves on SiC

$$r_v = V_x/V_z = V_c\pi R/180V_z \tag{3-1}$$

$$\gamma = \arctan r_v \tag{3-2}$$

At this time, as shown in Fig. 3-2, the friction force in the rake face is also subject to the rotation force F_x by the rotation of tool. In the conventional machining without tool rotation, the cutting mechanism is two dimensions machining. The direction of friction force is the same as the ejection direction of chip which is the same as Y direction. Then, in the use of cutting point swivel machining, the direction, which the friction force is subject to, is inclined with Y direction by rotating cutting tool, so the ejection direction of chip is changed and it is become three dimensions machining by using the cutting point swivel machining, as the oblique cutting or sliding cutting.

Then, when the tool rotating direction is changed from plus to minus direction of C axis, there is the threat of deterioration of the machined surface because of the back rush of the rotation axis. Figure 3-1 (d) shows the part where the tool rotating direction is changed. It is known that the tool rotating direction changes by the direction change of cutting mark. As shown in this figure, the good microgroove shape can be obtained even in case that the tool rotating direction is changed.

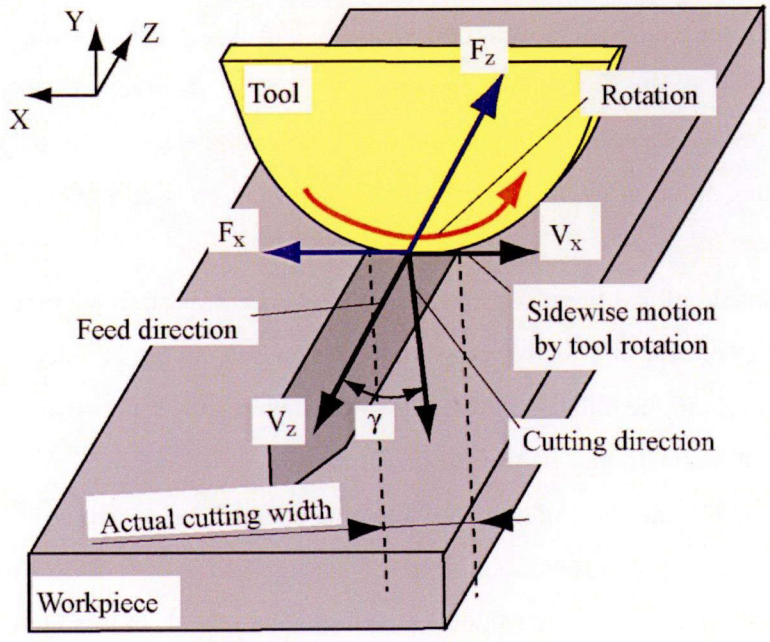

Fig. 3-2 Effect of cutting point swivel machining

3.3 Three dimensions cutting mechanism

The cutting mechanism is important to be investigated because the problem which can influence the cutting accuracy such as the force and energy in the cutting, deformation and vibration can been estimated by understanding the cutting mechanism. Then, Krystof and Merchant et al. proposed several cutting models of two dimensions cutting by predicting the shear angle in the cutting with maximum shearing stress theory and minimum energy theory [117-119]. However, the practical machining such as turning, drilling and end-milling are almost the three dimensions cutting. So there are several three dimensions cutting models since Stable proposed the cutting model.

At first, Stabler derived the force relation by using the velocity relation which is derived by Merchant [120-121]. Then, geometry formula which is called Stabler Formula is made by adding the partial maximum shearing stress theory to the force relation. This model is built on the hypothesis that the ejection direction of chip is the same as the inclination of tool in the oblique cutting, which is proposed by Stabler. So this model is based on the heuristics. By using the Stabler Formula, Aemarego et al. proposed the model with heuristics of chip ejection direction which is proposed by Russell et al. [122], [123] and Lin et al. proposed the model with prediction and measurement of shear angle in two dimensions cutting [124], [125]. Chisholm et al. used the Stabler Formula and the hypothesis that the chip is ejected to the direction which has the minimum cutting energy [120]. However, the ejection angle which is calculated by this model is different from that which is measured in the cutting experiment, because this model is the combination of two different physical laws. Then, Usui et al. proposed the model which is calculated by the hypothesis that the chip is ejected to the direction which has the minimum cutting energy, and combined to the both velocity and force relations and the concept of effective rake angle, and it is the best known in Japan [126]. The effective rake angle is that the projection of rake angle to the plane including the cutting velocity and ejection direction of chip. It is considered that the cutting force is reduced because that the effective rake angle is larger than the actual rake angle [127].

However, Shamoto pointed out that there is a mistake on the concept of effective rake angle [128], [129]. The reason is that, by the concept of effective rake angle, the cutting energy is reduced by increasing the inclination of cutting tool in the oblique cutting. However, there is the report that cutting energy is rising with the increase of inclination [130]. And then, it is supposed that the friction angle is zero. At this time, as shown in Fig. 3-2, the form of chip, the direction and volume of cutting force and cutting energy is not changed when the sidewise motion of tool is changed. However, it is different from that the effective rake angle becomes large when sidewise motion is increased. In this model, as shown in Fig. 3-2, it is considered that the moving distance of cutting edge is longer than that without sidewise

motion to remove the same volume of workpiece. So the actual cutting width becomes small, and the cutting force in tool feed direction can be reduced. The energy is almost the same because the cutting force is reduced while moving distance of cutting edge becomes longer. Actually, the cutting energy becomes a little larger because of the existence of friction force. However, there is no numerical calculation of cutting parameter in this model.

Kato et al. used the geometric relationship and balance of force to analyze the rotary shaving by using die-type cutting tool [131]. As a result, the relationship among ejection angle of chip, inclination of tool, shear angle and friction coefficient is obtained, as shown in Eq. (3-3). Here, α is the rake angle, ϕ is the shear angle, θ is the ejection angle of the chip, and the relationship between the inclination angle of tool γ and the speed ratio r_v is shown in Eq. (3-2). As shown in Table 3-1, it is found that the calculated ejection angle of chip is almost the same as the measured result [132]. Then, it is confirmed that cutting force can be reduced by rotating the tool, while the rotation force is increased at the same time.

$$\mu \cos\alpha \sin\theta = (r_v \cos(\phi - \alpha) - \tan\theta \sin\phi) \times (\cos(\phi - \alpha) - \mu \sin(\phi - \alpha) \cos\theta) \quad (3\text{-}3)$$

Table 3-1 Comparision of ejection angle

Experiment result (Zorev)				Calculation result θ deg
Inclination angle γ deg	Shear angle ϕ deg	Friction coefficient μ	Ejection angle θ deg	
0	14.0	0.77	0	0.00
10	14.1	0.78	11	10.86
25	15.2	0.80	27	27.47
40	16.6	0.88	42	44.36
49	18.2	0.95	52	54.39
60	21.7	1.06	63	65.53
70	28.1	1.25	74	72.82

3.4 Relationship between cutting forces and speed ratio

As shown in Fig. 3-2, when the tool is fed while being rotated, the moving distance of cutting edge is longer than conventional machining. So the actual cutting width becomes small, and the cutting force in tool feed direction can be reduced to suppress tool wear. In addition, the tool wear can be averaged by using broad part of cutting edge and the cutting fluid is easily to be supplied between the tool and workpiece. By these reasons, tool wear can be reduced substantially in the use of cutting point swivel machining. Then, the cutting forces by using cutting point swivel machining are investigated.

3.4.1 Estimation of cutting forces

The cutting forces by using cutting point swivel machining are estimated by using Eq. (3-3). The ejection direction of chip is considered to be the same as that with the minimum cutting power. At this time, as shown in Fig. 3-3, the cutting force in feed direction, F_z, can be shown in Eq. (3-4). Here, A is shear area and τ_s is the maximum shear stress. β is the friction angle on the rake face, which can be shown in Eq. (3-5). ξ can be shown in Eq. (3-6), $\tan\xi$ is the ratio of velocity in Z direction to that in Y direction.

$$F_z = \mathrm{R}\cos(\beta - \alpha) = \frac{A\tau_s cos\xi \cos(\beta-\alpha)}{\sin\phi\cos(\phi+\beta-\alpha)} \tag{3-4}$$

$$\beta = \tan^{-1}(\mu\cos\theta) \tag{3-5}$$

$$\xi = \tan^{-1}\frac{\mu\sin\theta\cos\beta}{\cos(\phi+\beta-\alpha)} \tag{3-6}$$

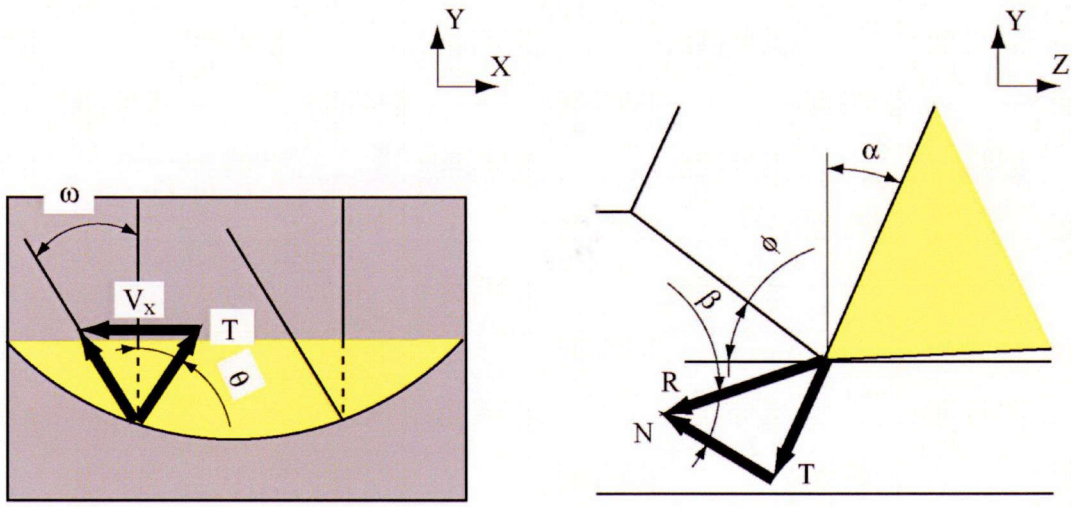

Fig. 3-3 Balance of force in the cutting

Then, because the cutting force in X direction, F_x, equals to the component force of shear force in the rotation direction, Eq. (3-7) can be derived.

$$F_x = \frac{A\tau_s \sin\xi}{\sin\phi} \tag{3-7}$$

In the cutting process, the cutting power P can be shown in Eq. (3-8). Here, the circumferential velocity of tool rotation is V_x, the feed rate is V_z.

$$\mathrm{P} = F_z V_z + F_x V_x \tag{3-8}$$

Then, the Eq. (3-9) can be obtained by substituting Eq. (3-4) and (3-7) into Eq. (3-8). β is shown in Eq. (3-5) by the friction coefficient μ and ejection angle θ. The cutting mode is set to be that cutting power P which is shown in Eq. (3-9) becomes the minimum.

$$\frac{P}{A\tau_s V_z} = \frac{\sin\xi}{\sin\phi}\left(\frac{\cos(\beta-\alpha)}{\mu\sin\phi\cos\beta} + r_v\right) \tag{3-9}$$

The calculation process is subjected as follows. The cutting condition is set to be (α, r_v, μ). Then, the shear angle ϕ is set and the ejection angle θ is calculated by Eq. (3-3). Then, cutting power is calculated by Eq. (3-9). After that, the shear angle is changed until the minimum cutting power is obtained, and the shear angle ϕ with the minimum cutting power is the solution of the cutting. In the calculation, it is presupposed that there is no relationship between rotation speed and friction coefficient μ. By the calculated shear angle ϕ, the cutting force in X direction and Z direction, F_x and F_z can be obtained. Then, cutting Force in Y direction, F_y, can be calculated by Eq. (3-10).

$$F_y = F_z \tan(\beta - \alpha) \tag{3-10}$$

Then, the dimensionless cutting forces F_z, rotation forces F_x and the thrust forces F_y by $A\tau_s$ with different speed ratio r_v are shown in Fig. 3-4. The rake angle is -30 deg, the feed rate V_z is 3.0 mm/min,

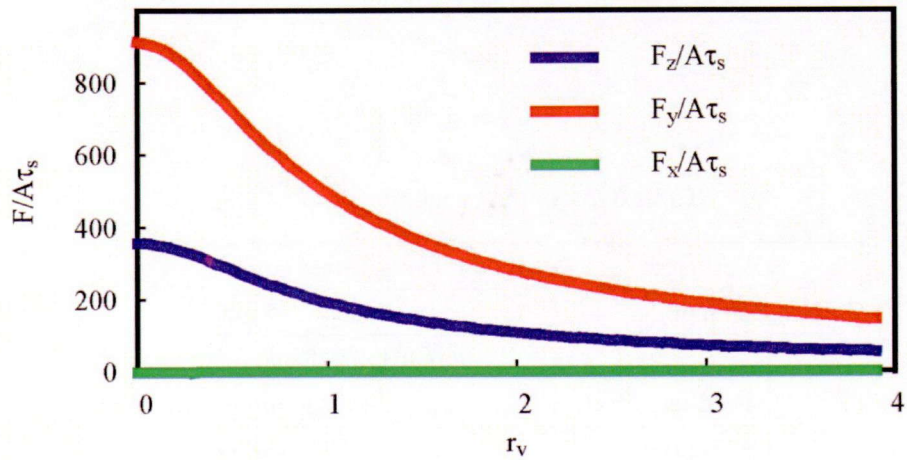

Fig. 3-4 Estimated cutting force

and the friction coefficient is 0.8.

As shown in this figure, it is known that the cutting force F_z and thrust force F_y can be reduced by using cutting point swivel machining, and it can be reduced additionally by increasing the speed ratio. To compare with cutting force and thrust force, the increase of rotation force F_x is too small that can be ignored. By the estimation of cutting forces, it can be known that the use of cutting point swivel machining has the ability to reduce cutting forces and cutting forces can be reduced additionally by increasing the speed ratio.

3.4.2 Experiment of cutting forces

Then, the actual cutting forces in the cutting point swivel machining are investigated to get the relationship between the speed ratio and cutting force. To remove the influence of the tool wear, Oxygen-free cooper is used as the workpiece. A microgroove with depth of 5 μm is machined preliminarily. Then, cutting forces are measured in the cutting with depth of cut as 5 μm over machined microgroove. The cross-section of the removed workpiece is like a ring with radius of 0.1 mm and thickness of 5 μm. At this time, the cross-section area of microgroove is 3.81×10^{-4} mm^2, and the length of microgroove is 1 mm. As shown in Fig. 3-2, the feed rate in Z direction is constant and only tool rotation speed is changed. Cutting conditions are shown in Table 3-2. The feed rate in Z direction is set to be 2 mm/min, the speed ratio r_v is set to be 0 (Conventional machining), 0.003, 0.028 and 0.5. Both dry and wet cutting are performed with the same conditions. In the wet cutting, the oil is put to form the oil film on the workpiece. The cutting dynamometer used in the experiment is Kistler 9117 with the minimum resolution of 0.01 N.

At first, the cutting forces in dry cutting are shown in Fig. 3-5. Figure 3-5 (a) shows the thrust force F_y, and Fig. 3-5 (b) shows the cutting force F_z. As shown in these figures, it can be known that the

Table 3-2 Cutting conditions

Workpiece	Oxygen-free copper
Depth of cut	5 μm
r_v	0, 0.003, 0.028 and 0.5
Feed rate	2 mm/min
Cutting fluid	Non and oil

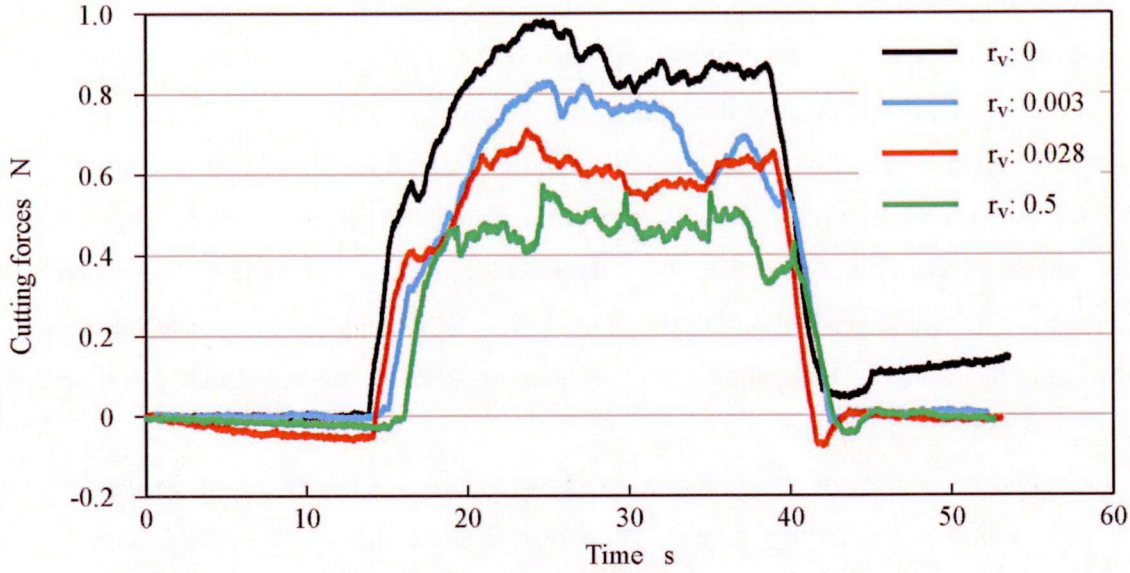

(a) Thrust forces F_y

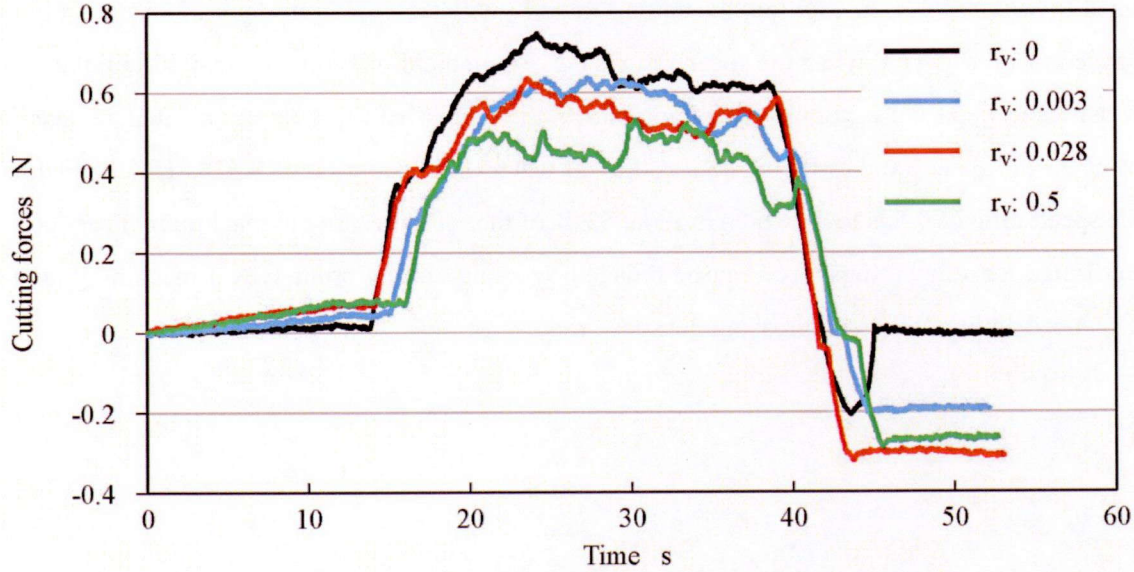

(b) Cutting forces F_z

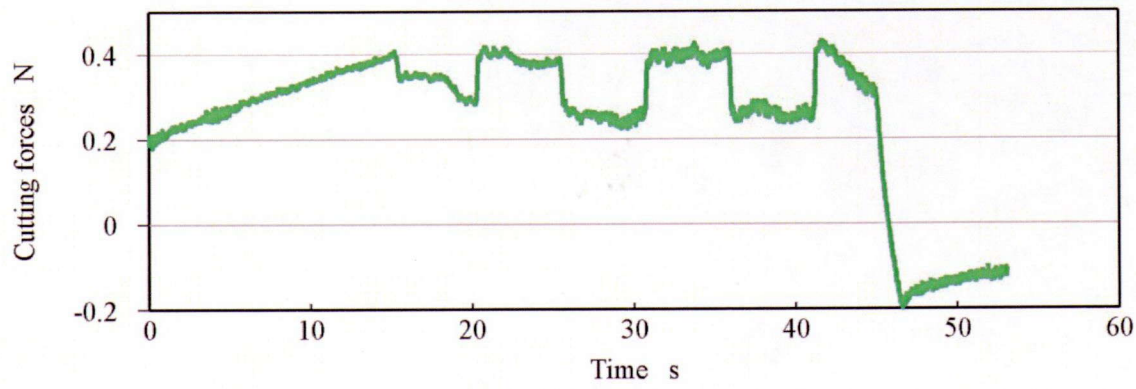

(c) Rotation force F_x with the speed ratio of 0.5

Fig. 3-5 Measured cutting force in dry cutting

cutting force can be reduced by rotating the tool, and it can be reduced additionally by increasing the speed ratio from 0.003 to 0.5. When the speed ratio is 0.5, it can be observed that there is the substantial change of cutting force for three times. It is because, when the speed ratio is 0.5, the tool rotation speed becomes large, and tool rotation direction is changed for three times. At this time, the cutting force becomes instability by the back rush of the machining center. Figure 3-5 (c) shows the measured rotation forces F_x in X direction. When the speed ratio is 0.003 and 0.028, the rotation force is too small to be measured. And when the speed ratio is 0.5, the rotation force becomes the shape like step, because of the change of rotation direction. The rotation speed F_x can be calculated as 0.07 N, by getting the difference of these steps.

Then, the average and range of cutting forces are shown in Fig. 3-6. Figure 3-6 (a) shows the thrust force F_y and (b) shows the cutting force F_z. As shown in these figures, the cutting force in feed direction F_z of conventional machining is the maximum, 0.66 N, and when the speed ratio is 0.003, it is reduced to 86%, 0.57 N. In addition, the cutting force F_z with the speed ratio of 0.028 is 0.55 N, and it is reduced to 71%, 0.47 N when the speed ratio is 0.5. Then, the thrust force F_y shows the same trend. The thrust force F_y of conventional machining shows the largest value, 0.89 N, and it is reduced to 0.71 N when the speed ratio is 0.003, and to 0.61 N when the speed ratio is 0.028. The thrust force with the speed ratio of 0.5 is 0.47, which is about 53 % of that of conventional machining. From above, it is confirmed that the cutting force can be reduced by using cutting point swivel machining, and it can be reduced additionally by increasing the speed ratio.

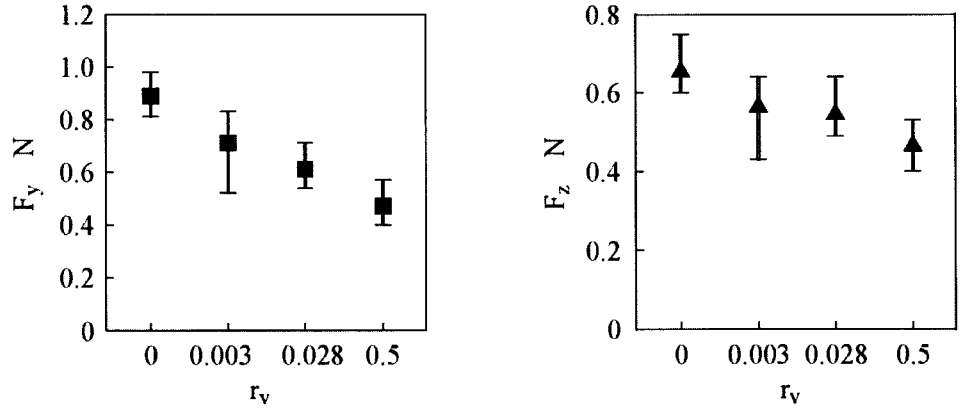

(a) Thrust force F_y (b) Cutting force F_z

Fig. 3-6 Cutting forces in dry cutting

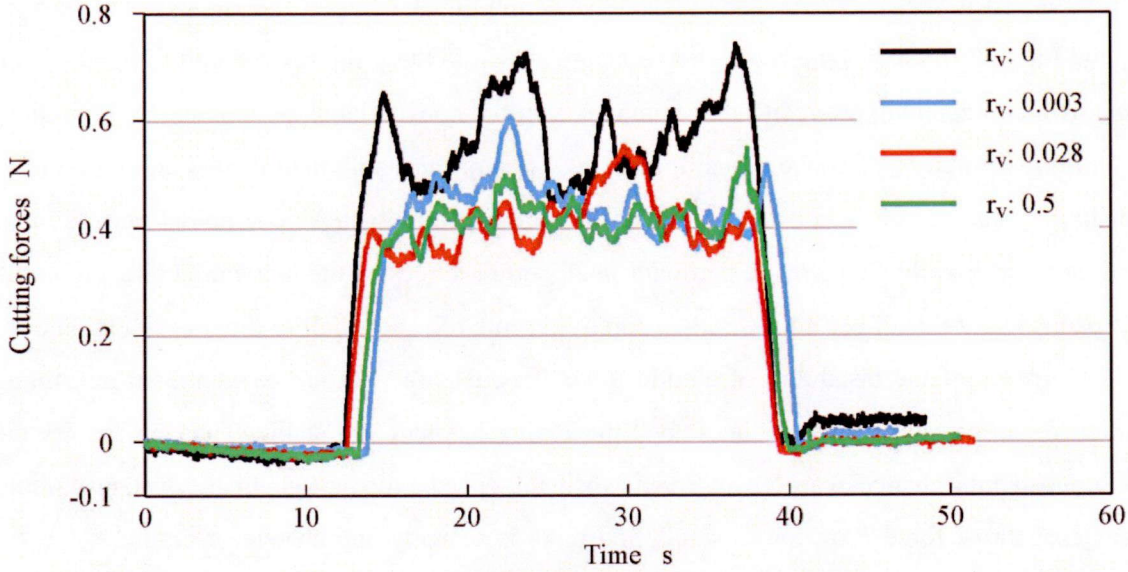

(a) Thrust forces F_y

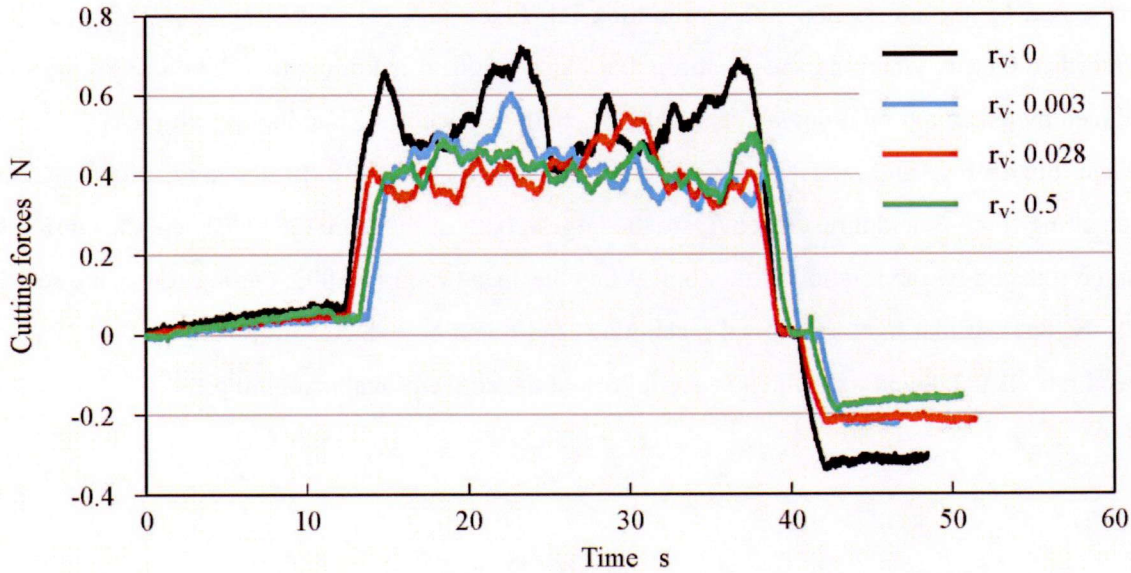

(b) Cutting forces F_z

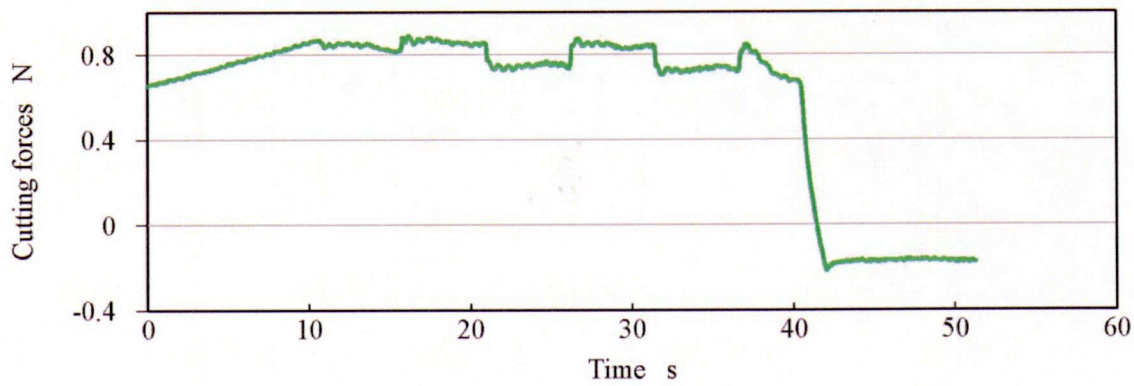

(c) Rotation force F_x with the speed ratio of 0.5

Fig. 3-7 Measured cutting force in wet cutting

Then, the cutting forces in wet machining are shown in Fig. 3-7. Figure 3-7 (a) shows the thrust force F_y, and Fig. 3-7 (b) shows the cutting force F_z. As shown in these figures, the cutting forces in cutting point swivel machining are reduced to compare with the conventional machining. Both cutting force F_z and thrust force F_y of conventional machining are more unstable than that of cutting point swivel machining. The reason is considered as that the cutting fluid cannot be supplied between tool and workpiece effectively. So there are part with small cutting forces by the lubrication effect of cutting oil and part without this effect, so the cutting forces become big and small in the machining, and there is the occurrence of the instability of cutting force. To compare with the conventional machining, the cutting force by using cutting point swivel machining is small and stable. Then, in the dry cutting, three substantial changes can be observed when the speed ratio is 0.5. In the wet machining, the change of thrust force F_y becomes small, and there is scarcely any change of cutting force F_z. It is considered that the influence which is caused by the back rush of the machining center can be suppressed by the lubrication effect of cutting oil. Figure 3-7 (c) shows the rotation force F_x, F_x is reduced to 0.05 N when the speed ratio is 0.5. As a result, it is known that the cutting forces can be reduced by using cutting point swivel machining both in dry cutting and in wet cutting.

Then, the average and range of cutting forces are shown in Fig. 3-8. In the conventional machining, the cutting force F_z and thrust force F_y are the largest, both of them are 0.54 N. Then, the cutting forces can be reduced by the rotation of the tool. When the speed ratio is 0.003, cutting forces are reduced to 0.45 N, 83% of that in conventional machining, and it can be reduce additionally to 0.41 N when the speed ratio is 0.028 and 0.5, which is about 76% of the conventional machining.

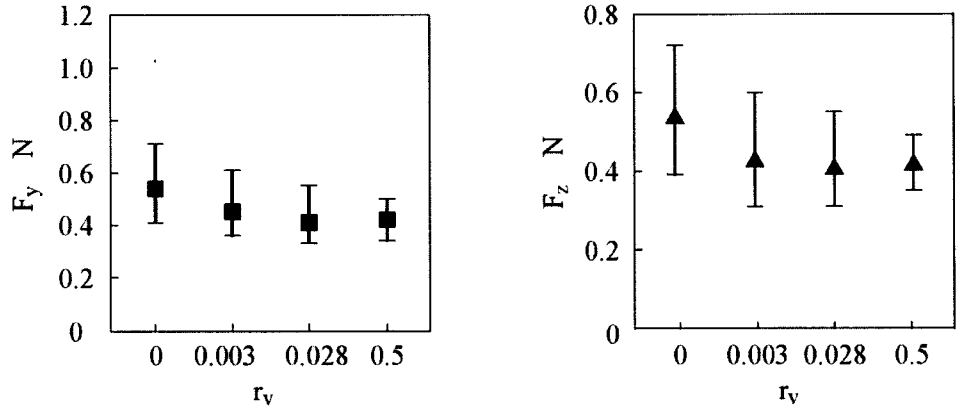

(a) Thrust force F_y (b) Cutting force F_z

Fig. 3-8 Cutting forces in wet cutting

3.4.3 Discussion

The average of measured cutting forces in dry and wet cutting is summarized in Table 3-3. When the speed ratio r_v is 0 to 0.028, thrust force F_y in wet cutting reduces significantly, compared with that of dry cutting. As shown in Fig. 3-9, the chip is subjected to the force in X direction by rotating the tool, so it is rejected inclined to the Y direction. When the speed ratio r_v is increased, the component force in Y direction of friction force which is subject on rake face becomes small, and the component force in X direction becomes large. On the other hand, when the speed ratio r_v is 0.5, F_y in wet cutting is almost the same as that of dry cutting. The reason is that the component force in Y direction of friction force is small so that the reduction of cutting force by the lubrication effect of cutting fluid becomes small.

Table 3-3 Cutting forces

r_v		0		0.003		0.028		0.5		
Measured cutting force N		F_y	F_z	F_y	F_z	F_y	F_z	F_y	F_z	F_x
	Dry	0.89	0.66	0.71	0.57	0.61	0.55	0.47	0.47	0.07
	Wet	0.54	0.54	0.45	0.43	0.41	0.41	0.42	0.42	0.05
Estimated cutting force		$F_y/A\tau_s$	$F_z/A\tau_s$	$F_y/A\tau_s$	$F_z/A\tau_s$	$F_y/A\tau_s$	$F_z/A\tau_s$	$F_y/A\tau_s$	$F_z/A\tau_s$	$F_x/A\tau_s$
		911.2	355.99	911.16	355.98	910.32	355.65	722.10	282.12	1.67

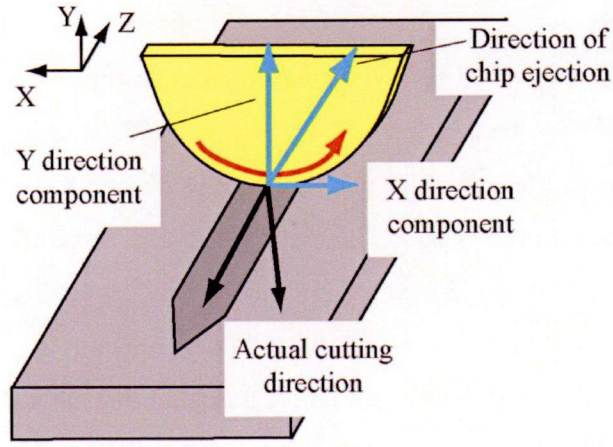

Fig. 3-9 Friction force in the rake face

Then, both measured and estimated cutting forces are listed in Table 3-3. In the estimated cutting force, when the speed ratio is increased from 0 to 0.028, there is scarcely any change of cutting forces, and the cutting forces are reduced substantially when the speed ratio is increased from 0.028 to 0.5. To compare with this, in the measured cutting forces, the cutting force reduced substantially when the speed ratio increases from 0 to 0.028. In the section 3.4.1, it is presupposed that the friction coefficient is not changed and the shear area is the same when the speed ratio is increased. However, as shown in Table 3-1, when the inclination angle γ is increased, there is the increase of the friction coefficient. At the same time, by the rotation of the tool, the actual cutting width is reduced to the cosγ times. At this time, the width of shear area becomes 1/cosγ times and the shear area A also increases to 1/cosγ times. In addition, by using the tool with negative rake angle, the mechanism of cutting becomes more complex, and it is too difficult to calculate the cutting force by specific numbers. However, the estimated cutting forces show the same trend as the measured cutting forces, which is the reduction of cutting forces by using cutting point swivel machining and by increasing the speed ratio r_v.

3.5 Relationship between tool wear and speed ratio

In the cutting force experiment in the Section 3.4, it is known that the both cutting force F_z and thrust force F_y can be reduced by using cutting point swivel machining. At the same, there is the occurrence of the rotation force F_x. However, the rotation force is very small to compare with the cutting force and thrust force. So it is expected to suppress tool wear in the cutting point swivel machining by the reduction of cutting forces. In addition, by increasing the speed ratio, the lubrication effect of cutting oil becomes large so that the tool wear can be suppressed.

3.5.1 Low speed ratio

Then, an experiment is conducted to investigate the relationship between tool wear and the speed ratio. The speed ratio is set to be 0.003, 0.007, 0.014 and 0.028. Machining shape is the microgroove with the depth of 4 μm and length of 25 mm. the feed rate is set to be 3 mm/min, and the rotation speed of tool at each speed ratio is 6, 12, 24 and 48 deg/min, respectively. Three microgrooves are machined with each speed ratio, and the cutting distance is 2,250 mm, respectively. The workpiece is SiC, and the cutting conditions are shown in Table 3-4 (Experiment A).

Figure 3-10 shows the rake face of the tool before and after machining with each speed ratio. (a) to (h) show the tools used before and after machining, with the speed ratio r_v of 0.003, 0.007, 0.014 and 0.028, respectively. As shown in these figures, when the speed ratio is 0.003 and 0.007, the tool wear

on cutting edge is about 0.5 μm, which is calculated from the width of chamfer before and after machining. Then, as shown in Fig. 3-10 (c) and (d), when the speed ratio is 0.014 and 0.028, the tool wear on the cutting edge is less than 0.1 μm. Then, the flank face of tool after machining which is observed by a metallurgical microscope (Olympus PME-3) is shown in Fig. 3-11. (a), (b), (c) and (d) show the tool with speed ratio of 0.003, 0.007, 0.014 and 0.028, respectively. When the speed ratio is 0.003, the maximum tool wear on flank face, VB_{max}, is about 0.4 μm. Then, when the speed ratio is increased to 0.007, the VB_{max} is reduced to 0.3 μm, and it is reduced additionally to 0.2 μm when the speed ratio is increased to 0.014. Then, as shown in Fig. 3-11 (d), there is scarcely any tool wear on the flank face when the speed ratio is 0.028. However, several chippings are observed on the cutting edge.

It is considered as, because the poreless process of workpiece is not executed, so a lot of pores exist in the workpiece. When the speed ratio is increased, the rotation speed is increased at the same time. The impact to the tool becomes large, and it is easy to cause the occurrence of chippings on the cutting edge. From these results, it can be confirmed that both tool wear on the cutting edge and the maximum tool wear on flank face can be suppressed by increasing the speed ratio. The reason is considered as the reduction of cutting forces.

Then, the measured roughness Rz in the tool feed direction is summarized in Table 3-5. As shown in this table, good surface can be obtained with each speed ratio even the variation of tool posture becomes steep.

Table 3-4 Cutting conditions

	Experiment A	Experiment B	Experiment C
Workpiece	SiC		Tungsten Carbide
Total depth	4 μm	5 μm	5 μm
Depth of cut	80 nm		50 nm
r_v	0.003 to 0.028	0.028 and 0.5	0.028 and 0.5
Feed rate	3 mm/min	1 mm/min	1 mm/min
Cutting fluid	Oil mist	Non and Oil mist	Oil mist

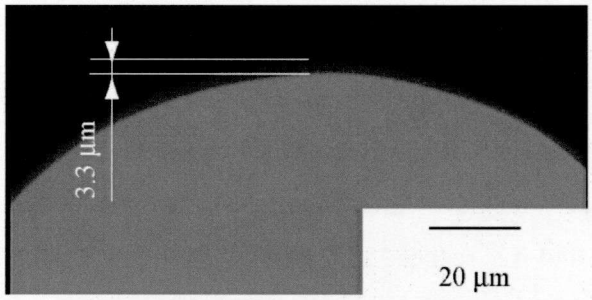

(a) Before machining (r_v: 0.003)

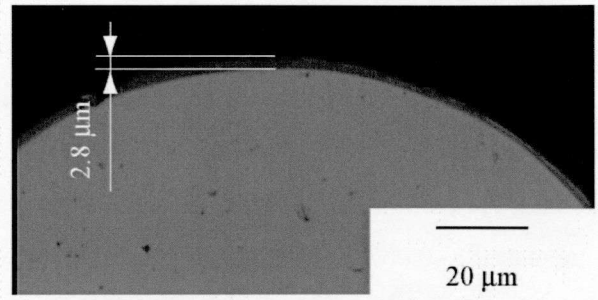

(b) After machining (r_v: 0.003)

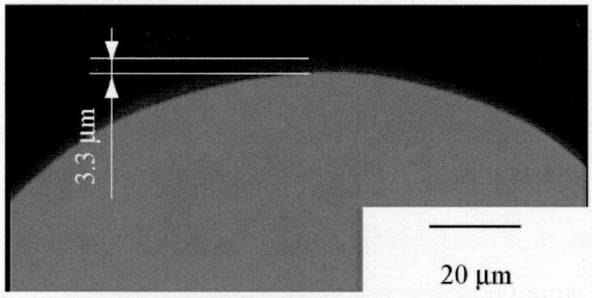

(c) Before machining (r_v: 0.007)

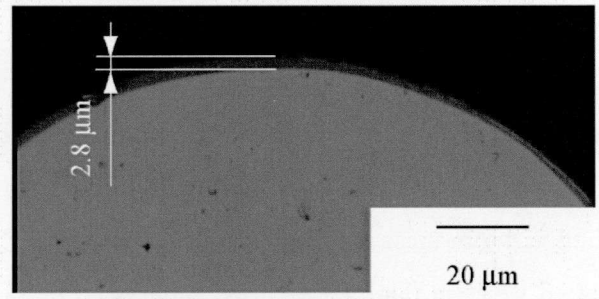

(d) After machining (r_v: 0.007)

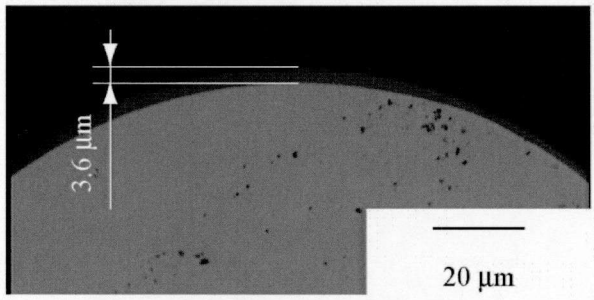

(e) Before machining (r_v: 0.014)

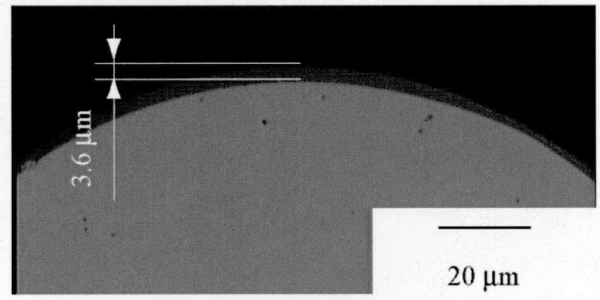

(f) After machining (r_v: 0.014)

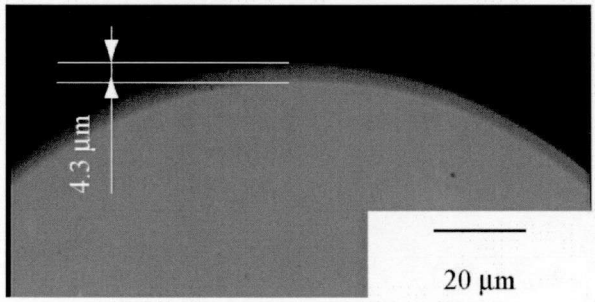

(g) Before machining (r_v: 0.028)

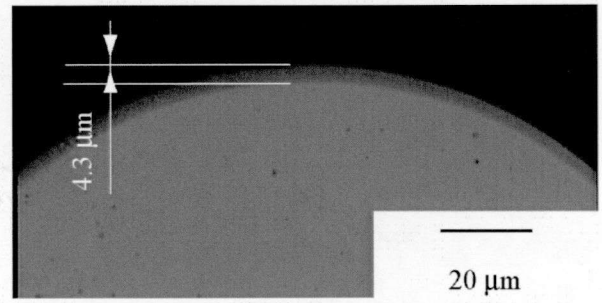

(h) After machining (r_v: 0.028)

Fig. 3-10 Rake face of tool used in the machining with each speed ratio

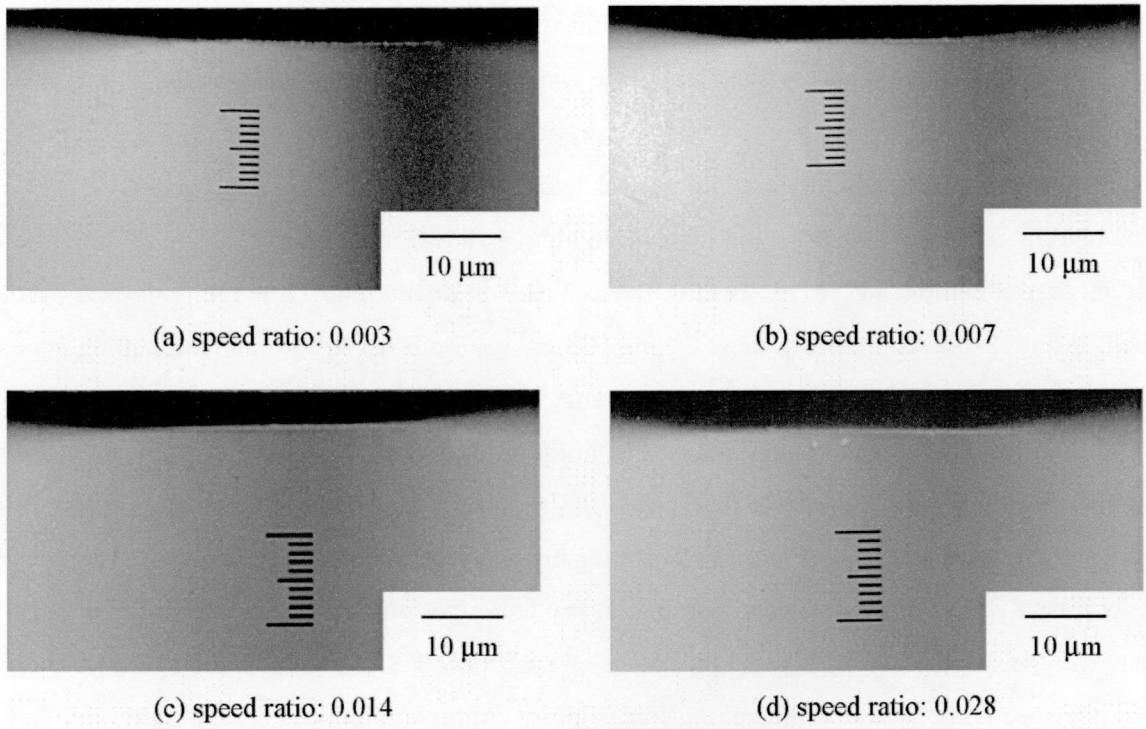

(a) speed ratio: 0.003 (b) speed ratio: 0.007

(c) speed ratio: 0.014 (d) speed ratio: 0.028

Fig. 3-11 Flank face of tool after machining

Table 3-5 Tool wear and roughness of machined microgrooves

r_v	Tool wear on cutting edge μm	VB_{max} μm	Roughness of grooves μm		
			1st	2nd	3rd
0.003	0.5	0.4	0.12	0.13	0.10
0.007	0.5	0.3	0.11	0.13	0.12
0.014		0.2	0.09	0.10	0.09
0.028			0.13	0.11	0.11

3.5.2 High speed ratio

Furthermore, an experiment is conducted with the speed ratio of 0.028 and 0.5. Because the maximum synthesis command speed of the machining center in the experiment is 720 min^{-1}, the feed rate is set to be 1 mm/min. At this time, the tool rotation speed is 16 and 286.5 deg/min, respectively. Cutting conditions are shown in Table 3-4 (Experiment B). The machining shape is the microgroove

with length of 12.5 mm, and depth of 5 μm. In the experiment with low speed ratio, there is scarcely any tool wear on both cutting edge and flank face when the speed ratio is 0.028, so the cutting distance is set longer. 15 microgrooves are machined with each speed ratio, and the cutting distance is 11,250 mm, respectively. Then, both dry cutting and wet cutting are executed in this experiment.

The rake face of the tool before and after machining is shown in Fig. 3-12. (a) to (d) show the tool used in the wet cutting, and (e) to (h) show the tool used in dry cutting. Then, the flank face of tool is shown in Fig. 3-13. As shown in these figures. Chippings are observed on the both cutting edge and flank face of all tools. As the trend of the occurrence of chippings, it is found that the chippings on the tool used in wet cutting is less than that on the tool used in dry cutting, and the chippings on the tool with the speed ratio of 0.028 is less than that with the speed ratio of 0.5. In the experiment of cutting force, it is known that cutting forces in wet cutting are less than that in dry cutting. So it is known that the tool wear in wet cutting are less than that in dry cutting by the lubrication effect of cutting fluid. Then, to compare the cutting force with the speed ratio of 0.028 to that with the speed ratio of 0.5, when the speed ratio r_v is 0.5, the cutting forces in dry cutting are reduced substantially, and they are almost the same in wet cutting. However, the chippings on the cutting edge are increased when the speed ratio is increased.

The roughness of microgrooves which are machined in wet machining in feed direction is shown in Fig. 3-14. The dotted line shows the roughness machined by conventional machining. The surface of microgroove machined by conventional machining becomes bad rapidly because of the severe tool wear. To compare with this, good surface can be obtained until the 12^{th} microgroove when the speed ratio r_v is 0.028. However, surface of microgroove machined with the speed ratio of 0.5 becomes bad from 7^{th} microgroove. The reason of the deterioration of surface is considered as the chippings on the cutting edge. When the speed ratio is 0.5, the chippings on the cutting edge occur from the 7^{th} microgroove, and they become more in the machining. Then, the reason of the increase of chipping when the speed ratio becomes large is considered at next section.

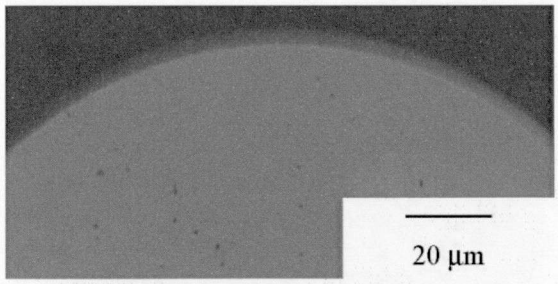

(a) Before machining (r_v: 0.028, wet)

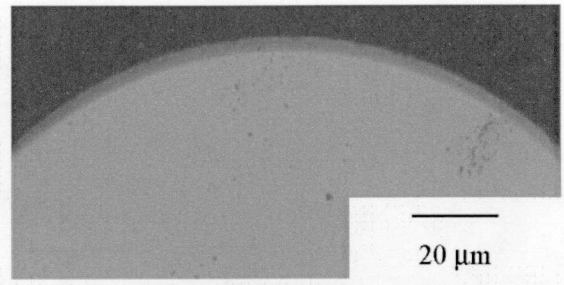

(b) After machining (r_v: 0.028, wet)

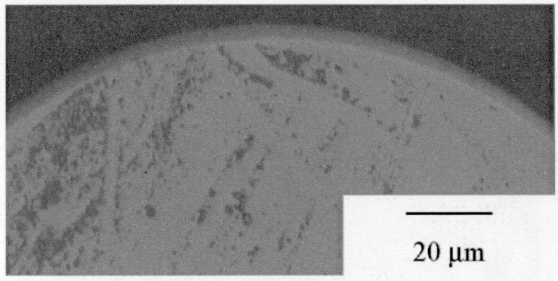

(c) Before machining (r_v: 0.5, wet)

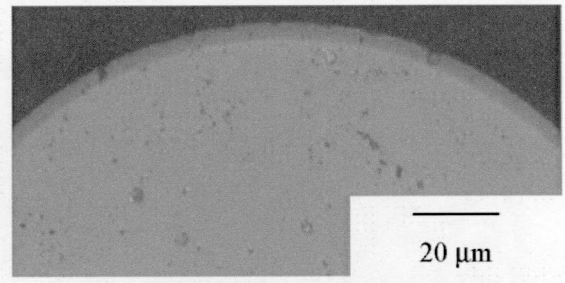

(d) After machining (r_v: 0.5, wet)

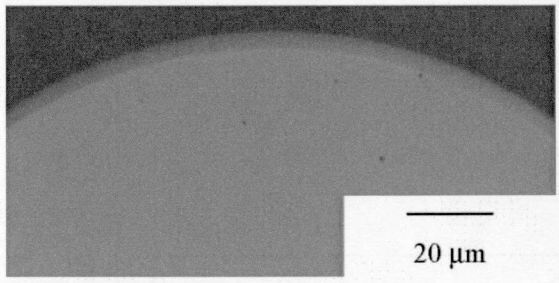

(e) Before machining (r_v: 0.028, dry)

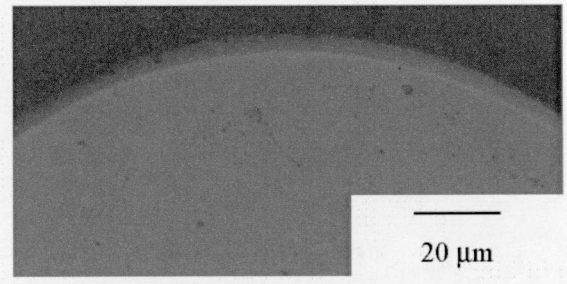

(f) After machining (r_v: 0.028, dry)

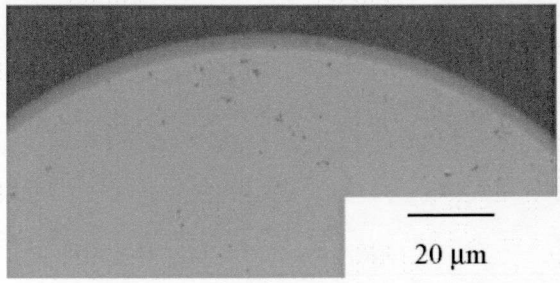

(g) Before machining (r_v: 0.5, dry)

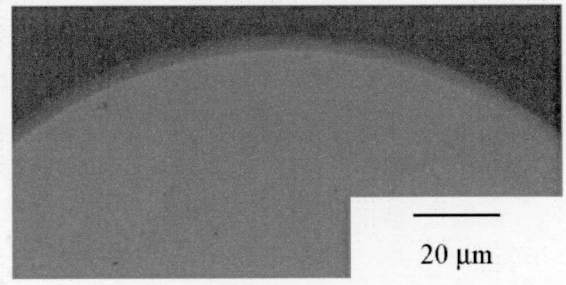

(h) After machining (r_v: 0.5, dry)

Fig. 3-12 Tool used in the machining with high speed ratio

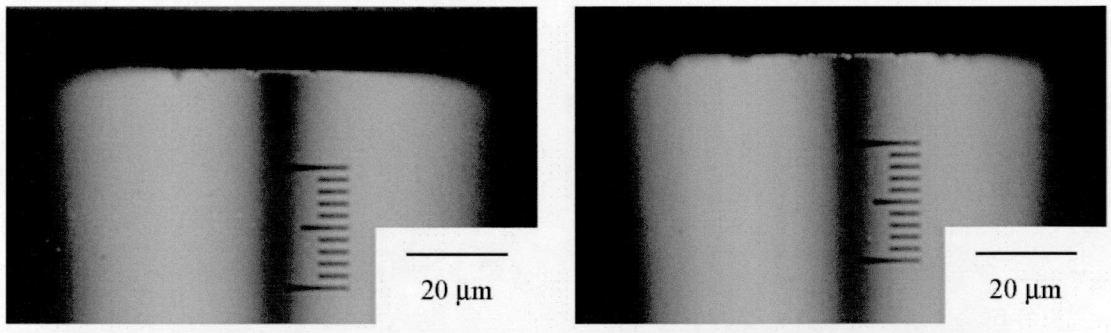

(a) Tool used after wet cutting (r_v: 0.028) (b) Tool used after wet cutting (r_v: 0.5)

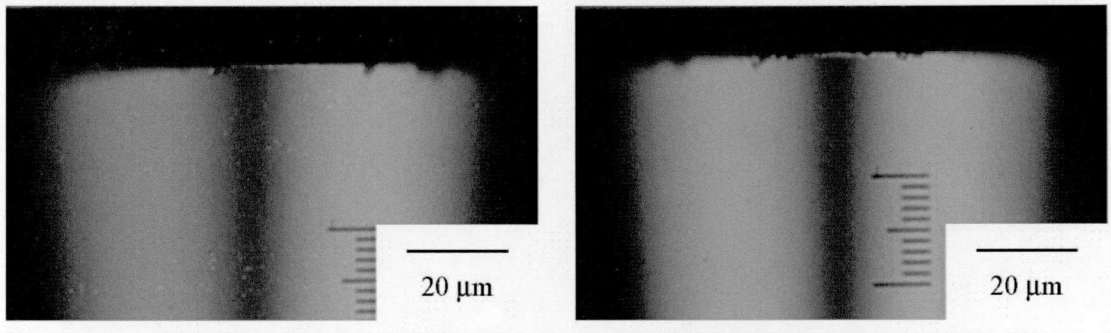

(c) Tool used after dry cutting (r_v: 0.028) (d) Tool used after dry cutting (r_v: 0.5)

Fig. 3-13 Flank face of tool after machining

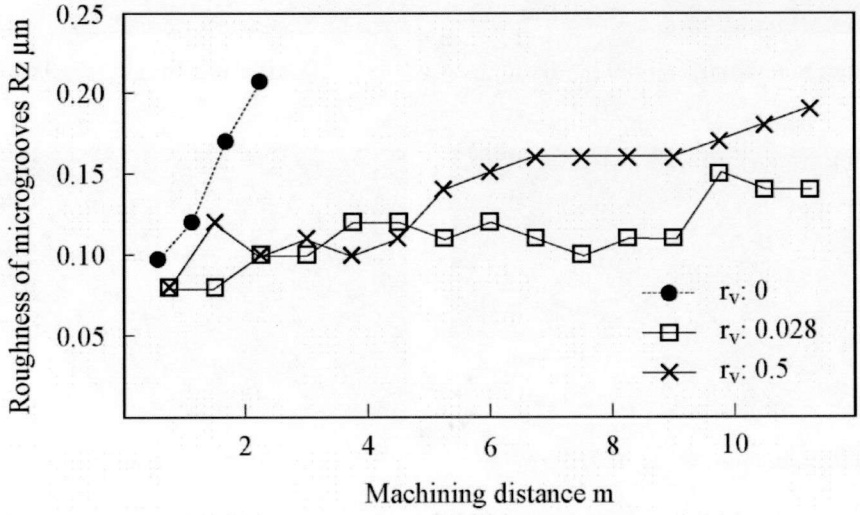

Fig. 3-14 Roughness of machined microgrooves

3.5.3 Discussion

There are two reasons which are considered why the chippings increase. One is the pore in the workpiece, and the other one is the increase of the contact distance between the flank face and workpiece when the speed ratio is increased.

Fig. 3-15 shows the microgrooves machined in the wet cutting with the speed ratio of 0.028 and 0.5. As shown in these figures, the poreless processing of the workpiece is not executed, so there are a large number of pores in the workpiece. The cutting forces are changed by the presence or absence of these pores. In addition, as shown in Fig.3-16, the workpiece used in the experiment is sintered SiC. So there are SiC grains and Si grains in the material. In the cutting experiment, the cutting forces of Si grains are different from that of SiC grains. So the cutting force in the cutting experiment is always changing, and the tool is subject to the impact by the change of cutting forces. When the speed ratio is increased, the impact to the tool becomes larger by the increase of tool rotation speed, and it is easy to cause the chipping on the cutting edge.

Then, the other reason is the increase of the contact distance between the flank face of the tool and

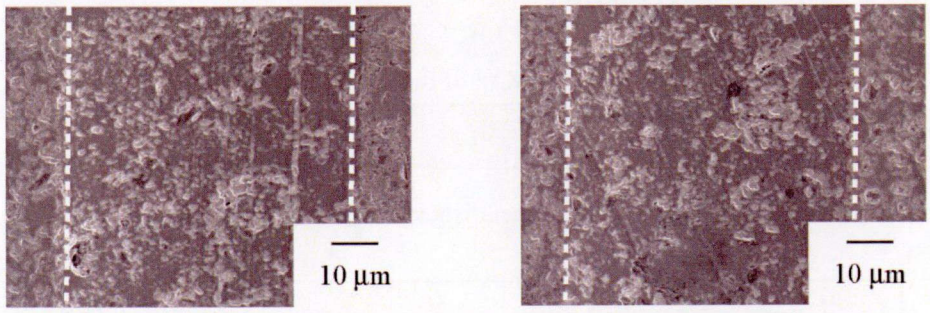

(a) r_V: 0.028 (b) r_V: 0.5

Fig. 3-15 Machined microgrooves

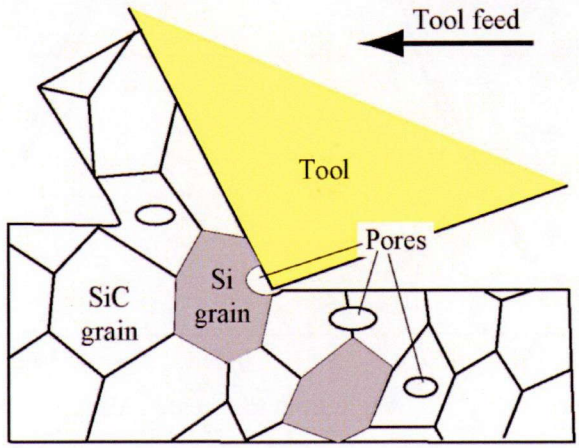

Fig. 3-16 Cutting of SiC

workpiece. As shown in Fig. 3-17, the tool is fed while being rotated by the use of cutting point swivel machining, so the actual cutting direction is inclined. At this time, the moving direction of cutting points becomes inclined to the feed direction, and the contact distance between the flank face of the tool is longer than that of the conventional machining to cause the ability of the increase of tool wear. On the other hand, as shown in Fig. 3-17, the cutting edge moves to the outside of the workpiece in this experiment, so the contact distance between the flank face of the tool and workpiece becomes shorter than the machining distance.

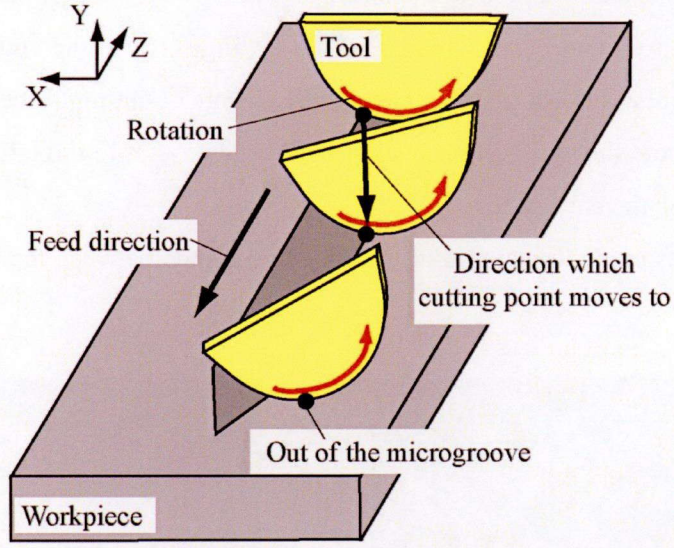

Fig. 3-17 Increase in the contact distance between flank face and workpiece

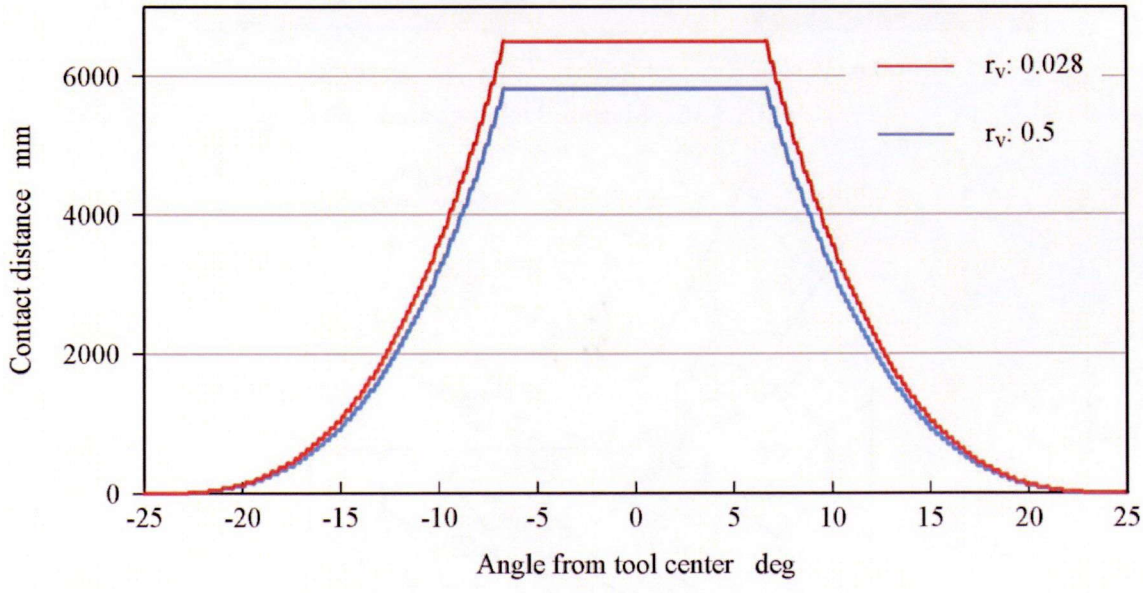

Fig. 3-18 Contact distance between the flank face of tool and workpiece

When the speed ratio r_v is increased, the contact distance is increased at the same time. The contact distance of each part of cutting edge, which is divided by 0.1 deg, is shown in Fig. 3-18. As shown in this figure, the contact distance between flank face and workpiece on the part which is between -10 deg to 10 deg is the same by the effect of cutting point swivel machining. Then, to compare with the cutting distance of 11,250 mm, the maximum contact distance when the speed ratio is 0.028 is 5,812 mm, and it is increased to 6,495 mm, which is about 1.12 times of that with speed ratio of 0.028, when the speed ratio is 0.5. This is a reason that the chippings on the cutting edge are increased by raising the speed ratio.

In the experiment of Section 3.5.1, to compare with the cutting distance of 2,250 mm, when the speed ratio is increased from 0.003 to 0.028, the distance between the flank face of tool and workpiece is 1,647 and 1,648 mm, respectively. Although the speed ratio is increased, the contact distances are almost the same, and there is almost scarcely any influence to the tool wear.

3.5.4 Experiment on cemented carbide

Then, an experiment is conducted on the cemented carbide with the speed ratio of 0.028 and 0.5. Cutting conditions are shown in Table 3-4 (Experiment C). The depth of cut is set to be 50 nm, and feed rate is set to be 1 mm/min. Machining shape is the microgroove with length of 12.5 mm and depth of 5 μm. 20 microgrooves are machined with each rotation speed, and cutting distance is 20,000 mm. Then, only wet cutting is executed in this experiment.

The workpiece used in the machining is binderless tungsten carbide (FUJI DIE Co. Ltd. J05). Its physicality is shown in Table 3-6. This material has the property of heat resistance, hardness and low coefficient of linear thermal expansion in high temperature. The SEM photo of this material is shown in Fig. 3-19. As shown in this figure, there is no binder like Cobalt and other metallic phase in the

Table 3-6 Physicality of Tungsten Carbide J05

Machanical properties	Density		14.65 g/cm^3
	Young's modulus		650 GPa
	Hardness HV		2000
	Poisson's ratio		0.20
Thermal properties	Thermal conductivity		63 W/m·K
	Coefficient of linear thermal expansion(α)	RT-400 °C	4.6×10^{-6}/K
		RT-600 °C	4.8×10^{-6}/K
		RT-800 °C	5.1×10^{-6}/K

workpiece. In addition, there is no pore in the workpiece, and it is used widely as the mold of glass lens.

The rake face of the tool before and after machining is shown in Fig. 3-20, (a) shows the tool used in the machining with the speed ratio of 0.028, and (b) shows the tool used in the machining with the speed ratio of 0.5. Then, Figure 3-21 shows the flank face of the tool used after machining. As shown in these figures, when the speed ratio is 0.5, several microchippings can be observed on the cutting edge. Both the size and the number of chippings is less than that on the tool used in the machining of SiC. Then, when the speed ratio is 0.028, only one that looks like microchipping can be observed on

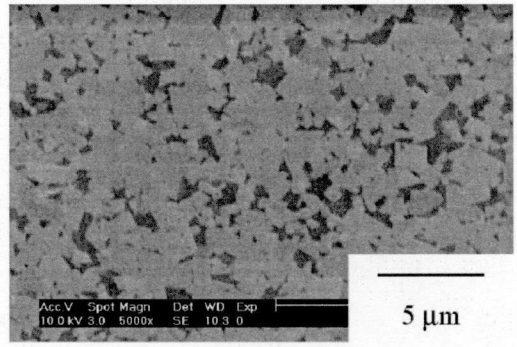

Fig. 3-19 SEM photo of Tungsten Carbide

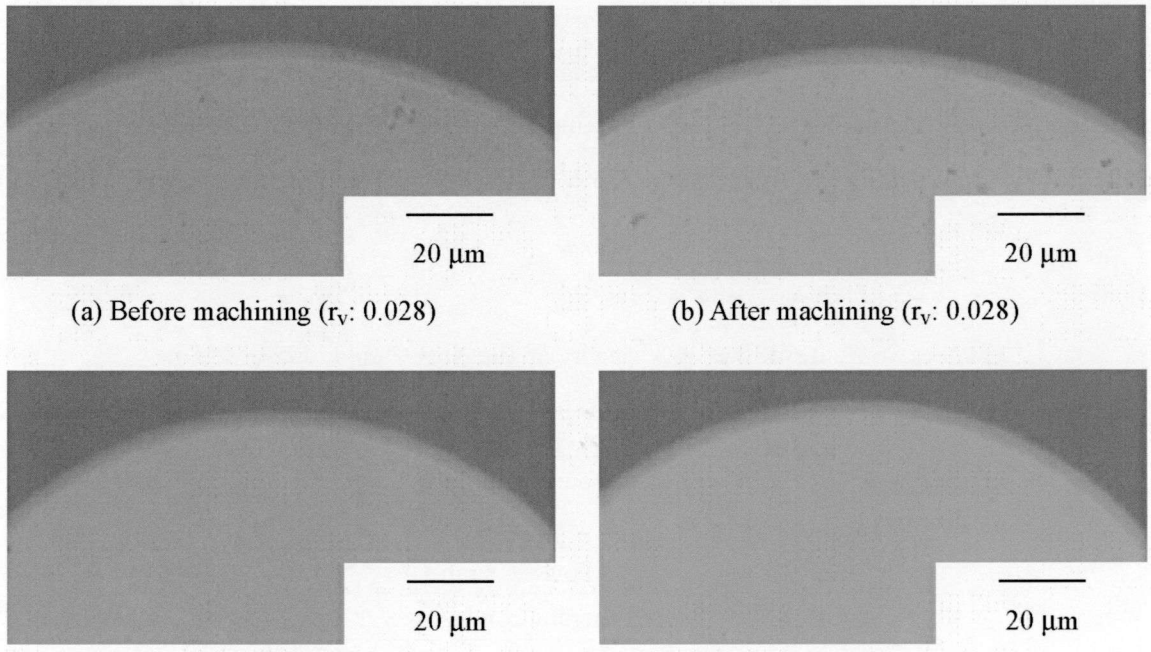

(a) Before machining (r_v: 0.028) (b) After machining (r_v: 0.028)

(c) Before machining (r_v: 0.5) (d) After machining (r_v: 0.5)

Fig. 3-20 Tool used in the machining of Tungsten Carbide

the cutting edge, and there is almost no tool wear on the cutting edge. The relationship between the speed ratio and tool wear shows the same trend as that in the machining of SiC. When the speed ratio is increased, both the number and size of chippings increase at the same time. Then, the tool wear becomes less and smaller than that of the tool used in the machining experiment of SiC. As shown in Table 2-5 and Table 3-6, the hardness of tungsten carbide J05 and SiC is 2000 and 2100 HV, respectively. Although the cutting distance of tungsten carbide is much longer than that of SiC, and the difference of hardness is very small, the tool wear in the cutting of tungsten carbide is much smaller than that of SiC. The reason is considered as the impact which is subject to the tool in the machining. As already described earlier, the cutting forces in the cutting of SiC are always changing in the machining, and the tool is subject to the impact by the change of cutting forces. To compare with this, there is no pore in the tungsten carbide, so the impact to the tool is much smaller than that in the machining of SiC, and the chippings on the cutting edge is reduced substantially.

3.6 Summary

This chapter aims at investigating the mechanism of the cutting point swivel machining, and making clear the relationship among the speed ratio, cutting forces and tool wear. As the result of the experiment of cutting forces with different speed ratio and that of tool wear on the SiC and tungsten carbide, by using cutting point swivel machining which is proposed in Chapter 2, the conclusion can be summarized as follows:

1) The cutting marks can be observed on the surface of machined microgrooves. From these cutting marks, it is known that the actual cutting direction can be changed by using cutting point swivel

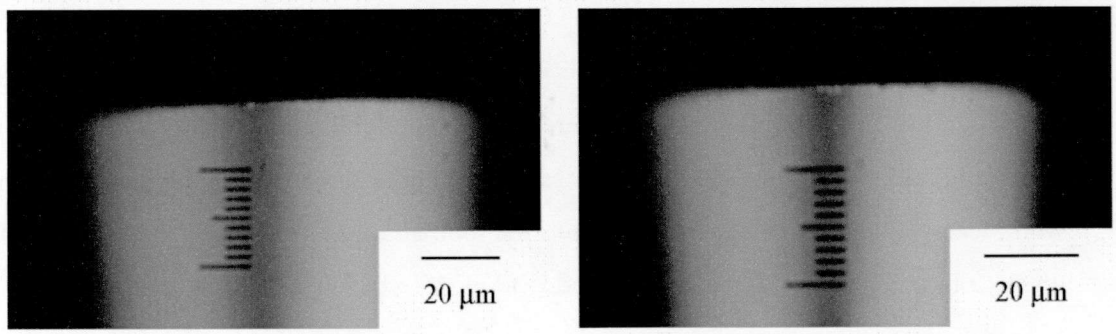

(a) Tool with speed ratio of 0.028 (b) Tool with speed ratio of 0.5

Fig. 3-21 Flank face of tool after machining

machining. The actual cutting direction is calculated and it is the same as the direction of cutting marks. In addition, it is confirmed that good shape can be obtained even the rotation direction is changed.

2) The tool is fed while being rotated in cutting point swivel machining. At this time, the moving distance of cutting edge is longer than that without rotating, to remove the same volume of workpiece. So the actual cutting width becomes small, and the cutting force in tool feed direction can be reduced to suppress tool wear. In addition, the tool wear can be averaged by using broad part of cutting edge, and the cutting fluid can be supplied between the tool and workpiece easier. By these reasons, tool wear can be suppressed substantially.
3) The cutting forces are estimated by using the equation which is proposed by Kato et al. and minimum energy theory. As a result, it is found that both the cutting force F_z and thrust force F_y can be reduced by rotating the tool and they can be reduced furthermore by increasing the speed ratio. To compare with these forces, the rotation force is so small that can be ignored.
4) In the experiment of cutting forces, it is found that the cutting forces in dry cutting can be reduced by using cutting point swivel machining, and it can be reduced furthermore by increasing the speed ratio from 0.028 to 0.5. Then, in the wet cutting, the cutting force can be reduced by using cutting point swivel machining. However, the reduction of cutting forces by increasing the speed ratio is very small. The reason is considered as that the component force in Y direction of friction force is so small that the lubrication effect of cutting fluid becomes small.
5) To compare with the estimated and measured cutting forces, the reduction of cutting force by increasing the speed ratio is different. However, they show the same trend that the cutting force can be reduced by the increase of speed ratio.
6) When the speed ratio is increased from 0.003 to 0.028, it is found that the tool wear can be suppressed by increasing the speed ratio. The reason is considered as the reduction of cutting force.
7) When the speed ratio is increased from 0.028 to 0.5, it is confirmed that both the size and the number of chippings on the cutting edge is increased with no relation to the presence and absence of the cutting fluid. By this reason, there is the deterioration of the roughness of machined microgroove. Two reasons are considered as this phenomenon: one is the pore and Si grains in the workpiece which cause the micro impact to the tool, and the other one is the increase of contact distance between the flank face of tool and workpiece, which is caused by the rotation of the tool. However, the contact distance between the flank face of tool and workpiece is shorter than that of conventional machining because the cutting edge moves to outside of the workpiece.

8) In the cutting experiment of binderless tungsten carbide, the relationship of tool wear shows the same trend with that of SiC. However, the hardness of these materials are almost the same, and the cutting distance of binderless tungsten carbide is much longer than that of SiC, the tool wear on the cutting edge becomes small substantially. It can presume that there is the large influence to the tool wear by the pore in the workpiece.
9) By the experiment of the relationship between the speed ratio and tool wear, it is confirmed that there is an appropriate speed ratio which has the ability to suppress the tool wear to minimum.

As summarized above, the effect of cutting point swivel machining is investigated, and the relationship among the speed ratio, cutting forces and tool wear are made clear. However, there are still several problems which need to be solved.

a) In the machining of hard brittle material, the critical depth of cut is very important. To realize high efficiency machining, the critical depth of cut is expected to be enlarged. It is known that the use of cutting point swivel machining has the ability to reduce the actual cutting width, and the depth of chip can become thinner than conventional machining. So it is interesting to investigate the relationship between the critical depth of cut and the speed ratio.
b) In this chapter, because of the limit of the machining center, the maximum speed ratio is set to be 0.5. So the cutting force may become smaller when the speed ratio becomes larger. In the investigation of the rotary machining, it is reported that the cutting force can convergence when the speed ratio is larger than 4. So it is necessary to enlarge the speed ratio, and to research the relationship between the speed ratio and cutting forces.
c) Although the trend of estimated cutting forces are the same as that of measured cutting force. There is a large difference between them. So it is necessary to get another method which can calculate the cutting forces correctly.
d) From the experiment of the speed ratio and tool wear, it is known that tool wear can be reduced by increasing the speed ratio. However, when the speed ratio is more than a certain value, the tool wear becomes severe because of the increase of contact distance. To realize the tool wear to the minimum, it is necessary to research the best speed ratio.

Chapter 4
APPLICATION OF CUTTING POINT SWIVEL MACHINING

4.1 Introduction

As introduced in the Chapter 1, ball end milling is mostly used in the machining of complex shape. There are several advantages of the ball end milling:

- It is easy to machine complex shape by controlling tool path and tool posture.
- Cutting forces are smaller than that of sharp machining.
- The tool can be fed with high feed rate by revolving at high speed, so the cutting efficiency is higher than that of sharp machining.
- In the machining of metal materials, it is reported that tool wear can be suppressed by the effect of intermittent cutting.

By this ball end milling, complex shape can be machined easily and efficiently. However, to compare with the sharp machining, there is a problem that there is the error of shape accuracy because of the use of rotational tool. In the micromachining, the radius of tool is small, so it is necessary to rotate the tool over 10,000 rpm. At this time, the vibration of tool occurs. The vibration of the tool is about several micrometers. However, it is too large to compare with the radius of the tool so there is the occurrence of the shape error. And because of the vibration, the machining becomes unsteadiness to cause the deterioration of machined surface. In addition, there is a point, which is called dead point, that the rotation speed on this point is zero. The surface becomes worse in the machining with dead point. To avoid the machining with dead point, the inclined axis cutting process is proposed [133]. And to realize high precision machining, the compensation machining is proposed after the first machining [134], [135]. However, it is difficult to get the actual shape of the tool, and there is still shape error in the machining. To realize high precision machining, the sharp cutting is used in the machining of curved surface. It is reported that both the shape accuracy and roughness which cannot be obtained in the ball end milling can be obtained by sharping machining. However, there is a large problem that the machining time of sharp machining is much longer than that of the ball end milling.

The cutting point swivel machining, which use the sharp machining is proposed in the Chapter 2, and the mechanism of the cutting point swivel machining is investigated in Chapter 3. Then, in this chapter, the cutting point swivel machining is applied to the machining of complex shape. In Section 4.2, the cutting point swivel machining is applied to the machining of curved microgroove. And then, in Section 4.3, the ball end milling is used to the machining of hard material. The tool wear and the shape

accuracy are investigated in this section. In Section 4.4, the cutting point swivel machining is applied to the machining of the curved surface.

4.2 Curved microgrooving

4.2.1 Application to curved microgrooving

The cutting point swivel machining is applied to the curved microgrooving. At first, as shown in Fig. 4-1, the curved microgroove is divided into small segments, and the coordinate values of each machining point are calculated.

Then, the coordinate value of B axis, which is the rotating degree of the workpiece set on the ZX plane, is calculated. The linear interpolation is used in the machining of the curved microgroove to approximate the curve. As shown in Fig. 2-15, the tool is fed by moving Z axis. So it is necessary to

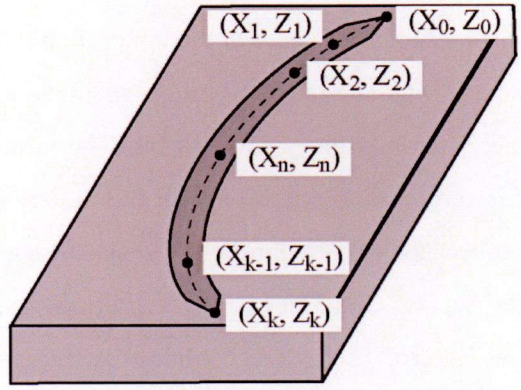

Fig. 4-1 Division of the microgroove

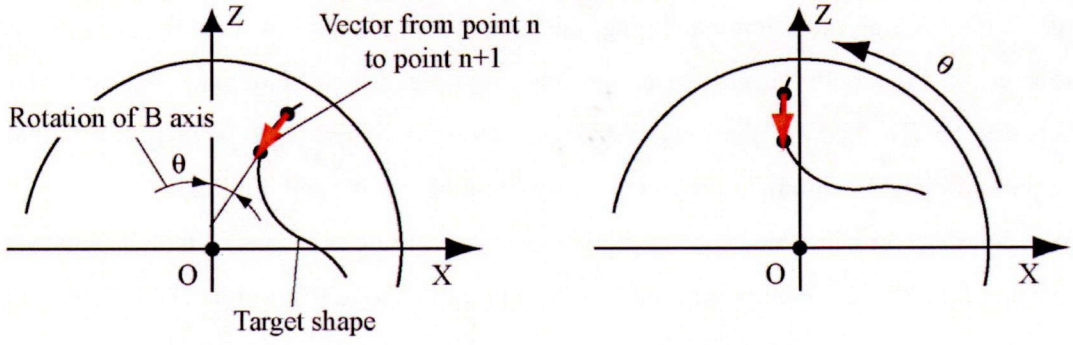

(a) Before B axis rotation (b) After B axis rotation

Fig. 4-2 Rotation of B axis rotation

rotate B axis to angle θ, which is between the vector from point n to point n+1 and negative direction of Z axis, to make sure that the vector is in the opposite direction with Z axis, as shown in Fig. 4-2. Here, the coordinate of point n is (X_n, Z_n), and that of point n+1 is (X_{n+1}, Z_{n+1}), so the degree θ between the vector and the negative direction of Z axis can be shown in Eq. (4-1).

$$\theta = \tan^{-1}\frac{X_{n+1}-X_n}{Z_{n+1}-Z_n} \tag{4-1}$$

Then, as shown in Fig. 4-3, if B axis is rotated to α degree, there is a displacement of machining point, and the coordinate of machining point changes into (X_n`, $Z_n$`). To compensate this displacement, it is necessary to make the coordinate transformation, as shown in Eq. (4-2).

$$\begin{cases} X_n` = X_n\cos\alpha - Z_n\cos\alpha \\ Z_n` = Z_n\cos\alpha + X_n\cos\alpha \end{cases} \tag{4-2}$$

At last, the coordinate value of C axis, that is, the posture of the tool is calculated. The range of C axis rotation is C_r deg, the distance between the machining point and the microgroove starting point is

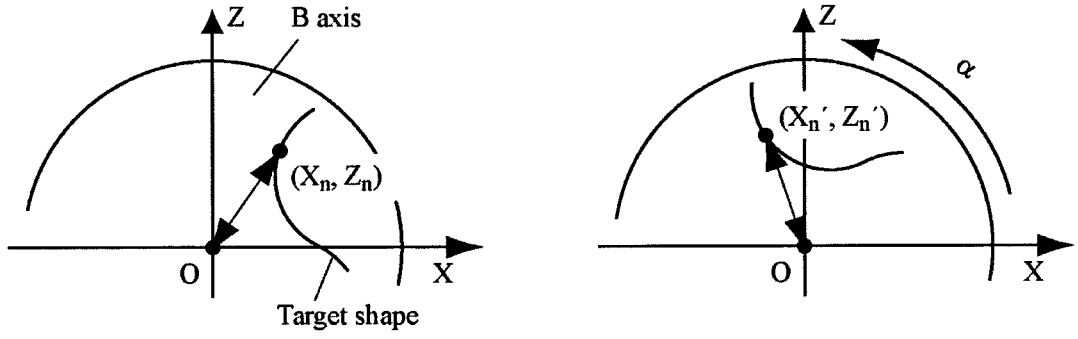

(a) Before B axis rotation (b) After B axis rotation

Fig. 4-3 Displacement of machining point

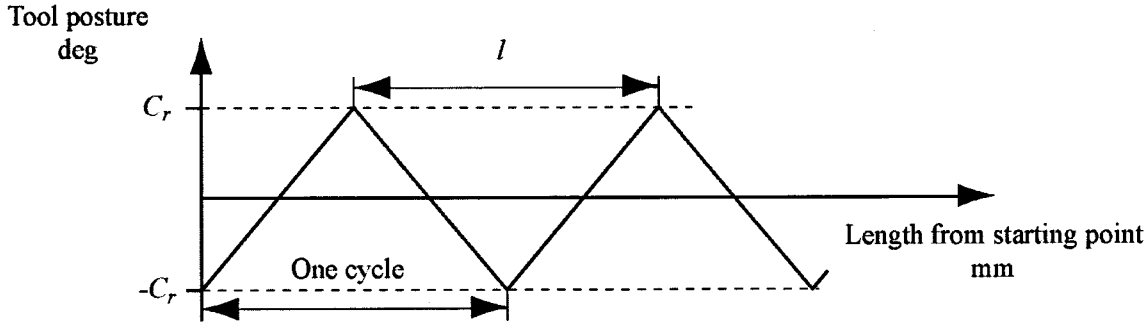

Fig. 4-4 Relationship between tool posture and distance from starting point

L mm, the relationship between tool posture and the distance L can be shown in Fig. 4-4. And the moving length l of tool in one cycle can be shown in Eq. (4-3). Here, r_v is the speed ratio, and R is the radius of tool tip. Tool posture changes $4C_r$ degrees in one cycle. As a result, the posture of the tool C can be calculated by Eq. (4-4).

$$l = \pi R C_r / 45 r_v \tag{4-3}$$

$$C = C_r - \left|0.5 - \left(\frac{45 r_v L}{\pi R C_r} - int\left(\frac{45 r_v L}{\pi R C_r}\right)\right)\right| \times 4C_r \tag{4-4}$$

4.2.2 Setting between tool center point and the center of B axis

As shown in Fig. 4-3, there is a displacement when B axis is rotated. So it is important to get the coordinates of X and Z axis. Usually, the origins of these axes are set the same as the center of B axis. The try cutting is conducted to set the origins of X and Z axis. As shown in Fig. 4-5(a), microgrooves in X and Z direction are machined on the workpiece with an arbitrary coordinate (X_a, Z_a). Then, the B table is rotated to 180 deg, and the same microgrooves are machined on the workpiece, as shown in Fig. 4-5(b). Next, the distances between these microgrooves in X direction, Δx, and that in Z direction, Δz, are measured by a microscope. At last, because Z axis controls the moving of the tool, and X axis

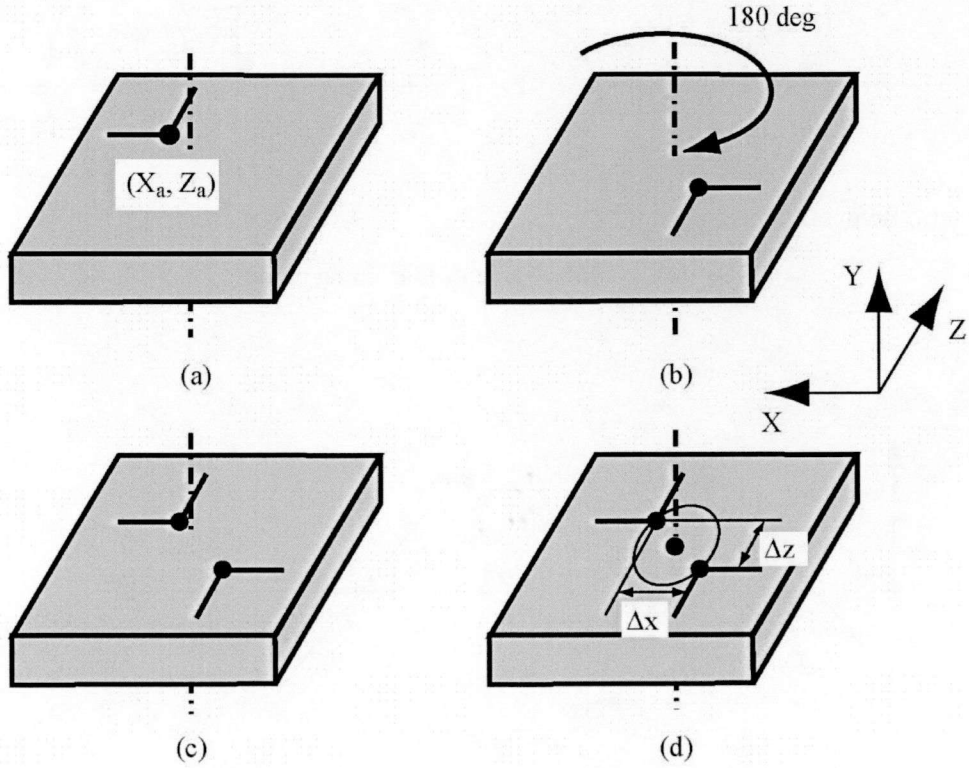

Fig. 4-5 Setting of the origins of X and Z axes

controls the moving of workpiece. To consider the relative motion between tool and workpiece, the origin of X and Z axis, (X_o, Z_o), is set as shown in Eq. (4-5). By the repetition of this setting, the origins of X and Z axis can be set the same as the center of B axis.

$$\begin{cases} X_0 = X_a + \Delta x/2 \\ Z_0 = Z_a - \Delta z/2 \end{cases} \tag{4-5}$$

As shown in Fig. 4-6, Δz can be measured by the edge of microgroove machined by rake face. However, because the tool used in the machining is an R-shape tool, so it is difficult to get the center of the machined microgrooves in X direction. At this time, the width of the machined microgrooves, w_a and w_b, and the distance between two edges of the microgroove d_s, are measured by the microscope. Then, the distance in X direction Δx can be shown in Eq. (4-6).

$$\Delta x = d_s - w_a/2 + w_b/2 \tag{4-6}$$

4.2.3 Verification experiment

There is a verification experiment of the curved microgrooving by using cutting point swivel machining. The target shape is a curved microgroove of 5 mm in length and 4 μm in depth, which is combined by two arcs with the radius of 3 mm. The depth of cut is set to be 50 nm, and the microgroove is machined by 80 times. The workpiece is binderless tungsten carbide, and the cutting conditions are shown in Table 4-1 (Experiment A). To consider the length of microgroove, and using all part of cutting edge in the machining, the speed ratio is set to be 0.018, the machining distance is 400 mm, and the machining time is 6.5 hours.

The rake face of tool before and after machining is shown in Fig. 4-7. Figure 4-7(a) shows the tool before machining and (b) shows the tool after machining. As shown in these figures, there is no damage like chippings on the rake face of the tool after machining. The width of chamfer before and

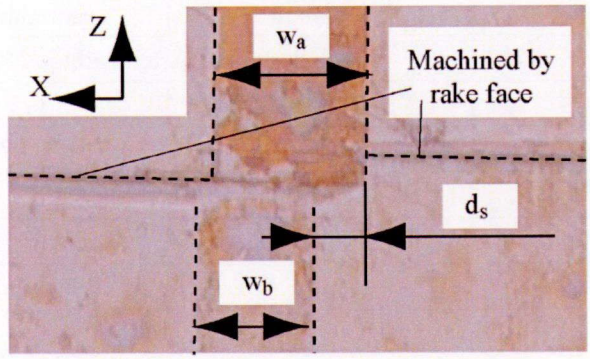

Fig. 4-6 Calculation the center of microgroove

after machining is about 3.6 μm, so there is scarcely any tool wear on the cutting edge.

The machined microgroove is shown in Fig. 4-8. Figure 4-8(a) shows the whole view, and (b) shows the enlarged parts of 0, 1.25, 2.5, 3.75 and 5 mm far from the starting point of the microgroove, respectively. Then, Fig. 4-8 (c) shows the cross-section of each part of microgroove, respectively. As shown in these figures, because of the inclination of workpiece, the machined microgroove becomes shallow in the machining, and there is about 800 nm difference in depth between the start and end point of the microgroove. Then, several black points can be observed on the surface of microgroove. There is no broken part on the edge of microgroove, so it is confirmed that there is no brittle fracture in the machining. These black points can be presumed as the grain drops in the machining. It can be known that the microgroove with good shape can be obtained by using cutting point swivel machining.

Then, the microgroove which is measured by surface roughness measuring instrument is shown in Fig. 4-9. The dashed line shows the target shape. Although there is the occurrence of the waviness in the measuring, it can be known that the microgroove is machined the same as the target shape. From the above, it is confirmed that the microgroove with good shape accuracy can be machined by using cutting point swivel machining.

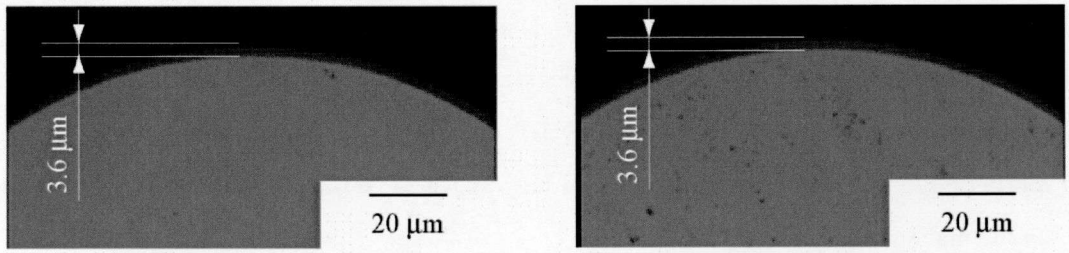

(a) Before machining (b) After machining

Fig. 4-7 Rake face of tool before and after machining

Table 4-1 Cutting conditions

	Experiment A	Experiment B
Workpiece	Binderless tungsten carbide J05	
Interpolation	0.5 μm	3.125 μm
r_v	0.0175	0.028
Rotation speed of tool	30 deg/min	48 deg/min
Range of C axis rotation	-25 to 25 deg	-12.5 to 12.5 deg
Total depth	4 μm	5 μm
Depth of cut	50 nm	
Feed rate	3 mm/min	
Cutting fluid	Oil mist	

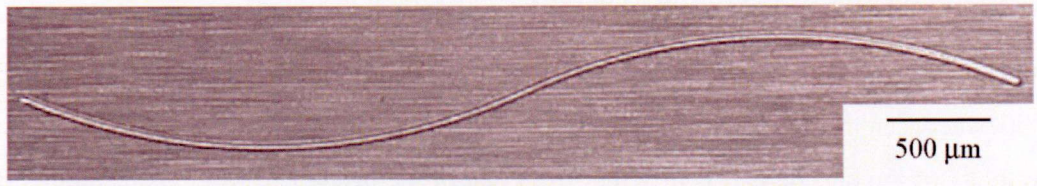

(a) Whole view

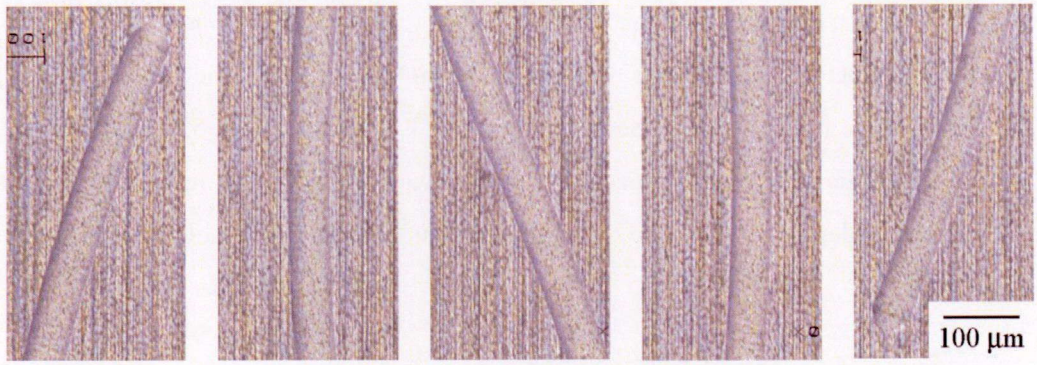

(1) 0 mm (2) 1.25 mm (3) 2.5 mm (4) 3.75 mm (5) 5 mm

(b) Enlarged view

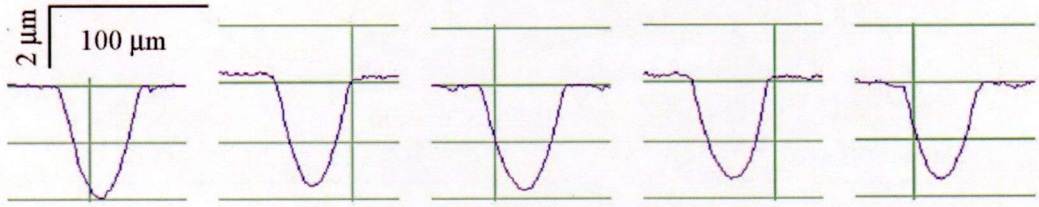

(1) 0 mm (2) 1.25 mm (3) 2.5 mm (4) 3.75 mm (5) 5 mm

(c) Cross-section of microgroove

Fig. 4-8 Machined curved microgroove

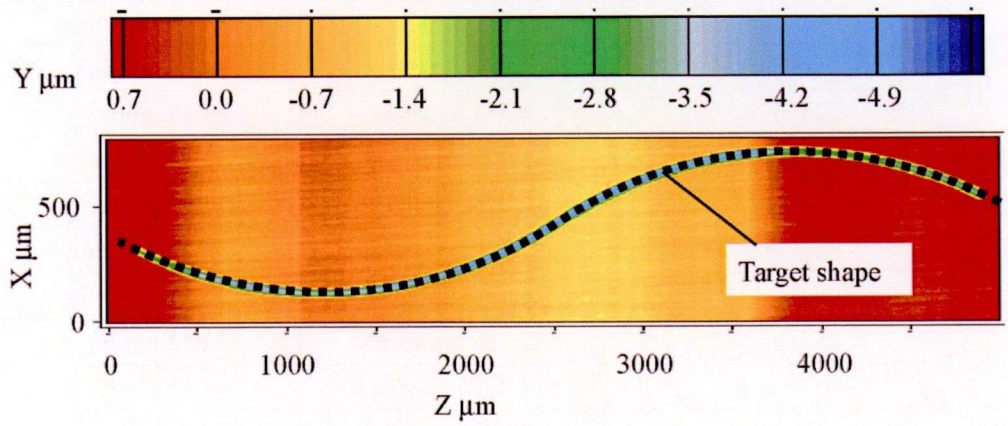

Fig. 4-9 Measured result

4.2.4 Microgrooving with arbitrary curvature

When the radius of the curved microgroove becomes small, both the volume and the direction of the velocities between the inside and outside part of microgroove become different. As shown in Fig. 4-10, the velocity of the outside part is different from that of the inside part. So the machining of outside is like down cutting, and that of the inside is like up cutting. In addition, the values of velocities are different so there is the threat of the occurrence of variation in the machined surface. Then, an experiment is conducted to investigate the influence which is caused by the curvature of microgrooves. The curvature of the microgroove is set to be 0.5, 1.0, 1.5, 2.0, 3.0, 4.0, 5.0, 6.0, 8.0, 10.0, 12.0 and 15.0 mm, and 12 microgrooves are machined in this experiment. The length of each microgroove is 3.125 mm, and the depth is 5 μm. The cutting conditions are shown in Table 4-1 (Experiment B). The

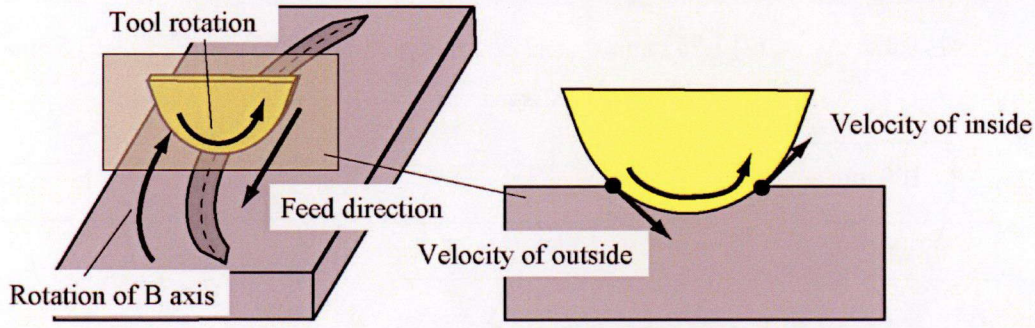

Fig. 4-10 Machining of curved microgroove

Table 4-2 Ralationship between the curvature and velocity

Curvature of microgroove	Velocity of inside part	Velocity of outside part
0.5 mm	2.814 mm/min	3.189 mm/min
1.0 mm	2.907 mm/min	3.095 mm/min
1.5 mm	2.939 mm/min	3.064 mm/min
2.0 mm	2.954 mm/min	3.048 mm/min
3.0 mm	2.970 mm/min	3.032 mm/min
4.0 mm	2.978 mm/min	3.025 mm/min
5.0 mm	2.982 mm/min	3.020 mm/min
6.0 mm	2.986 mm/min	3.017 mm/min
8.0 mm	2.989 mm/min	3.013 mm/min
10.0 mm	2.992 mm/min	3.011 mm/min
12.0 mm	2.993 mm/min	3.009 mm/min
15.0 mm	2.995 mm/min	3.007 mm/min

total machining time is 54.5 hours and total machining distance is 3,750 mm. The velocities of the inside and outside part of microgroove with each curvature of microgroove are summarized in Table 4-2. When the feed rate is set to be 3.0 mm/min, the velocity of the inside and outside part with the curvature of 0.5 mm is 2.8 and 3.2 mm/min, respectively. To compare with this, when the curvature of microgroove is 15 mm, the velocities of both the inside and outside parts are almost 3.0 mm/min.

Then, to omit the influence of the tool wear, two patterns of machining are conducted. Pattern 1 is machined from the microgrooves with small radius to that with large radius, and pattern 2 is inverted to the pattern 1. The tool is rotated 2 times in one microgrooving. At the anterior half of microgrooves, C table is rotated to plus direction while B axis being rotated to minus direction, and at the posterior

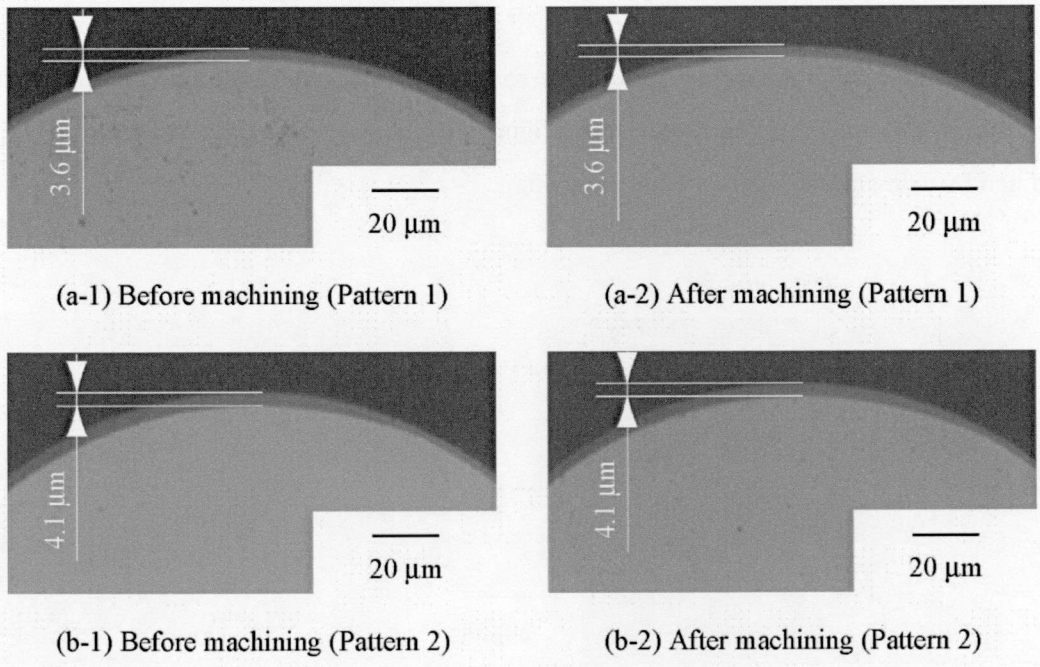

(a-1) Before machining (Pattern 1) (a-2) After machining (Pattern 1)

(b-1) Before machining (Pattern 2) (b-2) After machining (Pattern 2)

Fig. 4-11 Tool used in the machining

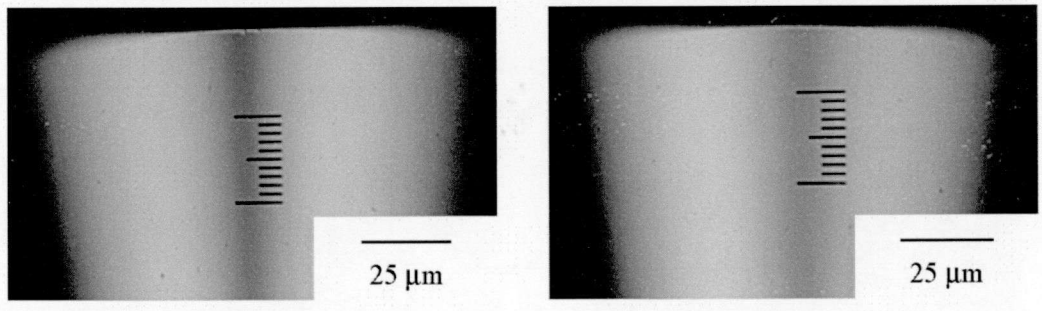

(a) Pattern 1 (b) Pattern 2

Fig. 4-12 Flank face of the tool after machining

half, both B axis and C table are rotated to minus direction.

Figure 4-11 shows the tool used in the machining. (a) shows the tool before and after machining used in the machining of pattern 1, and (b) shows the tool used in the pattern 2. From the width of chamfer, it is conformed that the tool wear on the cutting edge is almost zero. Then, the flank face of the tool is shown in Fig. 4-12. There is scarcely any tool wear on the flank face.

Because there is almost no tool wear on both cutting edge and flank face, it can presume that the microgrooves machined by two patterns show the same accuracy. Then, the SEM photos of machined microgrooves in pattern 1 are shown in Fig. 4-13. (a) shows the microgroove with curvature of 0.5 mm, and (b) shows the microgroove with curvature of 15 mm. Then, (1) shows the anterior half of the microgroove, and (2) shows the posterior half of the microgroove. As shown in these figures, grain drops can be observed on the surface of microgroove, but the edge of microgroove shows good shape accuracy. Although the volume and direction of the velocity of the microgrooving with the curvature of 0.5 is different, both the inside and outside parts show sharp edge, and good shape accuracy can be obtained on both sides. As shown in these figures, the microgroove with arbitrary curvature can be obtained by using cutting point swivel machining.

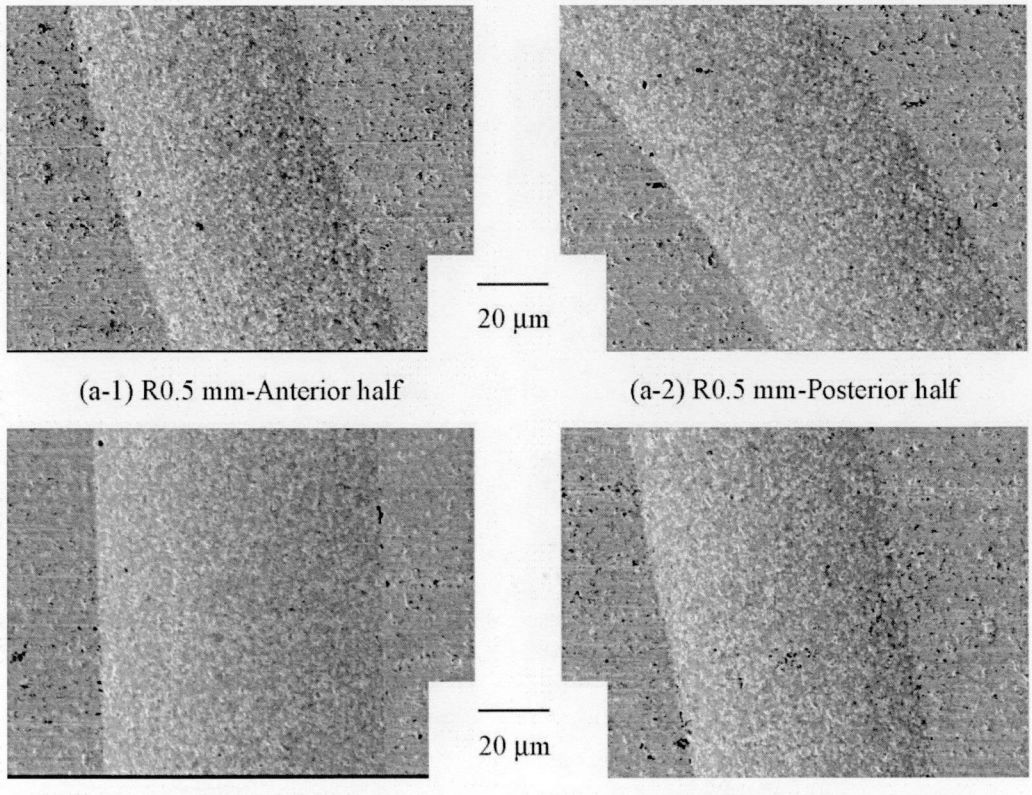

(a-1) R0.5 mm-Anterior half (a-2) R0.5 mm-Posterior half

(b-1) R15 mm-Anterior half (b-2) R15 mm-Posterior half

Fig. 4-13 Machined microgrooves

4.3 Machining of hard material with ball end mill

4.3.1 Ball end milling of hard material

The machining of hard brittle material is introduced in Chapter 2. It is necessary to machine the hard material under the critical depth of cut. In the machining with ball end mill, the actual depth of cut is changed along the cutting edge. The machining with ball end mill is shown in Fig. 4-14, the radius of cutting tool is R, the feed per revolution is f, the depth of cut is d, and the critical depth of cut is d_c. As shown in this figure, the maximum depth of cut is h_a, which can be shown in Eq. (4-7). So when h_a is shorter than the critical depth of cut, the ductile mode machining can be realized by using ball end mill.

$$h_a = R - \sqrt{(\sqrt{R^2 - (R-d)^2} - f))^2 + (R-d)^2} \tag{4-7}$$

However, as shown in Fig. 4-14, because the arc part between point T and R can be removed in the machining, so if there is brittle fracture on this part, it can be removed in the machining, and good surface can be obtained if there is no brittle fracture on the part of TQ. At this time, the actual depth of cut becomes h. By this way, with the same tool rotation speed, the feed rate of tool can be set faster, and the efficiency of cutting can be raised. The actual depth of cut h can be calculated as follows. At first, point O is considered as the origin of the relative coordinate system. At this time, the inclination of line OT is θ, which is shown in Eq. (4-8). Then, the equation of circle 1 can be shown in Eq. (4-9), and that of circle 2 can be shown in Eq. (4-10). Nest, the coordinate of point P (Y_P, Z_P) and point T (Y_T, Z_T) can be calculated by using these equations. At last, the length of segment PT can be calculated by the coordinate of point P and T.

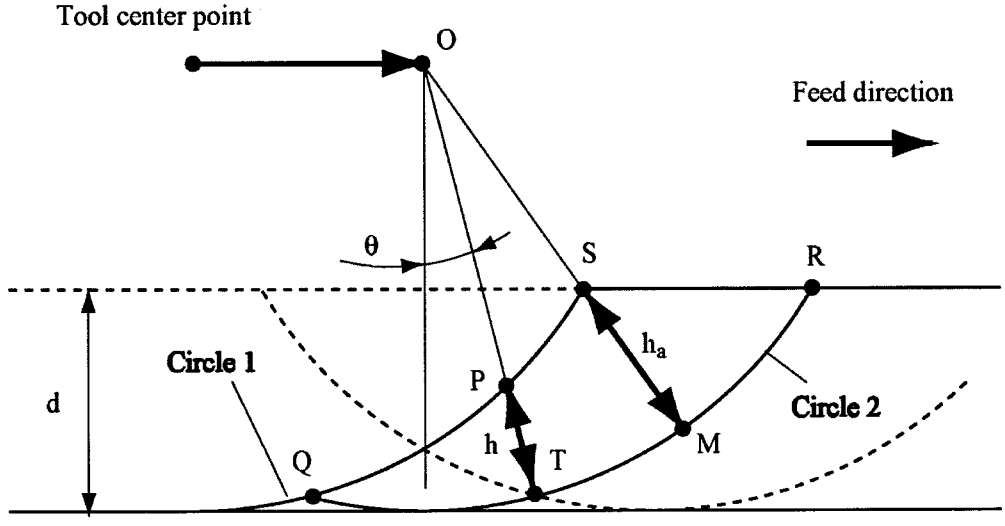

Fig. 4-14 Ball end milling

$$\theta = \sin^{-1} f/2R \tag{4-8}$$

$$(x + f)^2 + y^2 = R^2 \tag{4-9}$$

$$x^2 + y^2 = R^2 \tag{4-10}$$

Then, an experiment is conducted to investigate the tool wear in the machining of hard material by ball end mill. The cutting conditions are shown in Table 4-3, two experiments are conducted. One is the experiment with high cutting speed and low feed rate, and the other one is the experiment with low cutting speed and high feed rate. The cutting speed v_c can be shown in Eq. (4-11). Here, R is the radius of tool, and v_r is the rotation speed of tool

$$v_c = 2R\pi v_r/1000 \tag{4-11}$$

When the cutting speed is high, it is known that the cutting force can be reduced so that the tool wear can be reduced at the same time. However, the heat in the cutting becomes large and there is the threat of the increase in cutting temperature which causes the severe tool wear. As shown in Eq. (4-11), the cutting speed depends on the rotation speed and the radius of tool, and it can be adjusted by the rotation speed of tool. In the experiment with high cutting speed and low feed rate, the rotation speed is set to be 30,000 rpm and the feed rate is set to be 2.0 mm/min. At this time, the cutting speed is 18.85mm/min, the feed per revolution is 67 nm, and the actual cutting depth h is 0.42 nm. To compare with this, in the experiment with low cutting speed and high feed rate, the rotation speed of tool is set to be 20,000 rpm, and the feed rate is set to be 40 mm/min. The cutting speed is 12.57 mm/min, the feed per revolution is 2 μm, and the actual cutting depth h is 39.46 nm. The machining shape is microgroove with length of 12.5 mm, and depth of 5 μm, which is the same as the experiment in

Table 4-3 Cutting conditions

	Ball end milling		Cutting point swivel machining
	Low feed rate	High feed rate	
Workpiece	SiC		
Rotation speed	30,000 rpm	20,000 rpm	
Cutting speed	18.850 mm/min	12.566 mm/min	
Depth of cut	500 nm		80 nm
Total depth	5 μm		
r_v			0.028
Feed rate in Z direction	2 mm/min	40 mm/min	1 mm/min
Cutting fluid	Oil mist		

cutting point swivel machining.

The rake face of cutting tool after machining is shown in Fig. 4-15. (a) shows the tool used in the experiment with low feed rate and (b) shows the tool used in the experiment with high feed rate. As shown in these figures, severe tool wear can be observed on the cutting edge. When the feed rate is 2.0 mm/min, there is about 9 μm tool wear on the cutting edge, and it is reduced by increasing the feed rate. When the rotation speed is increased, and the feed rate is reduced, the removed volume of workpiece per revolution becomes small, and the cutting force can be reduced. So it is expected to suppress tool wear. However, the tool wear becomes worse conversely in the cutting experiment. Then, Fig. 4-16 shows the flank face of the tool used in the machining with high feed rate. There is about 5 μm wear on the flank face. To compare with these ball end mills, the tool used in the cutting point swivel machining is shown in Fig. 4-17, the speed ratio r_v is 0.028, and the machining shape is the same. Several microchippings can be observed on the cutting edge of the non-rotational tool. However, there is scarcely any tool wear on the cutting edge. It is confirmed that there is no chipping on the cutting edge by using the ball end mill. However, the tool wear on the cutting edge becomes much

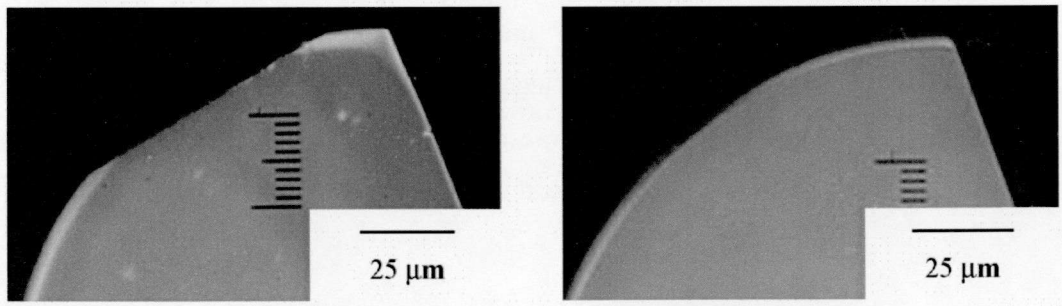

(a) Low feed rate (b) High feed rate

Fig. 4-15 Rake face of tool after machining

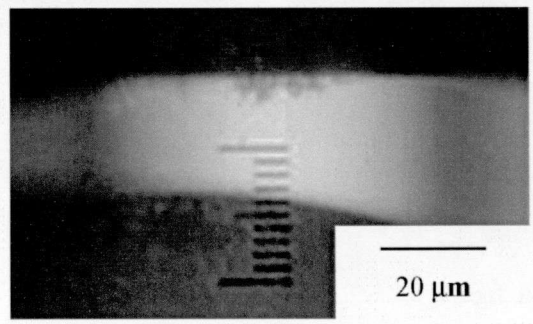

Fig. 4-16 Flank face of tool with high feed rate

larger than that of non-rotational tool.

Then, the surfaces of machined microgrooves are shown in Fig. 4-18. Figure 4-18 (a) shows microgrooves machined with low feed rate, (b) shows microgrooves machined with high feed rate and (c) shows microgrooves machined by cutting point swivel machining, respectively. As shown in these figures, the cutting mark can be observed on the microgroove, so it can be known that the microgrooves are machined in ductile mode. The microgrooves machined by ball end mill with low feed rate shows the best surface. It is considered as, in the machining of SiC, by the drop of Si grains and SiC grains, there is the occurrence of grain drops on the surface. In the machining with low feed rate, the feed per revolution is small, and the cutting force is less than the combining forces between the grains. So the occurrence of grain drops on the surface becomes less. However, as shown in these figures, there is large deterioration on the shape accuracy of the microgroove. In the first microgroove, there is the shape error on the cross section of the microgroove, and it becomes worse and worse. There is even no microgroove at the end of machining. To compare with this, the microgroove machined with high feed rate shows better shape accuracy. The first microgroove shows circle cross section, and there is the shape error on the 15^{th} microgroove. However, the depths of machined microgrooves are the same. Then, the microgroove machined by cutting point swivel machining shows the best shape accuracy. Although there is the setting error to cause the depth of microgroove deeper than target shape, the shape of both 1^{st} and 15^{th} microgroove shows good shape accuracy. The reason is considered as severe tool wear occurs in the machining and it is transferred into the surface to cause the deterioration of the shape accuracy. As a result, although the microgroove machined by ball end milling with low feed rate shows good surface, there is large error in the shape accuracy.

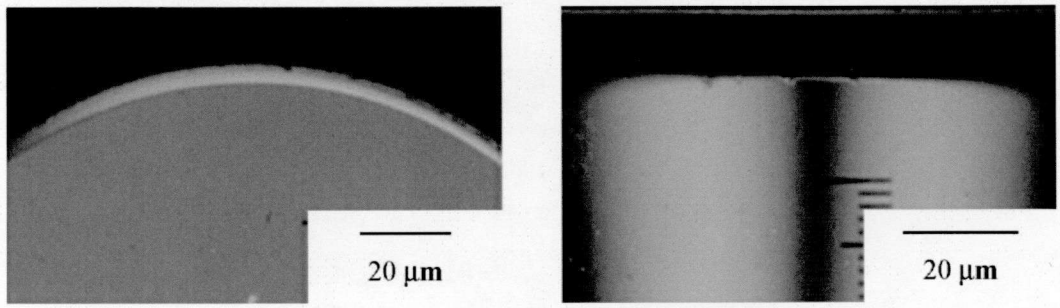

(a) Rake face (b) Flank face

Fig. 4-17 Tool after machining by cutting point swivel machining

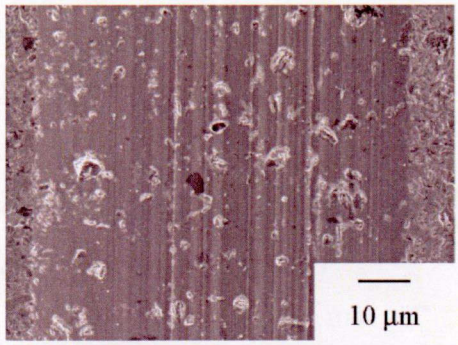

(1) SEM photo of 1st microgroove

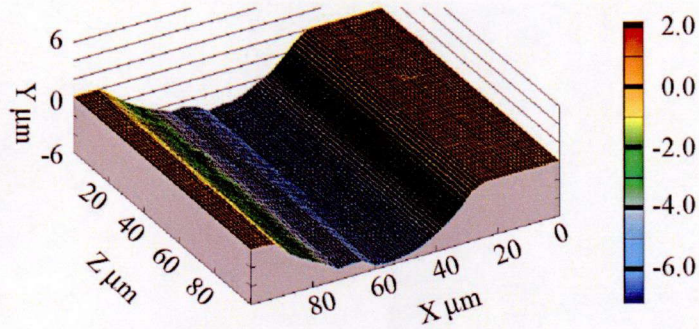

(2) Measured result of 1st microgroove

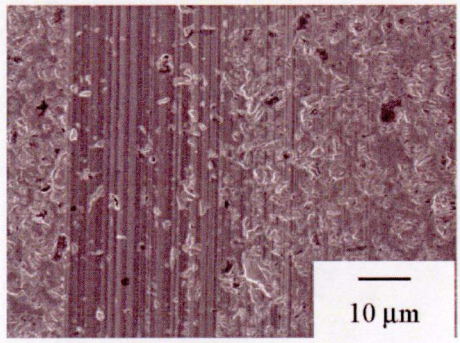

(3) SEM photo of 15th microgroove

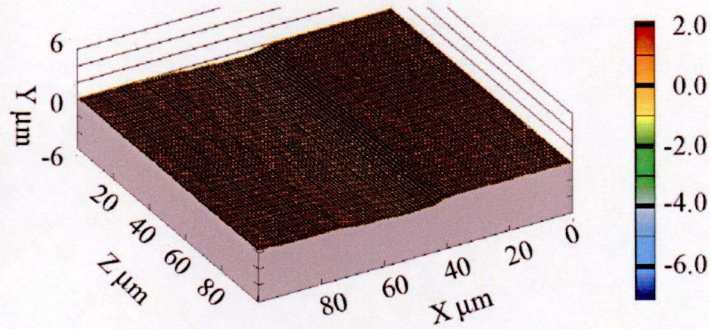

(4) Measured result of 15th microgroove

(a) Microgrooves machined by end milling with low feed rate

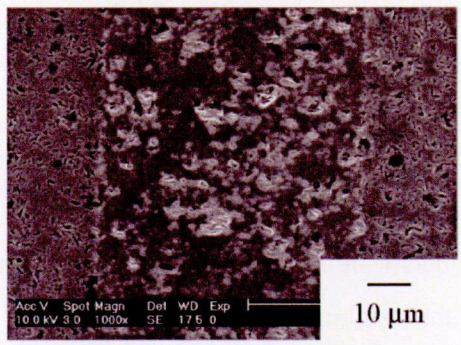

(1) SEM photo of 1st microgroove

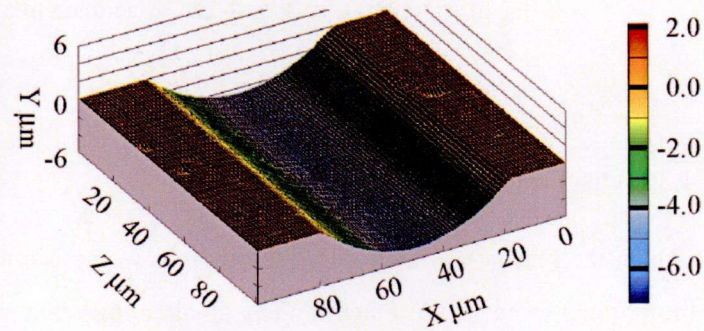

(2) Measured result of 1st microgroove

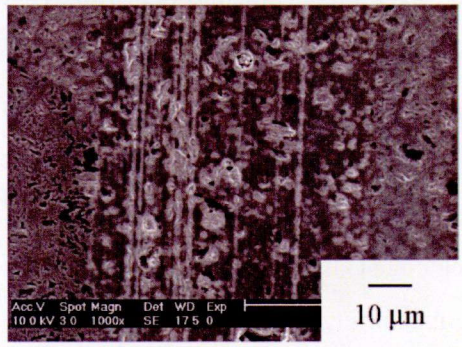

(3) SEM photo of 15th microgroove

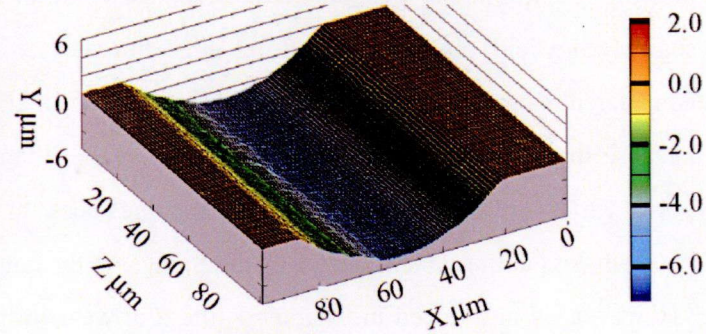

(4) Measured result of 15th microgroove

(b) Microgrooves machined by ball end mill with high feed rate

Fig. 4-18 Machined microgrooves

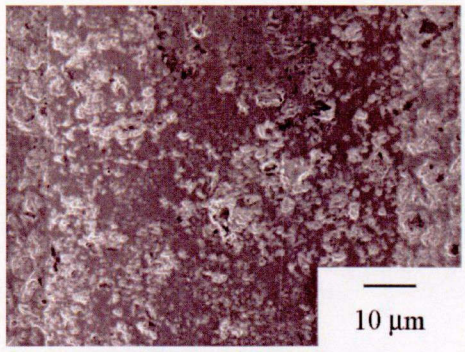

(1) SEM photo of 1st microgroove

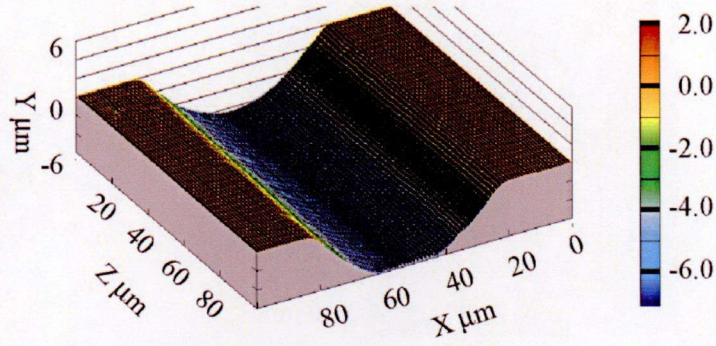

(2) Measured result of 1st microgroove

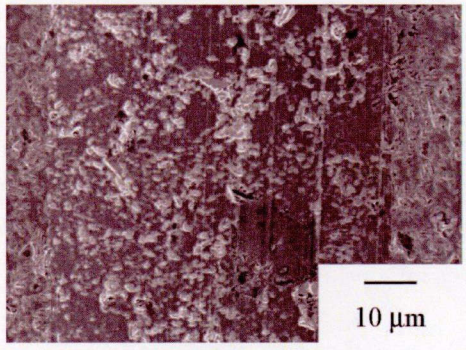

(3) SEM photo of 15th microgroove

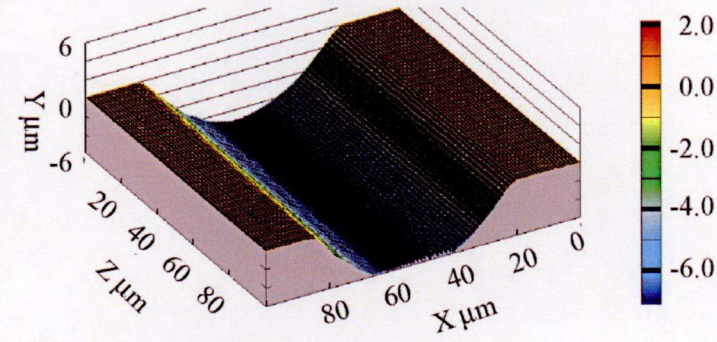

(4) Measured result of 15th microgroove

(c) Microgrooves machined by cutting point swivel machining

Fig. 4-18 Machined microgrooves

4.3.2 Discussion

Then, the reason that the tool wear becomes worse is considered. In the machining by ball end mill, the cutting force in the machining is smaller than that of the machining by non-rotational tool. In addition, the tool wear can be suppressed by the effect of intermittent cutting. However, in the machining experiment, the tool wear becomes worse in the machining with ball end mill. There is scarcely any chipping on the cutting edge but the tool wear is more severe. The reason can be considered as, the cutting force in ball end milling is smaller than the depth of cut in sharp machining, because the feed rate per revolution is much smaller than that of sharp machining, so the number of pores which are removed by the tool becomes less, and the impact which is subject to the tool becomes less at the same time. So the chippings on the cutting edge can be suppressed effectively.

However, as introduced in Chapter 1, the tool wear in the machining of hard material is almost the flank wear, which is caused by the friction between the flank face and workpiece. As shown in Fig. 4-19, in the ball end milling, because the tool is feed while being rotated, the contact distance between the flank face of tool and workpiece becomes much longer. Feed per revolution is f, the depth of

microgroove is D, the depth of cut is d, the number of microgroove is n, and the length of microgroove is l, so the maximum contact distance between tool and workpiece can be shown in Eq. (4-12). To compare with the contact distance of cutting point swivel machining, 5,812 mm, the distance in the ball end milling with high feed rate is 10,316 mm which is 1.8 times to that of the sharp machining, and that with low feed rate is 271,923 mm which is about 47 times to the sharp machining. This is the main reason that the tool wear become more severe.

$$\mathrm{L} = (\cos^{-1}\frac{\sqrt{R^2-f^2}}{R} + \cos^{-1}\frac{R-d}{R}) \times \frac{2\pi nRDl}{360df} \tag{4-12}$$

Then, the machining time of one microgroove is 3 minutes (ball end milling with high feed rate), 60 minutes (ball end milling with low feed rate) and 15 hours (cutting point swivel machining) respectively. To compare with the cutting point swivel machining, the machining times of ball end milling can be reduced substantially. However, the tool wear becomes severe and the shape accuracy becomes worse at the same time.

4.4 Curved surface machining

4.4.1 Application to curved surface machining

In the experiment of Section 4.3, it is confirmed that to compare with ball end milling, the cutting point swivel machining has the ability to suppress tool wear, and to keep the high precision machining for longer time. Then, the cutting point swivel machining is applied to the machining of curved surface. The setting of tool and workpiece is shown in Fig. 2-15, the tool is fed in Z direction, and X direction is the pick feed direction. The algorithm is shown in Fig. 4-20. There are two parts of calculation. One

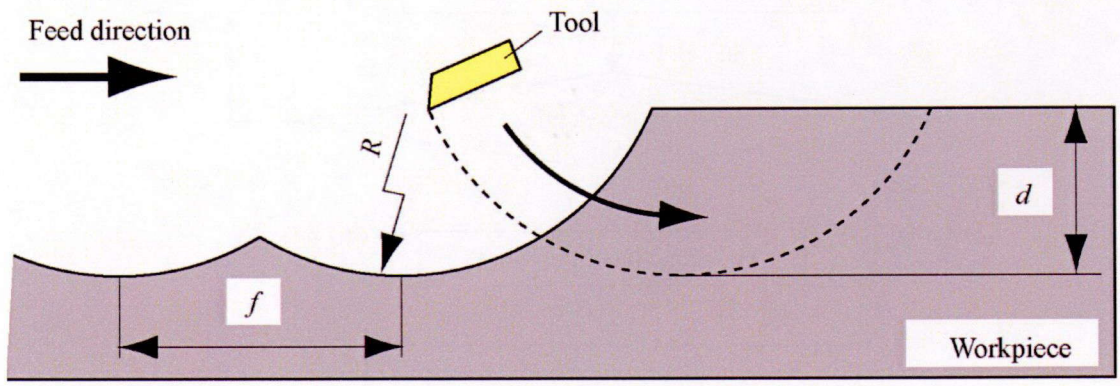

Fig. 4-19 Calculation of the contact distance between the flank face and workpiece

is the pick feed in X direction, and the other is the tool posture. The machining is presumed as the finish machining of the hard material, so the depth of cut is always set smaller than the critical depth of cut.

At first, the pick feed in X direction is calculated. When n+1th path is machined in X direction, the cross-section in XY plane of *i*th cutting point in Z direction is shown in Fig. 4-21. The dashed line shows the part which need to be removed in n+1th path machining. Here, the pick feed in X direction is pf_i, the cutting depth of nth path is h_n, and that of n+1th path is h_{n+1}, and the angle between segment PQ and X axis is θ, the critical depth of cut is *cd*, and the radius of tool is *R*. At first, the length of segment OQ is set to be the same as the critical depth of cut. Here, the length of segment OQ *l* is shown in Eq. (4-13). By this equation, the pick feed in X direction pf_i can be calculated as Eq. (4-14).

$$l = pf_i - \sqrt{R^2 - (R - h_n)^2} + \sqrt{R^2 - (R - h_{n+1})^2} \tag{4-13}$$

$$pf_i = \mathrm{cd} + \sqrt{R^2 - (R - h_n)^2} - \sqrt{R^2 - (R - h_{n+1})^2} \tag{4-14}$$

Then, the angle θ is calculated as shown in Eq. (4-15) and Eq. (4-16). By the calculated θ and other parameter, the length of segment OT L_i can be calculated by Eq. (4-17) and Eq. (4-18).

$$\theta = \tan^{-1} \frac{\sqrt{c^2 - 4bd} - c}{2b\sqrt{R^2-(R-h_n)^2} + 2bpf_i + 2ab + 2(h_n - h_{n+1})(c - \sqrt{c^2 - 4bd})} \tag{4-15}$$

Here,

$$\begin{cases} a = (pf_i^2 + h_{n+1}^2 - h_n^2 + 2h_nR - 2h_{n+1}R)/(2pf_i) \\ b = 1 + 4(h_n - h_{n+1})^2/pf_i^2 \\ c = 2(R - h_n + a(h_n - h_{n+1})/pf_i) \\ d = (R - h_n)^2 + a^2 - R^2 \end{cases} \tag{4-16}$$

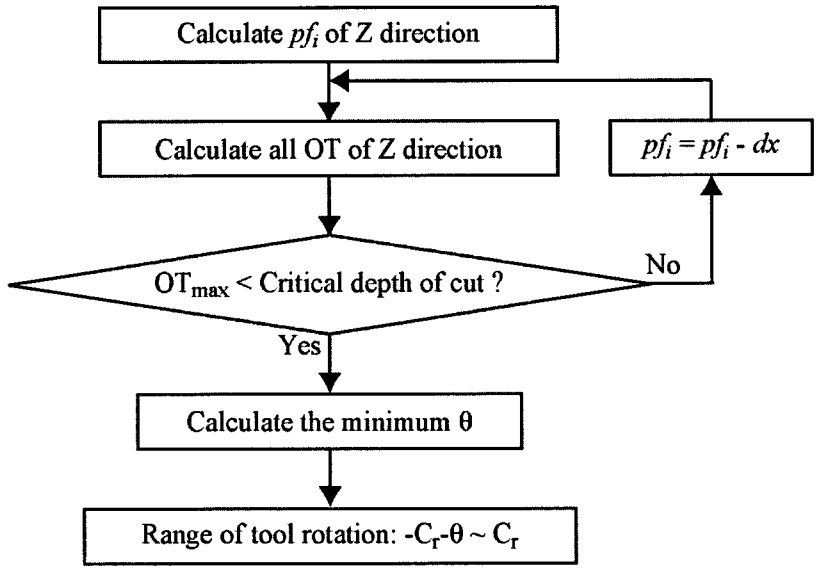

Fig.4-20 Algorithm for applying to surface machining

$$L_i = -\frac{e\tan\theta+g-\sqrt{(e\tan\theta+g)^2-(1+\tan\theta)(e^2+g^2-R^2)}}{\cos\theta(1+\tan^2\theta)} \tag{4-17}$$

Here,

$$\begin{cases} e = \sqrt{R^2-(R-h_1)^2} - pf_i \\ g = R - h_2 \end{cases} \tag{4-18}$$

Then, the length L_i is compared to the critical depth of cut. If the length L_i is larger than the critical depth of cut, the pick feed pf_i is reduced until the length L_i is smaller than the critical depth of cut. At last, the length L_i of all cutting points in Z direction is calculated, and the pick feed pf_i is reduced to make sure that the length L_i of all cutting points are smaller than the critical depth of cut.

Then, the posture of the tool is calculated. As shown in Fig. 4-21, when the n+1th path is machined, because the left part of workpiece has been removed in the nth path machining, there is no tool interference which is the machining with the part that is not like circle of the tool in the left side. To use the broad part of the tool, the tool rotation angle is set to be ($-Cr-\theta \sim Cr$). Here, Cr is the original tool rotatable angle. And the tool posture can be calculated in Eq. (4-19).

$$\mathrm{C} = C_r - \left|0.5 - \left(\frac{45r_v l}{\pi R(C_r+\theta/4)} - int\left(\frac{45r_v l}{\pi R(C_r+\theta/4)}\right)\right)\right| \times (4C_r+\theta) - \frac{\theta}{4} \tag{4-19}$$

4.4.2 Plane machining

An experiment is conducted to investigate the surface which is machined by cutting point swivel machining. The target shape is a plane with length of 0.8 mm, width of 0.6 mm, and depth of 16 μm. The cutting conditions are shown in Table 4-4 (Experiment A). The speed ratio is set to be 0.05, and the depth of cut is set to be 50 nm. The calculated pick feed in X direction is 50 nm. To compare with

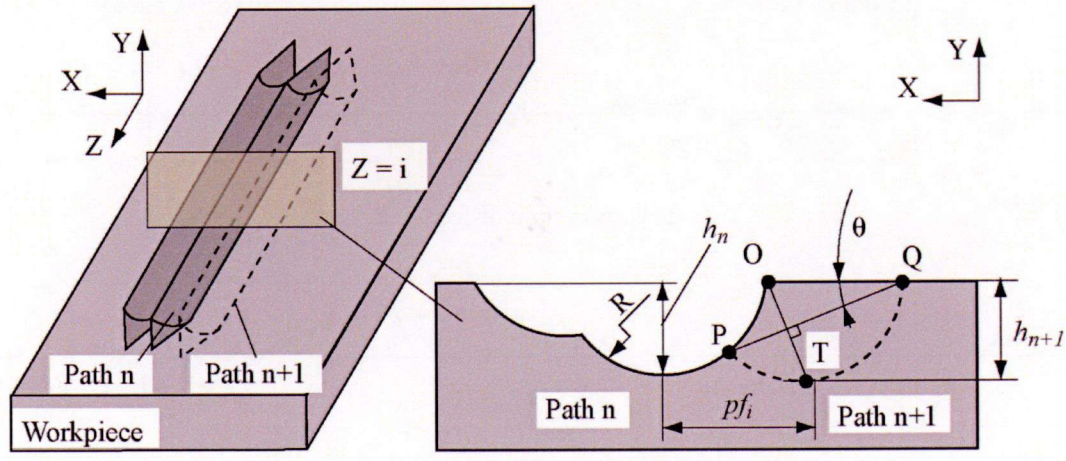

Fig.4-21 Calculation of pick feed

the time which costs in the machining of one path, the number of path is too large. So the long side is set to be feed direction and the short side is set to be pick feed direction, to reduce the machining time. The machining time is 78.8 hours, and the machining distance is 9,856 mm.

Machined result is shown in Fig. 4-22. Figure 4-22 (a) shows the measured result, (b) shows the SEM photo of the machined plane and (c) shows the cross-section in the feed direction and pick feed

Table 4-4 Cutting conditions

	Experiment C	Experiment D	Experiment E
Workpiece	Binderless Tungsten carbide J05		
Interpolation	3 μm	2.5 μm	0.05 μm
Speed ratio r_v	0.05		
Depth of cut	50 nm		
Feed rate	5 mm/min		3 mm/min
Cutting fluid	Oil mist		

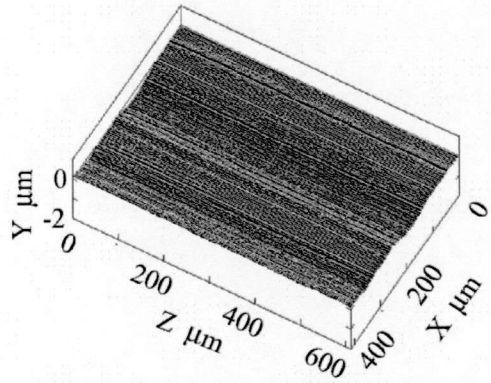

(a) Whole view

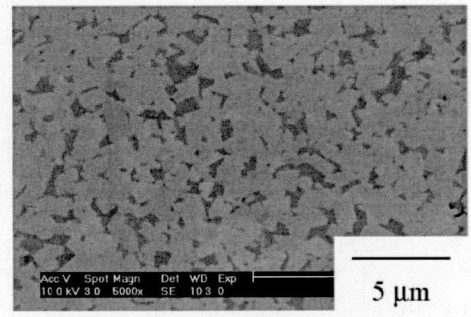

(b) SEM photo

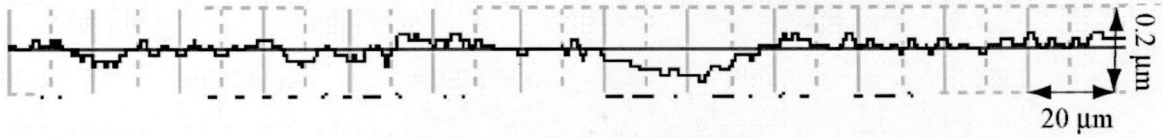

(c-1) Cross setion of feed direction

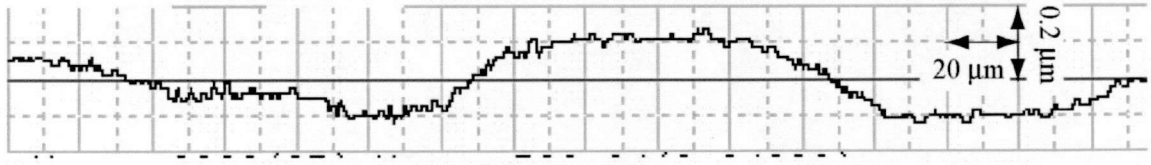

(c-2) Cross setion of pick feed direction

Fig.4-22 Machined plane

direction, respectively. From the measured result, 5 cross-sections are selected in both feed direction and pick feed direction to calculate the roughness of the surface. Roughness Ra and Rz in feed direction and pick feed direction are summarized in Table 4-5. In the feed direction, the roughness Ra of all cross-sections are 10 nm, and roughness Rz is from 0.05 to 0.07 μm. The average of the roughness Rz in this direction is 0.060 μm. Then, the roughness Rz in the pick feed direction is from 0.07 to 0.08 μm, and the average is 0.074 μm. As a result, good surface roughness can be obtained in both feed direction and pick feed direction.

4.4.3 Curved surface machining

Then, a curved surface is machined by using cutting point swivel machining. The target shape is shown in Fig. 4-23, which is combined with concave surface and convex surface in Z direction. The cross-section in X direction is a curve, and the elevation difference from two sides is 10 μm. the cutting conditions are shown in Table 4-4 (Experiment B). The machining time is 69.5 hours. Then, there is a curved microgrooving on the machined curved surface. This curved microgroove is

Table 4-5 Measured roughness

Measured roughness μm							Average μm
Feed direction	R_a	0.01	0.01	0.01	0.01	0.01	0.010
	R_Z	0.05	0.06	0.06	0.06	0.07	0.060
Pick feed direction	R_a	0.01	0.01	0.01	0.01	0.01	0.010
	R_Z	0.07	0.08	0.07	0.08	0.07	0.074

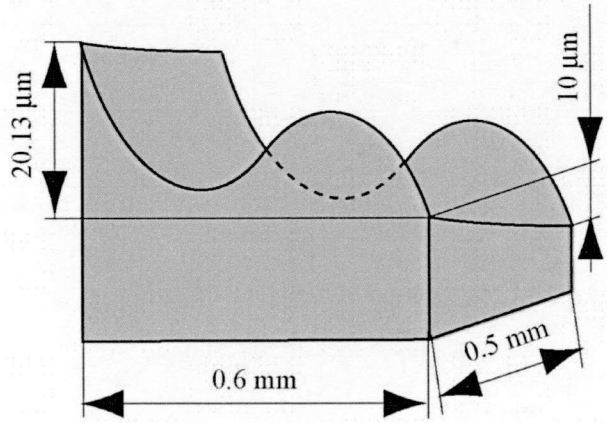

Fig. 4-23 Target shape

combined by two arcs with the radius of 0.4 mm, and the length of the microgroove is 0.4 mm. the cutting condition of curved microgrooving are shown in Table 4-4 (Experiment C). The machining time of microgrooving is 2.3 hours. The machining distance of curved surface is 6,312 mm, and that of the curved microgroove is 40 mm.

The measured result is shown in Fig. 4-24. Figure 4-24 (a) shows the whole view, and (b) shows the cross-section of pick feed direction with two different X coordinate. From these result, it is confirmed that the curved surface and curved microgroove are machined the same as target shape.

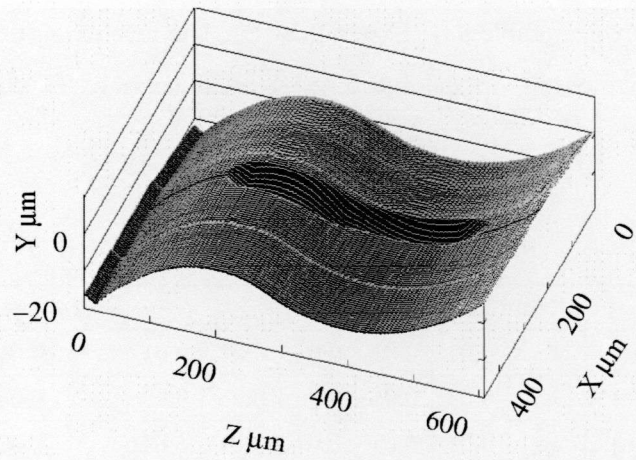

(a) Whole view

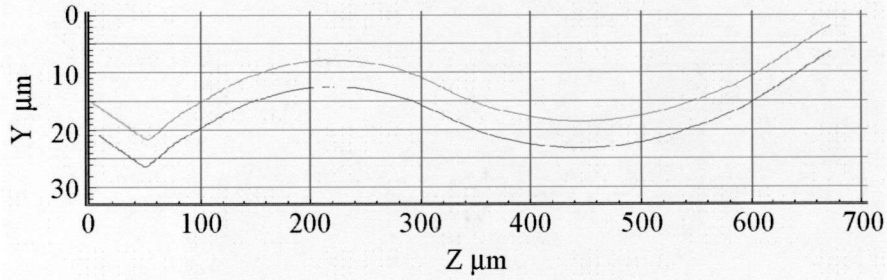

(b) Cross-section of pick feed direction

Fig. 4-24 Measured result

The SEM photos of machined surface are shown in Fig. 4-25. (a) shows the concave part, (b) shows the convex part and (c) shows the microgroove. As shown in (a) and (b), it is confirmed that good surface is obtained in the machining. However, there is a large number of the grain drops in the

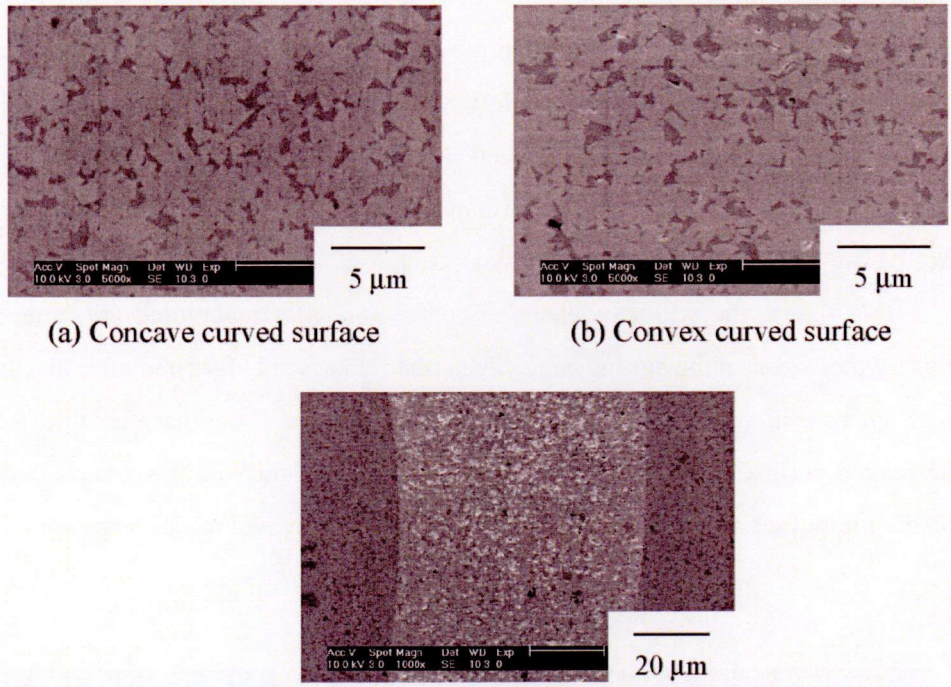

(a) Concave curved surface (b) Convex curved surface

(c) Curved microgroove

Fig.4-25 SEM photo of machined curved surface and microgroove

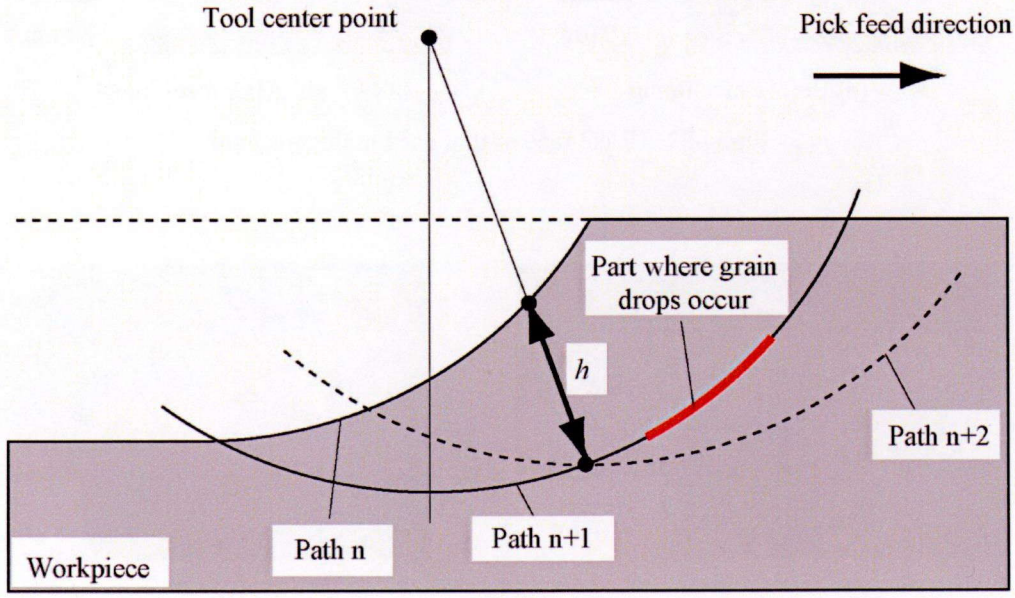

Fig. 4-26 Remove of the part with grain drop

microgrooving. The depth of cut in the curved surface machining and microgrooving is set to be the same. However, there are a lot of grain drops on the surface of microgroove. The reason is considered as, in the machining of curved surface, the maximum depth of cut is set to be 50 nm, so there are several parts with grain drops. However, as shown in Fig. 4-26, these parts are removed by the next path of machining. The actual depth of cut, *h*, is smaller than the setting value. In the machining of these parts, the cutting force is smaller than the combining forces of tungsten carbide grains, so there is no grain drop on the machined surface. However, in the machining of microgroove, the cutting force is larger than the combining forces of tungsten carbide grains, so the grain drops in the machining.

The same tool is used in the plane machining, curved surface machining and microgrooving. The rake face before and after machining is shown in Fig. 4-27. Total machining distance is 16,208 mm. As shown in this figure, the width of chamfer before and after machining are both 3.6 μm, there is scarcely any tool wear on the cutting edge. Then, the flank face before and after machining is shown in Fig. 4-28. There is no tool wear or chipping on the flank face. From these results, it can be confirmed that the curved surface which is the same as target shape and with good surface roughness can be machined with tool wear suppression by using cutting point swivel machining.

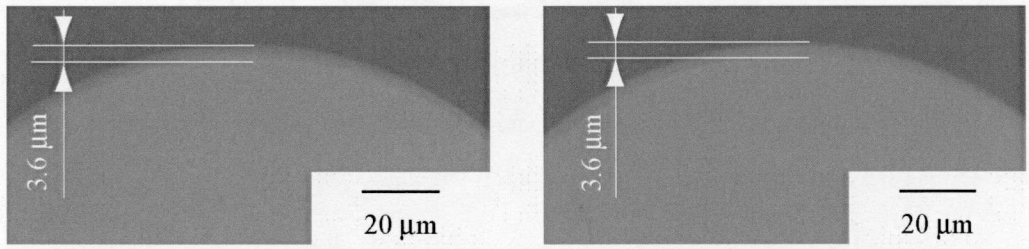

(a) Before machining (b) After machining

Fig. 4-27 Rake face of tool used in the machining

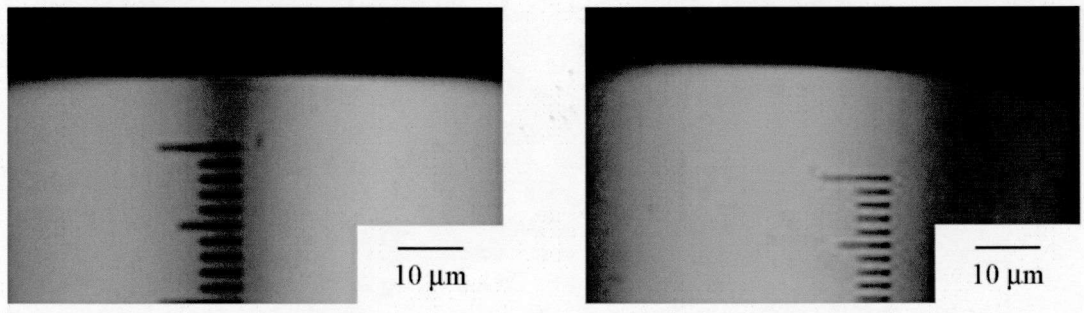

(a) Before machining (b) After machining

Fig. 4-28 Flank face of tool used in the machining

4.5 Summary

This chapter aims at applying the cutting point swivel machining to the curved microgrooving and the machining of the curved surface. As the result of the experiment on binderless tungsten carbide, the conclusion can be summarized as follows.

1) The cutting point swivel machining is applied to the machining of the curved microgroove. By the verification experiment of the S shape microgroove, it is confirmed that the curved microgroove can be machined with good shape accuracy.
2) It is known that in the machining of the curved microgroove, the direction and volume of the relative velocity between the tool and workpiece on the inside and outside of microgroove are different. In the experiment of the microgrooving with arbitrary curvature, it is confirmed that by using the cutting point swivel machining, microgroove with arbitrary curvature can be machined with good accuracy.
3) The ball end mill is mostly used in the machining of curved surface. However, in the machining of hard material, the contact distance between the flank face and workpiece becomes too long because of the rotation of the tool. By this reason, the tool wear is more severe than that of the cutting point swivel machining. In the machining with low feed rate, the grain drop on the surface can be reduced. However, the tool is worn and the deterioration of the shape accuracy becomes rapidly.
4) In the machining of hard material by ball milling, the machining time is so short that good machining efficiency can be obtained. However, the tool is worn rapidly, and the worn tool shape is transferred into the surface to cause the deterioration of shape accuracy. To compare with this, although the efficiency of cutting point swivel machining is bad, the tool wear is much less than that of ball end milling and good shape accuracy can be obtained for longer time.
5) The cutting point swivel machining is applied to the machining of curved surface. in the machining of the plane, it is confirmed that good roughness can be obtained in both feed direction and pick feed direction. Then, in the verification experiment, a free-form surface is machined the same as the target shape with no tool wear on both rake face and flank face of cutting edge.

As summarized above, the cutting point swivel machining is applied to the curved microgrooving and machining of curved surface with tool wear suppression. However, there are still several problems need to be solved.

a) In the machining of curved surface by the cutting point swivel machining, it is presumed as the finish machining of hard material, so the depth of cut is set smaller than the critical depth of cut. As shown in Fig. 4-26, if the actual depth of cut h is set the same as critical depth of cut, the machining efficiency can be increased.

b) In the experiment of Section 4.3, it is known that the machining efficiency of ball milling is good, and the machined surface of cutting point swivel machining is well. So it is need a composition machining method, that the rough machining is ball end milling and finish machining is cutting point swivel machining. By this way, both machining efficiency and accuracy can be obtained.

Chapter 5
SUMMARY

5.1 Achieved results in this study

The cutting operation, which has lots of advantages and is the most fundamental machining method, acts an important part in the manufacturing. Then, as an important element, the cutting tool, which is pushed into the workpiece, has a potent influence on the accuracy of machined shape and surface. Among them, the tool life is always focused because it is combined with the productivity and manufacturing cost directly. In recent years in particular, it is requested to cutting the hard material with high precision and miniaturization because of the improvement of optical equipments. In the machining of hard material, the most important proposition is how to make the tool life as long as possible, to keep the high precision machining for long time.

There are large numbers of investigations to increase the tool life. Almost of them are focused on the material of tool, tool shape, surface treatment, cutting conditions and so on. By the combination of these elements, the tool wear in the machining can be suppressed. However, the number of investigations about the machining method is so small, and some of the machining method needs special machine like the vibration machine tool. Under this background, this study focused on the machining method to suppress tool wear and to increase tool life in the machining of hard material. This study aims to create a new machining method which has the ability to suppress tool wear and to realize high precision machining at the same time. By using 5-axes machining center, a machining method called cutting point swivel machining is proposed, and its effect is verified by the cutting experiment. By applying the cutting point swivel machining to complex shape, it is expected to create a new machining method in the machining of hard material.

Then, the results of this study are summarized as follows.

In Chapter 2, the mechanism of brittle fracture and the effect of the tool with negative rake angle in the machining of hard material are summarized. By using these past investigations, the rake angle, which is an important part in the machining of hard material, is decided. Then, from Section 2.3, the cutting point swivel machining is proposed. By the verification experiment, the result can be summarized as follows.

1) By using the tool with special chamfer, the cutting point swivel machining, that the tool is swiveled in the plane perpendicular to the tool feed direction, is proposed. To compare with other

machining method, the cutting point swivel machining can be realized easily by using the rotation axis, and it is expected to suppress and average the tool wear.

2) In the cutting point swivel machining, there is a problem of the setting error between the tool center point and the center of C axis. Then, a try cutting is proposed to calculate the coordinate of tool center point. By using this calculated coordinate, the setting error can be compensated by modifying the NC data, which controls the tool path and tool posture. By the result of the verification experiment, it is confirmed that the proposed method has the ability to compensate the setting error and to realize ultraprecision machining.
3) By the verification experiment of SiC, it is confirmed that to compare with the conventional machining, the cutting point swivel machining can extend tool life to more than two times. In addition, good roughness and shape accuracy can be obtained by using cutting point swivel machining, because of the suppression of tool wear, and the machining with high precision can be continued for long time.

In Chapter 3, it aims at investigating the mechanism of the cutting point swivel machining, and making clear the relationship among the speed ratio, cutting forces and tool wear. As the result of the experiment of cutting forces with different speed ratio and the experiment of tool wear on SiC and tungsten carbide, by using cutting point swivel machining which is proposed in Chapter 2, the results can be summarized as follows.

1) The cutting marks can be observed on the surface of machined microgrooves. From these cutting marks, it is known that the actual cutting direction can be changed by using cutting point swivel machining. The actual cutting direction is calculated and it is the same as the direction of cutting marks. In addition, it is confirmed that good shape can be obtained even the rotation direction is changed.
2) The tool is fed while being rotated in cutting point swivel machining. At this time, the moving distance of cutting edge is longer than that without rotating, to remove the same volume of workpiece. So the actual cutting width becomes small, and the cutting force in tool feed direction can be reduced to suppress tool wear. In addition, the tool wear can be averaged by using broad part of cutting edge, and the cutting fluid can be supplied between the tool and workpiece easier. By these reasons, tool wear can be suppressed substantially.
3) The cutting forces are estimated by using the equation which is proposed by Kato et al. and minimum energy theory. As a result, it is found that both the cutting force F_z and thrust force F_y can be reduced by rotating the tool and they can be reduced furthermore by increasing the speed ratio. To compare with these forces, the rotation force is so small that can be ignored.

4) In the experiment of cutting forces, it is found that the cutting forces in dry cutting can be reduced by using cutting point swivel machining, and it can be reduced furthermore by increasing the speed ratio from 0.028 to 0.5. Then, in the wet cutting, the cutting force can be reduced by using cutting point swivel machining. However, the reduction of cutting forces by increasing the speed ratio is very small. The reason is considered as that the component force in Y direction of friction force is so small that the lubrication effect of cutting fluid becomes small.
5) To compare with the estimated and measured cutting forces, the reduction of cutting force by increasing the speed ratio is different. However, they show the same trend that the cutting force can be reduced by the increase of speed ratio.
6) When the speed ratio is increased from 0.003 to 0.028, it is found that the tool wear can be suppressed by increasing the speed ratio. The reason is considered as the reduction of cutting force.
7) When the speed ratio is increased from 0.028 to 0.5, it is confirmed that both the size and the number of chippings on the cutting edge is increased with no relation to the presence and absence of the cutting fluid. By this reason, there is the deterioration of the roughness of machined microgroove. Two reasons are considered as this phenomenon: one is the pore and Si grains in the workpiece which cause the micro impact to the tool, and the other one is the increase of contact distance between the flank face of tool and workpiece, which is caused by the rotation of the tool. However, the contact distance between the flank face of tool and workpiece is shorter than that of conventional machining because the cutting edge moves to outside of the workpiece.
8) In the cutting experiment of binderless tungsten carbide, the relationship of tool wear shows the same trend with that of SiC. However, the hardness of these materials are almost the same, and the cutting distance of binderless tungsten carbide is much longer than that of SiC, the tool wear on the cutting edge becomes small substantially. It can presume that there is the large influence to the tool wear by the pore in the workpiece.
9) By the experiment of the relationship between the speed ratio and tool wear, it is confirmed that there is an appropriate speed ratio which has the ability to suppress the tool wear to minimum.

In Chapter 4, it aims at applying the cutting point swivel machining to the curved microgrooving and the machining of the curved surface. As the result of the experiment on binderless Tungsten Carbide, the conclusion can be summarized as follows.

1) The cutting point swivel machining is applied to the machining of the curved microgroove. By the verification experiment of the S shape microgroove, it is confirmed that the curved microgroove can be machined with good shape accuracy.

2) It is known that in the machining of the curved microgroove, the direction and volume of the relative velocity between the tool and workpiece on the inside and outside of microgroove are different. In the experiment of the microgrooving with arbitrary curvature, it is confirmed that by using the cutting point swivel machining, microgroove with arbitrary curvature can be machined with good accuracy.
3) The ball end mill is mostly used in the machining of curved surface. However, in the machining of hard material, the contact distance between the flank face and workpiece becomes too long because of the rotation of the tool. By this reason, the tool wear is more severe than that of the cutting point swivel machining. In the machining with low feed rate, the grain drop on the surface can be reduced. However, the tool is worn and the deterioration of the shape accuracy becomes rapidly.
4) In the machining of hard material by ball milling, the machining time is so short that good machining efficiency can be obtained. However, the tool is worn rapidly, and the worn tool shape is transferred into the surface to cause the deterioration of shape accuracy. To compare with this, although the efficiency of cutting point swivel machining is bad, the tool wear is much less than that of ball end milling and good shape accuracy can be obtained for longer time.
5) The cutting point swivel machining is applied to the machining of curved surface. in the machining of the plane, it is confirmed that good roughness can be obtained in both feed direction and pick feed direction. Then, in the verification experiment, a free-form surface is machined the same as the target shape with no tool wear on both rake face and flank face of cutting edge.

As summarized as above, a new machining method which is called cutting point swivel machining is proposed in this study. Then, the cutting point swivel machining is applied to the curved microgrooving and the machining of curved surface, it is confirmed that the machining of complex shape with tool wear suppression can be realized. By using this technology, the machining with high precision and complex shape, which is requested in the machining of mold, can be realized. As a result, the machining method shows the originality and practical utility in industry.

5.2 Future prospects

Even though this research makes some original contributions to suppress tool wear and to realize high precision machining in the machining of hard material, there are still several problems need to be solved.

1. Three dimensions cutting theory by using tool with negative rake angle

In Chapter 3, the cutting force is estimated by using the balance of force and the minimum energy theory. However, the estimated cutting force only shows the same trend to the measured cutting force, and there is big difference between the values of these forces. The reason is considered that the cutting theory by using tool with negative rake angle is different from that with plus rake angle. In the machining, the tool with negative rake angle is used common because the stiffness of tool with negative rake angle is larger. So it is necessary to make clear the mechanism of the machining by using the tool with negative rake angle.

2. Verification of cutting point swivel machining by universal machining center.

In this study, the cutting point swivel machining is used only on ROBOnano, an ultraprecision machining center. There is problem that the feed rate of ROBOnano is too slow, so the effect of cutting point swivel machining cannot be verified completely. There is another problem that the accuracy of ROBOnano is so high that some problems cannot be found in the experiment. So it is necessary to verify the cutting point swivel machining on a universal machining center. New result can be obtained by increasing the speed ratio much higher, and there may be some new problems by using a universal machining center.

3. Construction of the composition machining method

In Chapter 4, it is found that the efficiency of ball end milling is well. However, the tool wear becomes severe and the shape accuracy becomes bad. To compare with this, the cutting point swivel machining has the ability to keep high precise machining for a long time, with bad efficiency. So it is considered to propose a new machining process that the rough machining is conducted by ball end milling, and only finish machining is done by cutting point swivel machining. By this way, the efficiency and the accuracy can be obtained at the same time. Although there are several problems like the positioning of cutting tool, and the measurement of shape before finish machining. It is very important for fabricating the mold of optical elements.

REFERENCE

[1] 中島利勝，鳴瀧則彦：機械加工学，(1983)，コロナ社

[2] 鶴田匡夫：光とレンズ，(1985)，日刊工業新聞社

[3] ニューガラスハンドブック編集委員会：ニューガラスハンドブック，(1991)，丸善

[4] 瀧野日出雄：カラスレンズの製造技術，精密工学会誌，70，5 (2004) 619

[5] J. L. Soret: Ueber Die Durch Kreisgitter Diffraction Shanomene, Annual Review of Physical Chemistry, 156 (1875) 99

[6] R. W, Wood: Phase-reversal Zone-plates and Diffraction-telescopes, Philosophical Magazine, 45 (1898) 511

[7] K. Miyamoto: The Phase Fresnel Lens, Journal of the Optical Society of America, 51 (1961) 17

[8] 鹿島伸悟：回折光学素子のレーザ顕微鏡への応用，光設計研究グループ第 10 回研究会予稿集，(1996) 42

[9] 丸山晃一：回折レンズの眼視系への応用，光設計研究グループ第 13 回研究会予稿集，(1997) 24

[10] 回折光学素子入門　増補改訂版，(2006)，オプトロニクス社

[11] 中井武彦：白色用回折レンズ，光学，32，8 (2003) 476

[12] 小野雄三：最近の回折光学素子 - 回折光学から周期構造の光学へ - ，光学，32，8 (2003) 468

[13] 高分子学会編：高分子工学講座，13，14，18 巻，(1964)，共立出版

[14] 泉谷徹郎：プラスチックレンズとガラスレンズ，精密機械，50，12 (1984) 15

[15] 日本機械学会編：超精密加工技術，(1998)，コロナ社

[16] 応用物理学会　光学懇話会編：新編　レンズ・プリズムの工作技術，(1969)，中央科学社

[17] ヴィリー・チョムラー著，浅野俊雄訳：レンズ・プリズムの工作技術，(1969)，恒星社厚生閣

[18] 吉田正太郎：レンズとプリズム - その研磨の実際 - ，(1985)，地人書館

[19] 光・薄膜技術マニュアル，(1989)，オプトロニクス社

[20] F. V. Tooley: The Handbook of Glass Manufacture, (1984), Ashlee Publishing Co., Inc.

[21] D. R. Vhlman and N. J. Kreidl: Glass: Science and Technology, (1984), Academic Press

[22] 河田圭一，佐藤　豊，水野和康：光学ガラスの超精密研削，愛知県工業技術センター研究報告，36 (2000) 30

[23] 松村　隆，矢島直樹：ガラスのボールエンドミル加工，2003 年度精密工学会春季大会学術講演会講演論文集，(2003)，366

[24] 松村　隆，大野威徳：ガラスのエンドミル加工における切削特性，日本機械学会第 5 回生産加工・工作機械部門講演会講演論文集，(2004)，275

[25] 大野威徳，松村　隆：ガラスのエンドミル切削における切れ刃形状が脆性損傷に及ぼす影響，2007 年度精密工学会秋季大会学術講演会講演論文集，(2007)，63

[26] 松村　隆，小澤秀之，大野威徳：エンドミルのシャンク形状がガラス切削の脆性損傷に及ぼす影響，2008 年度精密工学会春季大会学術講演会講演論文集，(2008)，153

[27] 割澤伸一，パイラットタンポーンプラサート，布川健太郎，光石　衛：ガラスの高速微細加工における塑性変形及び延性・脆性モード切削間遷移挙動の観察，日本機械学会第 4 回生産加工・工作機械部門講演会講演論文集，(2002)，81

[28] 帯川利之，白樫高洋，小田英一：ガラス切削における延性—脆性遷移のシミュレーション解析，1996 年度精密工学会秋季大会学術講演会講演論文集，(1996)，635

[29] 帯川利之，国枝泰博，篠塚　淳：マイクロボールエンドミルによるガラスの高能率切削，日本機械学会第 5 回生産加工・工作機械部門講演会講演論文集，(2004)，21

[30] 飯塚　保，上野　滋，森田　昇：フライカットによるガラスの延性モード切削に関する研究(第 1 報) - 工具材種による加工面の影響 - ，2008 年度精密工学会春季大会学術講演会講演論文集，(2008)，1033

[31] 勝木雅英：高精度光学ガラス素子成形技術，(独)日本学会振興会将来加工技術第 136 委員会第 16 回研究会資料，(2006)

[32] A. Pramanik, K. S. Neo, M. Rahman, X. P. Li, M. Sawa and Y. Maeda: Cutting performance of diamond tools during ultra-precision turning of electroless-nickel plated die materials, Journal of Materials Processing Technology, 140 (2003) 308

[33] 庄司克雄：超精密加工と非球面加工，(2004)，NTS

[34] Y. Liu, S. Hata, K. Wada, and A. Shimokohbe: Thermal, Mechanical and Electrical Properties of Pd-based Thin Film Metallic Galss, Japanese Journal of Applied Physics, 40, 9 (2001) 5382

[35] 田中隆史，増田　淳，藤本亮輔，不破久順：特殊 Ni 合金メッキ製金型によるガラスレンズ成形例，日本機械学会第 7 回生産加工・工作機械部門講演会講演論文集，(2008)，307

[36] 日本機械学会編：JSME テキストシリーズ - 加工学 I，(2006)，丸善

[37] 鳴瀧則彦：切削工具概論，精密工学会誌，61，6 (1995) 751

[38] 藤原順介，花崎伸作，金山博和，宮本　猛：超硬合金の切削 - 組成の違いが被削性に及ぼす影響 - ，2006 年度精密工学会秋季大会学術講演会講演論文集，(2006)，81

[39] 許　盛中，宮本　猛，花崎伸作，藤原順介：耐摩耗・耐衝撃工具用超硬合金の SEM 内微小切削，精密工学会誌，71，7 (2005) 926

[40] 許　盛中，宮本　猛，花崎伸作，藤原順介：超硬合金の切削に関する研究 - 旋削における PCD 工具の摩擦機構と切削抵抗 - ，精密工学会誌，69，12 (2003) 1724

[41] J. Yan, Z. Zhang and T. Kuriyagawa: Mechanism for Material Removal in Diamond Turning of Reaction-bonded Silicon Carbide, International Journal of Machine tools & Manufacture, 49 (2009) 366

[42] Z. Zhang, J. Yan and T. Kuriyagawa: Wear Mechanism of Diamond Tools in Ductile Machining of Reaction-bonded Silicon Carbide, Proceedingsof 6th International Conference on Leading Edge Manufacturing in 21st Century, (2009) 425

[43] E. Paul, C. J. Evants, A. Mangamelli, M. L. McGlauflin and R. S. Polvan: Chemical Aspects of Tool Wear in Single Point Diamond Turning, Precision Engineering, 18, 1 (1996) 4

[44] 加工データファイル，CBN 工具による難削材の切削，(財)機械振興協会技術研究所，(1976)

[45] 木村忠彦，木曽弘隆，鈴木雅春：多結晶焼結体工具による超硬合金の旋削，1985 年度精密工学会春季大会学術講演会講演論文集，(1985)，603

[46] 小林　豊：超硬合金切削用ダイヤモンド工具，砥粒加工学会誌，56，4 (2012) 222

[47] 小林　豊：焼結ダイヤモンド切削工具について，NewDiamond，27，3 (2011) 13

[48] 和田任弘，広　和樹，国友謙一郎，片岡篤司：超硬合金切削における PCD 工具の摩耗特性，日本機械学会関東支部・精密工学会山梨講演会講演論文集，(2005) 107

[49] 和田任弘：超硬合金切削におけるダイヤモンド焼結体の工具摩耗，粉体に関する討論会講演論文集，44 (2006) 156

[50] 和田任弘，広　和樹，国友謙一郎，片岡篤司：超硬合金切削における PCD 工具の摩耗特性，日本機械学会関東支部・精密工学会山梨講演会講演論文集，(2006) 127

[51] 和田任弘：超硬合金切削におけるダイヤモンド焼結体の工具摩耗，粉体及び粉末冶金，54，5 (2007) 311

[52] 仙波卓弥, 岡崎隆一, 角谷　均:ナノ多結晶ダイヤモンド製マイクロボールエンドミル，2009 年度精密工学会秋季大会学術講演会講演論文集，(2009)，21

[53] 仙波卓弥, 岡崎隆一, 角谷　均:ナノ多結晶ダイヤモンド製マイクロボールエンドミル，日本機械学会論文集　C 編，76，763 (2010) 768

[54] 角谷　均：ダイヤモンド合成用超高圧装置の最近の動向，高圧力の科学と技術，19，4 (2009) 264

[55] Miyamoto T., Fujiwara J. and Wakao K.: Influence of WC and Co in Cutting Cemented Carbides with PCD and CBN Tools, Key Engineering Materials, 407-408 (2009) 428

[56] M. Belmonte, A. J. S. Fernandes, F. M. Costa, R. F. Silva, P. Ferro and J. Sacramento: Wear Resistant CVD Diamond Tools for Turning of Sintered Hardmetals, Diamond and Related Materials, 12, 3-7 (2003) 738

[57] F. A. Almeida, F. J. Oliveira, M. Sousa, A. J. S. Fernandes, F. M. Costa, R. F. Silva and J. Sacramento: Machining Hardmetals with CVD Diamond Direct Coated Ceramic Tools: Effect of Tool Edge Geometry, Diamond Related Materials, 14, 3-7 (2005) 651

[58] 山本雄士，鈴木浩文，川端大樹，森脇俊道，藤井一二，後藤勇二，小野　孝：PCD フライス工具による超硬製マイクロ非球面金型の超精密切削に関する研究，日本機械学会第 6 回生産加工・工作機械部門講演会講演論文集，(2006)，179

[59] 山本雄士，鈴木浩文，森脇俊道，沖野　正，樋口俊朗：マイクロフレネルレンズ成形型の超精密研削(第2報) - モリブデン製ツルアによる鋭利なエッジを有する研削ホイールの精密ツルーイングとフレネル形状の研削加工の高精度化 - ，精密工学会誌，73，6 (2007) 688

[60] 鈴木浩文，古木辰也，町田一道，藤井一二，伊藤洋介，三浦太久真，小野　孝，後藤隆司：PCD マイクロフライス工具による超硬製微細金型の超精密加工 - フレネルレンズ金型加工用工具の開発，砥粒加工学会学術講演論文集，(2010) 63

[61] 鈴木浩文，岡田　睦，古木辰也，藤井一二：マイクロフライス工具による超硬金型の超精密切削 - 単結晶ダイヤモンド製マイクロフライス工具の試作と超硬合金の超精密切削の検証，2012 年度精密工学会秋季大会学術講演会講演論文集，(2012)，821

[62] 福井雅彦，田口勝也，本橋健次，大坪　寿：超硬合金材の直彫り加工，2003 年度精密工学会春季大会学術講演会講演論文集，(2003)，108

[63] 福井雅彦，田口勝也：超硬合金材の直彫り加工とその実用化，2004 年度精密工学会春季大会学術講演会講演論文集，(2004)，751

[64] 福井雅彦，田口勝也，原田建人：超硬合金材を用いた冷間鍛造用金型の直彫り加工，2005 年度精密工学会春季大会学術講演会講演論文集，(2005)，959

[65] 嘉戸　寛，一宮勇志：マイクロ・ナノ金型加工技術　超硬合金の直彫りによる微細形状加工，型技術，19，13 (2004) 10

[66] 許　盛中，宮本　猛，花崎伸作，藤原順介，天野詳毅：耐摩耗工具用超硬合金切削における切削油の効果，精密工学会誌，73，8 (2007) 896

[67] A. Yui, H. Matsuoka, T. Kitajima and S. Okuyama: Planning of Cobalt-Free Tungsten Carbide with PCD and CBN Tools, Key Engineering Materials, 389-390 (2009) 132

[68] 由井明紀，松岡浩司，田中隆之，奥山繁樹，北嶋孝之：単結晶ダイヤモンド工具による超硬合金の切削加工 - 第1報　ダイヤモンドと超硬合金の摩擦特性 - ，砥粒加工学会誌，54，9 (2010) 545

[69] 由井明紀，松岡浩司，奥山繁樹，北嶋孝之，岡畑　豪：単結晶ダイヤモンド工具による超硬合金の切削加工 - 第2報　加工雰囲気が切削点温度と工具摩耗に及ぼす影響 - ，砥粒加工学会誌，54，10 (2010) 613

[70] 由井明紀，松岡浩司，奥山繁樹，北嶋孝之，岡畑　豪：単結晶ダイヤモンド工具による超硬合金の切削加工 - 第3報　切削油剤が工具の摩擦・摩耗特性に及ぼす影響 - ，砥粒加工学会誌，54，11(2010) 654

[71] 飯島　昇，竹山秀彦，柏瀬雅一：焼結ダイヤモンド工具の切削性能と摩耗解析(第1報) - 焼結ダイヤモンド工具の力学的損傷機構 - ，精密機械，50，7 (1984) 1110

[72] 社本英二，家永　健，森脇俊道：超音波楕円振動切削による超硬合金の延性モード加工，砥粒加工学会誌，47，2 (2002) 83

[73] 鈴木教和，樋野　励，益田真輔，社本英二：超硬合金の超精密楕円振動切削加工 - 延性モード切削機構の検討 - ，精密工学会誌，72，4 (2006) 539

[74] 鈴木教和，閻　甄敏，針谷　誠，楊　積彬，浜田晴司，樋野　励，益田真輔，社本英二：超音波楕円振動切削によるタングステン合金の超精密切削加工，精密工学会誌，73，3 (2007) 360

[75] C. Nath, M. Rahman and K. S. Neo: Machinability Study of Tungsten Carbide Using PCD Tools under Ultrasonic Elliptical Vibration Cutting, International Journal of Machine Tools and Manufacture, 49, 14 (2009) 1089

[76] C. Nath, M. Rahman and K. S. Neo: A Study on the Effect of Tool Nose Radius in Ultrasonic Elliptical Vibration Cutting of Tungsten Carbide, Journal of Materials Processing Technology, 209, 17 (2009) 5830

[77] 岡崎隆一，伊東好樹，川上智也，仙波卓弥，久木野暁：バインダレス PCD ならびに cBN 製マイクロボールエンドミルの試作と加工特性，日本機械学会第 7 回生産加工・工作機械部門講演会講演論文集，(2008)，55

[78] 田中義弘，奥山藤夫，吉川典孝，瀧山　努，水迫祐太郎：小径ボールエンドミルによる超硬合金の鏡面切削 - 微小金型製作への応用 - ，2008 年度精密工学会秋季大会学術講演会講演論文集，(2008)，85

[79] 鈴木浩文，田中克敏，武田　弘，川上邦治，西岡昌彦：マイクロ非球面の超精密研削技術に関する研究(第 2 報)，精密工学会誌，64，8 (1998) 1221

[80] 佐伯　優，厨川常元，庄司克雄：パラレル研削法による非球面金型の加工に関する研究，精密工学会誌，68，8 (2002) 1067

[81] 厨川常元，立花　亨，庄司克雄，森由喜男：円弧包絡研削法による非軸対称非球面セラミックスミラーの加工，日本機械学會論文集　(C 編)，63，611 (1997) 2532

[82] T. Kuriyagawa, M. S. Sepasyzahmaty, H. Suzuki, K. Syoji and T. Tachibana: Nonaxisymmetric Aspheric Grinding Technique for Ceramic Mirrors, Advanced in Abrasive Technology, 1 (1997) 217

[83] 隈部淳一郎：超音波縦振動といしによる内面研削に関する研究：第 1 報，切削方向と左右方向超音波振動切削，日本機械学會論文集 ，27，181 (1961) 1404

[84] 隈部淳一郎：精密加工　振動切削 - 基礎と応用 - ，(1979)，共立出版

[85] E. Shamoto and T. Moriwaki: Study on Elliptical Vibration Cutting, Annals of the CIRP, 43, 1 (1994) 35

[86] 社本英二，森本祥之，森脇俊道：楕円振動切削加工法(第 1 報) - 加工原理と基本特性 - 精密工学会誌，62，8 (1996) 1127

[87] 社本英二，森本祥之，森脇俊道：楕円振動切削加工法(第 2 報) - 振動条件の影響に関する討論 - 精密工学会誌，65，3 (1999) 411

[88] 社本英二，馬　春翔，森脇俊道：楕円振動切削加工法(第 3 報) - 三次元切削への適用と実用的諸効果の検討 - 精密工学会誌，65，4 (1999) 586

[89] 社本英二，鈴木教和，森脇俊道，直井嘉和：楕円振動切削加工法(第 4 報) - 工具振動制御システムの開発と超精密切削への適用 - ，精密工学会誌，67，11 (2001) 1871

[90] 社本英二，宋　詠燦，吉田秀樹，鈴木教和，森脇俊道，幸田盛堂，山西哲司：機械式円振動発生機構を利用した楕円振動切削加工機の開発，精密工学会誌，69，4 (2003) 542

[91] (株)アライドマテリアル：製品カタログ

[92] 鈴木浩文，藤井一二，沖野　正，横山高士，小野　孝，渡邊昌司，和嶋　直，北嶋孝之，奥山繁樹：非軸対称非球面のダイヤモンド切削に関する研究(第 1 報) - アールバイトを用いた 3 軸制御シェーパ加工による形状創成 - ，精密工学会誌，65，11 (1999) 1611

[93] 竹内芳美，横山信人，久木達也，鈴木　裕，佐藤　真：6 軸制御による自由曲面平滑加工，精密工学会誌，60，12 (1994) 1786

[94] T. Bifano, T. Dow and R. Scattergood: Duticle Regime Grinding: A New Technology for Machining Brittle Materials, ASME, Journal of Engineering for Industry, 113, 5 (1991) 184

[95] 杉田忠彰，上田完次，遠藤勝義： 硬ぜい材料のマイクロ切削における塑性変形型材料除去の可能性，精密工学会誌, 52, 12 (1988) 1038

[96] 宮下政和：ぜい性材料の延性モード研削加工技術-ナノ研削技術への道，精密工学会誌，56, 5 (1990) 782

[97] K. E. Puttick, M. R. Rudman, K. J. Smith, A. Franks and K. E. Lindsey: Single-point Diamond Machining of Glasses, Proceedings of Royal Society of London., A 426 (1989) 19

[98] I. Inasaki: Grinding of Hard and Brittle Materials, Annals of the CIRP, 36, 2 (1987) 463

[99] P. N. Blake and R. O. Scattergood: Ductile Regime Machining of Germanium and Silicon, Journal of American Ceramic Society, 73, 4 (1990) 949

[100] T. Nakasuji, S. Kodera, S. Hara, H. Matsunaga, N. Ikawa and S. Shimada: Diamond Turning of Brittle Materials for Optical Components, Annals of the CIRP, 39, 1 (1990) 89

[101] 閻紀旺，庄司克雄，厨川常元：大きな負のすくい角工具による延性・ぜい性遷移，精密工学会誌，66，7 (2000) 1130

[102] E.Brinksmeier, W.Preub and O. Riemer: From Friction to Chip Removal: An Experimental Investigation of the Microcutting Process, Proceedings of 8th International Precision Engineering Seminar, 335

[103] P. A. Mckeown, K. Carlisle, P. Shore and R.F.J. Read: Ultraprecision High Stiffness CNC Grinding Machines for Ductile Mode Grinding of Brittle Materials, Journal of Japan Society for Precision Engineering, 56, 5 (1990) 806

[104] 山口　収，西口　隆，桝田正美，内田浩二：ガラスの臨界切込み深さに及ぼす工具すくい角の影響，1990 年度精密工学会秋季大会学術講演会講演論文集，(1990) 751

[105] M. G. Schinker: Subsurface Damage Mechanisms at High-Speed Ductile Machining of Optical Glasses, Precision Engineering, 13, 3 (1991) 208

[106] 閻紀旺，庄司克雄，厨川常元：単結晶 Si の超精密切削における切りくず形態，精密工学会誌，65，7 (1999) 1008

[107] 水谷勝己，谷先盛彦，田中芳雄，井戸守：セラミックスの切削における材料除去-大規模破壊過程におけるクラック進展経路の線形破壊力学による考察，精密機械，49，4 (1983) 435

[108] 杉田忠彰，上田完次，橋本知明：セラミックスのマイクロ切削に関する破壊力学的研究-き裂の残留を伴う材料除去機構の解析，精密工学会誌，51，10 (1985) 1940

[109] 後藤学：塑性学，コロナ社 (1982)

[110] B.R. Lawn and M.V.Swain: Micro-fracture beneath Point Indentations in Brittle Solids, Journal of Material Science, 10 (1975) 113

[111] 吉岡正人，室井邦雄：ガラス表面への引っかきによるクラック形成過程の動的観察，精密工学会誌，60，9 (1994) 1274

[112] Z.J. Pei, S.R. Billingsley and S. Miura: Grinding Induced Subsurface Cracks in Silicon Wafers, International Journal of Machine Tools and Manufacture, 39 (1999) 1103

[113] 藤井太一，平野 稔，渋川哲郎，石田 徹，竹内芳美：微細構造を有するガラスレンズ成形型の高精度加工に関する研究 - 複合加工手法によるフレネル形状ガラスレンズ金型の高精度加工，精密工学会誌，74，12 (2008) 1298

[114] 小林篤史：超精密ダイヤモンド切削工具「UPC」による最新の金型加工，型技術，24，6 (2009) 59

[115] 沢田 潔，竹内芳美：超精密マシンニングセンターとマイクロ加工，(1998)，日刊工業新聞社

[116] 園 真，石田 徹，寺本孝司，榎本俊之，竹内芳美：超精密 5 軸制御加工におけるセッティング誤差の一般化補正法，精密工学会誌，73，10 (2007) 1154

[117] J. Krystof: Berichte uber Betriebswissenschaftliche Arbeiten, Bd., 12, VDI Verlag, (1939)

[118] M. E. Merchant: Mechanics of the Metal Cutting Process. II .Plasticity Conditions in Orthogonal Cutting, Journal of Applied Physics, 16 (1945) 318

[119] E. H. Lee and B. W. Shaffer: The Theory of Plasticity Applied to a Problem of Machining, Journal of Applied Physics, 73 (1951) 405

[120] G. V. Stabler: The Fundamental Geometry of Cutting Tools, Proceedings Institution of Mechanical Engineers. 165 (1951) 14

[121] M. E. Merchant: Basic Mechanics of the Metal-Cutting Process, ASME Journal of Applied Mechanics, 11 (1944) A168

[122] E. J. A. Armarego and R. H. Brown: The Machining of Metals, Prentice Hall, Inc., Englewood Cliffs, New Jersey, (1969)

[123] J. K. Russel and R. H. Brown: The Measurement of Chip Flow Direction, International Journal of Machine Tool Design and Research, 6 (1966) 129

[124] G. C. I. Lin and P. L. B. Oxley: Mechanics of Oblique Machining: Predicting Chip Geometry and Cutting Forces from Work Material Properties and Cutting Conditions, Proceedings Institution of Mechanical Engineers, 186 (1972) 813

[125] E. Budak, Y. Altintas and E. J. A. Armarego: Predicition of Milling Force Coefficient from Orthogonal Cutting Data, ASME Journal of Manufacturing Science and Engineering. 118 (1996) 216

[126] E. Usui, A. Hirota and M. Masuko: Analytical Prediction of Three-Dimensional Cutting Process. Part 1 Basic Cutting Model and Energy Approach, Transaction of ASME, 100 (1978) 222

[127] 臼井英治：現代切削理論，共立出版，(1990)

[128] 社本英二：3 次元切削機構に関する研究 (第 1 報) - 傾斜切削プロセスの理解とベクトルによる定式化，精密工学会誌，68，3 (2002) 408

[129] E. Shamoto and Y. Altintas: Prediction of Shear Angle in Oblique Cutting with Maximum Shear Stress and Minimum Energy Principles, ASME Journal of Manufacturing Science and Engineering. 121 (1999) 399

[130] E. J. A. Armarego: Practical Implications of Classical Thin Shear Zone Cutting Analysis, UNESCO-CIRP Seminar on Manufacturing Technology, (1982) 1

[131] 加藤　仁，山口勝美，中村　隆：回転ダイス型工具による円周加工法の研究(第 2 報，実用範囲内での実験と理論的考察)，日本機械学会論文集　(C 編)，47，421 (1980) 1200

[132] N. N. Zorev: Metal Cutting Mechanics, Pergamon Press, (1966)

[133] 小林裕一，柴田順二，鈴木　亨，石川惣一，大森　整，林　偉民：マイクロレンズアレイ金型の超精密切削加工 - 斜軸切削加工法による試み - ，日本機械学会関東支部・精密工学会茨城講演会講演論文集，(2004) 147

[134] 小林裕一，柴田順二，森田晋也，鈴木　亨，劉　慶，大森　整，林　偉民，石川惣一：マイクロレンズアレイ金型の超精密切削加工(第 2 報) - 斜軸切削加工法による補正加工の試み - 2005 年度精密工学会春季大会学術講演会講演論文集，(2005)，769

[135] 神崎紀久，長坂昭吾，畑村章彦，吉田　仁，荒井　剛，岡安　裕：小径ボールエンドミル法における非球面マイクロレンズアレイ金型加工の高精度化 - 工具輪郭度補正の検討 - ，2006 年度精密工学会秋季大会学術講演会講演論文集，(2006)，795

LIST OF PUBLICATIONS

A) Journal Papers

1. 唐　辛鋭，吉永実樹，中本圭一，石田　徹，竹内芳美：特殊チャンファ付きダイヤモンド工具の摩耗抑制をした高硬度材の超精密マイクロ溝加工, 精密工学会誌, Vol.76, No.9, pp.1082，2010
2. 唐　辛鋭，中本圭一，小畠一志，石田　徹，竹内芳美：特殊チャンファ付き工具を用いた刃先移動加工法の効果，精密工学会誌，Vol.78，No.8，pp.705，2012
3. 唐　辛鋭，中本圭一，小畠一志，竹内芳美：刃先移動加工法を用いた曲線溝と曲面の超精密マイクロ加工，精密工学会誌，Vol.79，No.2，2013 (掲載予定)
4. Xinrui Tang, Keiichi Nakamoto, Kazushi Obata and Yoshimi Takeuchi: Ultraprecision Micromachining of Hard Material with Tool Wear Suppression by Using Diamond Tool with Special Chamfer, Annals of the CIRP, (投稿中)

B) International Proceedings

1. Xinrui Tang, Miki Yoshinaga, Keiichi Nakamoto, Tohru Ishida and Yoshimi Takeuchi: High Efficiency Machining of Hard Material by Non-rotational Diamond Tool with Chamfer, Proceedings of 3rd International Conference of Asian Society for Precision Engineering and Nanotechnology, 2B-2, 2009
2. Xinrui Tang, Miki Yoshinaga, Keiichi Nakamoto, Tohru Ishida and Yoshimi Takeuchi: Ultraprecision Microgrooving of Hard Material by Means of Cutting Point Swivel Machining, Key Engineering Materials, Vol.447-448, pp.36, 2010
3. Xinrui Tang, Kazushi Obata, Keiichi Nakamoto, Tohru Ishida and Yoshimi Takeuchi: Ultraprecision Low-wear Micro Curved Grooving of Hard Material, Proceedings of 6th International Conference on Micro Manufacturing, pp.605, 2011
4. Xinrui Tang, Keiichi Nakamoto, Kazushi Obata, Tohru Ishida and Yoshimi Takeuchi: Ultraprecision Microgrooving on Hard Material with Tool Wear Suppression, Proceedings of 26th Annual Meeting of the American Society for Precision Engineering, 2011
5. Keiichi Nakamoto, Toshiki Matsuura, Xinrui Tang and Yoshimi Takeuchi: Ultraprecision Cutting of Micro Lens on Roll Mold, 16th International Conference on Mechatronics Technology, pp.548, 2012
6. Xinrui Tang, Keiichi Nakamoto, Kazushi Obata and Yoshimi Takeuchi: The Effect of Cutting

Point Swivel Machining by Using Round Tool with Special Chamfer, Key Engineering Materials, Vol.523-524, pp.119, 2012

C) Conference

1. 唐　辛鋭，石田　徹，竹内芳美：エンドミルによる超精密マイクロ凹球面加工の誤差補正，2008 年度精密工学会学生会員卒業研究発表講演会論文集，pp.87，2008
2. 唐　辛鋭，石田　徹，竹内芳美：エンドミルによる超精密マイクロ凹球面加工とその誤差補正，2008 年度精密工学会関西地方定期学術講演会講演論文集，pp.71，2008
3. 唐　辛鋭，吉永実樹，中本圭一，石田　徹，竹内芳美：チャンファー付きダイヤモンド製工具による高硬度材料の高効率加工，2009 年度精密工学会秋季大会学術講演会講演論文集，pp.45，2009
4. 唐　辛鋭，吉永実樹，中本圭一，石田　徹，竹内芳美：刃先移動加工法を用いた超精密マイクロ溝加工，2010 年度精密工学会春季大会学術講演会講演論文集，pp.3，2010
5. 唐　辛鋭，吉永実樹，中本圭一，石田　徹，竹内芳美：刃先移動加工法を用いた超精密マイクロ溝加工(第 2 報) - 曲線溝加工への適用 - ，2010 年度精密工学会秋季大会学術講演会講演論文集，pp.789，2010
6. 唐　辛鋭，小畠一志，中本圭一，石田　徹，竹内芳美：刃先移動加工法を用いた超精密マイクロ溝加工(第 3 報) - 曲線溝における曲率の影響 - ，2011 年度精密工学会春季大会学術講演会講演論文集，pp.261，2011
7. 唐　辛鋭，中本圭一，小畠一志，石田　徹，竹内芳美：刃先移動加工法を用いた超精密マイクロ溝加工(第 4 報) - 刃先移動加工法のメカニズム - ，2011 年度精密工学会秋季大会学術講演会講演論文集，pp.451，2011
8. 唐　辛鋭，中本圭一，小畠一志，竹内芳美：刃先移動加工法を用いた超精密マイクロ溝加工(第 5 報) - 異なる工具回転速度に対する切削抵抗と工具摩耗 - ，2012 年度精密工学会春季大会学術講演会講演論文集，pp.903，2012
9. 唐　辛鋭，中本圭一，小畠一志，竹内芳美：刃先移動加工法を用いた超精密マイクロ曲面加工，2012 年度精密工学会秋季大会学術講演会講演論文集，pp.823，2012

D) Others

1. Xinrui Tang, Keiichi Nakamoto and Yoshimi Takeuchi: Ultraprecision Machining of Hard Material by Suppressing Diamond Tool Wear, Proceedings of the 15th International Machine Tool Engineer`s Conference, pp.88, 2012

ACKNOWLEDGEMENT

This study was carried out from 2008 to 2013 at the Department of Mechanical Engineering, Graduate School of Engineering, Osaka University. I would like to express my deepest gratitude to my supervisor, Prof. Y. Takeuchi in Chubu University for his continuous guidance, helpful suggestions, and hearty encouragement through the course of this study.

It is an honor for me to have three reviewers: Professor T. Enomoto, Professor Y. Takaya and Professor K. Yamauchi in Osaka University. Professors spare their valuable time guiding my dissertation, so that I will find more depth in this research.

In particular, I would like to express my grateful appreciation to Professor T. Ishida in the University of Tokushima, and Associate Professor K. Nakamoto in Tokyo University of Agriculture and Technology, for their continuous guidance, fruitful discussions and helpful suggestions to this work.

Then, I would like to feel grateful to related parties in A. L. M. T. Corp., for their supplying the cutting tool used in this study. Especially, I would like to express my deepest gratitude to Mr. K. Obata and Mr. M. Yoshinaga for their suggestion in cutting tool, machining technology and collaboration to this study.

Also I would like to express my appreciation to Assistant Professor T. Sugihara in Osaka University for his advices in cutting technology, measurement and my daily life in Japan. At the same time, I would like to thank Dr. J. Lin in Industrial Technology Research Instrument for his suggestions in the study and my future life.

I would like to thank Associate Professor T. Hayashi and Assistant Professor M. Michihata in Osaka University for supplying the measuring equipments. At the same time, I would like to thank related parties in Nippon Steel Materials Co. Ltd. and JTEKT Corp. for supplying the workpieces, and related parties in FANUC for their advices in using the ultraprecision machining center.

Then, I would like to express my appreciation to Professor M. Tsutsumi and Professor H. Sasahara in Tokyo University of Agriculture and Technology, for their suggestions to this study. Then, I would like to thank all the members in Lab. Takeuchi, Lab. Enomoto, Lab. Nakamoto, Lab. Tsutsumi and Lab. Sasahara for their help, not only in the research, but also in the life in Osaka and Tokyo.

Finally, I would like to express my heartfelt appreciation to my parents and family to complete my research work. Thank to their understanding and support.

January 2013

Tang Xinrui